CHAPTER ONE

INTRODUCTION

1.1 General Overview of Thesis: Problem Statement

The quick determination of trace quantities of analytes by simple methods is of special interest in analytical chemistry. The construction and application of sensitive electrode as a sensor offers interesting advantages such as simplicity, relatively fast response, low cost, wide linear dynamic range and ease of preparation and procedures. These characteristics have inevitably led to the preparation of numerous sensors for several analytes, and the list of available electrodes has grown substantially over the past years. Despite this, the electrochemical and electrocatalytic behaviour of carbon nanotubes-metal (CNTs-M) or carbon nanotubes-metal oxides (CNTs-MO) nanoparticles (NPs) modified electrode as potential nanocomposite for chemically modified electrodes, especially on a non-convectional electrode platform such as edge plane pyrolytic graphite electrode as a support have not received much attention or hugely explored. It is also anticipated that the supercapacitive properties of such electrode system for potential application in supercacitor still remain a virgin area for prospective research opportunities if explored.

This work describes the electron transport and electrocatalytic properties of single or double-walled carbon nanotubes (SWCNTs/MWCNTs) integrated with metal (M) and metal oxide (MO) nanoparticles supported on edge plane pyrolytic graphite electrode (EPPGE) platform towards the detection of biologically and environmentally important analytes: diethylaminoethanethiol (DEAET), hydrazine, dopamine and nitrite.

1.1.1 Carbon nanotube-metal and metal oxide nanocomposite in electrochemistry

1.1.1.1 Carbon nanotubes as electrical conducting nanowires

Carbon nanotubes (CNTs), discovered in 1978 [1] and rediscovered in 1991 [2] by Ijima, have attracted immense attraction around the world. Carbon nanotubes have found application in plethora of areas such as in nanoscale hydrodynamics [3], field emission devices [4], catalysis of redox reactions [5–7], nanoelectronics [8], hydrogen storage [9], electrochemical capacitors [10,11] and electrochemical sensors [12]. The material receives considerable attention in the area of electrochemistry not only due to their reported structural, mechanical or electronic properties but because they represent the world's smallest electrodes allowing electrochemistry to be performed where other electrode materials cannot penetrate. Its first application in electrochemical sensing was first carried out by Britto and Co-workers [13] but was largely neglected until Joseph Wang and co-workers demonstrated their beneficial use for the electroanalytical detection of nicotinamide adenine dinucleotide (NADH) [14]. Since then CNTs application in electrochemistry has grown profusely, where CNTs-modified electrodes have shown interesting catalytic properties toward electrochemical processes since it acts as electrical conducting nanowires between the base electrode and the electroactive species on the surface. Despite its numerous application, CNTs integration with metal nanoparticles (especially Co, Ni and Fe which are important members of mixed-valence transition metals) to give hybrid systems which form the basis of this project as electroactive material for sensor have not been fully explored.

1.1.1.2 Metal (M) and metal oxide (MO) nanoparticles as electrocatalyst

Metal nanoparticles are potentially useful for sensing, catalysis, transport, and other applications in biological and medical sciences [15, 16]. Transition metals nanoparticles (especially Ni, Fe and Co) are found to demonstrate better sensing and catalytic properties towards detection and determination of both environmental and biological analytes [17-21]. Metal oxide nanoparticles on the other hand are extensively used in a considerable number of applications in food, material, chemical and biological sciences [22]. It is well known that bulk materials based on TiO_2, SiO_2 and aluminium (Al) and iron oxides have been massively produced for many years. Recently, nanoparticulate versions of these metal oxides have been manufactured. They are introduced in commercial products such as cosmetics and sunscreens (TiO_2, Fe_2O_3 and ZnO) [23], fillers in dental fillings (SiO_2) [24], catalysis (TiO_2) [25], and as fuel additives (CeO_2) [26]. In contrast, nickel (Ni), iron (Fe) and Cobalt (Co) are important transition metals which application in catalysis and other industrial applications have been neglected for many years. More importantly, their nanocomposite with CNTs and their redox active behaviour to influence electron transfer kinetics on chemically modified electrode for application in catalysis are hardly reported or not fully explored. Therefore, this thesis dwell deeply into the synthesis, characterization and electrocatalytic behaviour of these important transition metals and their oxides (NiO, Fe_2O_3, Co_3O_4) towards sensing of some important environmental molecules.

1.1.1.3 Carbon nanotube-metal and metal oxide modified electrode as sensor for the hydrazine, diethylaminoethanethiol, dopamine and nitrite.

Recently there has been renewed interests in the preparation and characterization of carbon nanotubes/metal (CNT–M) hybrid systems as electroactive material for sensors [27–32] and catalysts [33,34]. Among these metals, Co, Ni and Fe have proven to have excellent properties in electrocatalysis. The detection of the hydrolysis products of V-type nerve agents is still hugely unexplored. But it was observed previously that surface-confined nickel micropowder (ca. 17 – 60 mm range) immobilized on basal plane pyrolytic graphite electrode showed good electrocatalytic response towards DEAET [35]. Even with that, research report on its detection on CNT/M nanocomposite modified electrode is very scarce or unavailable. On the other hand, there are huge literature on the electro-oxidation of hydrazine on carbon-based electrodes [36–45], but the use of CNTs decorated with metal nanoparticle is limited [46]. Authors have also reported the electrocatalytic properties of other modified electrodes towards the electrocatalytic response of dopamine [47-57], nitite and nitric oxide [58-67] but the detection of these molecules on CNT/M or CNT/MO modified electrodes is rarely established. Thus, this thesis did not only explore catalysis of these analytes on CNT/M modified electrode, but also reported the mechanism behind their electrocatalytic oxidation using different electrochemical techniques.

1.1.1.4 Electron transport behaviour of CNT-M/MO modified electrodes.

Studies have shown that CNTs provided a large surface for metal deposition on electrodes and thus provided a synergistic relationship for an improve electron transfer between the base

electrode and the CNT–M hybrids [16,68-70]. However, the extent and the mechanism for the electron transfer of the CNT–M and carbon nanotubes–metal oxide (CNT–MO) modified electrodes are not clearly understood. Electron transport (ET) process between the surface active material and the underlying electrode is important in achieving a maximal overlap between electrode modifier, the electrolyte or the analyte in solution for enhanced or active electrocatalysis. An effective electron transfer lowers the formal potential of catalysis, reduces the peak to peak separation (ΔE) and ensures that the ratio of the anodic to cathodic peak current is close to unity which in principle indicates a favourable reversible process. This principle is more important in biological system where the orientation of the active biological catalyst to the electrode is of great importance for effective electron transport and catalysis. For example, nickel oxide film has a great effect on the electrode kinetics and provides a suitable environment for the glucose oxidase to transfer electron with underlying GC electrode in blank phosphate buffer solution pH 7.0 [16]. This can be as a result of the strong interaction between GOx molecules and NiOx nanoparticles.

The electron transport (ET) behaviour of iron nanocomposite modified electrodes has been studied in different electrolytes. For example, ET of iron-5,10,15,20-tetrakis[aaaa-2-trismethylammoniomethyl-phenyl]porphyrin,nanocomposite modified gold electrode (MWNTs-FeTMAPP/Au) was determined in 0.1 M KCl containing 1.0 mM $[Fe(CN)_6]^{3-}$ .The redox peak currents of $[Fe(CN)6]^{3-/4-}$ redox couple greatly increased and was attributed to the larger apparent surface of the electrode due to the presence of the nanocomposite [71]. In a related experiment, electron transfer behaviour of nanostructured iron(II)phthalocyanine (nanoFePc) at edge plane pyrolytic graphite electrodes (EPPGEs) was investigated using cyclic voltammetry and electrochemical impedance spectroscopy (EIS). This showed that the nanoFePc-

based electrode exhibits faster heterogeneous electron transfer constant, k_{app} (about a magnitude higher) than the bulk FePc in $[Fe(CN)6]^{3-/4-}$ redox probe [72]. In another study, presence of Fe_3O_4 nanoparticles on chitosan iron oxide indium tin oxide electrode ($CH/Fe_3O_4/ITO$) results in increased active surface area of chitosan iron oxide nanocomposite and resulted in increased electron transport between $[Fe(CN)_6]^{3-/4-}$ redox species and the electrode [73]. Electrochemical impedance spectroscopy (EIS) studies of chitosan indium tin oxide modified electrode (CH/ITO film) and chitosan magnetic iron oxide nanoparticles indium tin oxide modified electrode ($CH–Fe_3O_4/ITO$) was investigated in phosphate buffer solution. From the Nyquist plots obtained, the semicircle part, which corresponds to the electron transfer limited process is smaller for the $CH–Fe_3O_4$ nanocomposite than CH film ITO modified electrode thus suggesting that the electron transfer in the $CH–Fe_3O_4$ nanocomposite film is easier between the solution and electrode [74]. Zhao et al. [75] reported that multilayer of $CH–Fe_3O_4$ promotes direct electron transfer of haemoglobin. Other studied on electron transport of iron and iron oxide nanoaparticles have been reported [76].

There are many literatures on the ET of CoOx NPs at electrode surface but in most cases, the CoOx NPs mediates ET between a biomolecule and the underlying electrode. For example, Haemoglobin (Hb) undergoes a quasi-reversible redox process at the glassy carbon electrode modified with cobalt oxide nanoparticles, not observed at the bare GC electrode and was attributed to the cobalt oxide providing a suitable environment for the hemoglobin to transfer electron with underlying GC electrode [77]. In another report, flavine adenine dinucleotide (FAD) undergoes a quasi-reversible redox process at glassy carbon electrode modified with cobalt oxide (CoOx) nanoparticles in pH 7.0 PBS. No peak was observed for GC/CoOx or bare GC electrode in

the same electrolyte [19]. The result suggests that CoOx influence kinetics of electrode reaction and provides a suitable environment for the FAD to transfer electron with underlying GC electrode. Other literatures on the ET behaviour of Co and CoOx NPs on electrode surface have been reported [78,79].

1.1.2 Aim of thesis.

The main objectives of this project are:

i. To characterise redox active metal and metal oxide nanoparticles made by both electrodeposition and simple chemical syntheis, and integrated with single or multi-walled carbon nanotubes using microscopy, spectroscopy and electrochemical techniques.

ii. To modify bare edge plane pyrolytic electrode with the CNT-M or CNT-MO films through a simple drop-dried method and establish their electrochemical properties which are:

(i) Heterogenous electron transfer kinetics and

(ii) Electrocatalysis towards the detection of DEAET, hydrazine dopamine and nitrite.

iii. To investigate the supercapacitive or energy storing properties of the CNT/MO nanocomposite materials in neutral and acidic pH conditions.

This introductory chapter will provide information on the general overview of electrochemistry, electrochemical techniques,electrochemical impedance spectroscopy, chemically modified electrodes, electrode modification process, nanoscience in electrochemistry, microscopy and spectroscopy techniques and the analytes (DEAET, hydrazine, dopamine and nitrite) used in this work as analytical probe. Chapter two provides the experimental procedure adopted. Chapter three to ten discuss the results obtained.

1.2 Overview of Electrochemistry

1.2.1 Basics of electrochemistry

Several analytical techniques have been developed over the years for the detection and quantification of arrays of biological and environmentally important analytes. Among these is titrimetric [80], flourimetry [81], high performance liquid chromatography (HPLC) [82], mass spectroscopy [83] among others. However, these methods require a lot of chemical derivatization procedures and are time consuming. Some are very cumbersome and expensive and not even portable enough for field analysis. Therefore in recent time, the properties and the application of these electrodes for analytical purposes have been investigated using electrochemical technique.

1.2.1.1 Electrochemical equilibrium: Introduction

An electrochemical equilibrium established when two solutions are separated by a membrane that is impermeable to some of the ions in the solution. In more physical terms, it is an equilibrium set up when two coexisting phases are subject to the restriction that one or more of the ionic components cannot pass from one phase into the other; commonly, this restriction is caused by a membrane which is permeable to the solvent and small ions but impermeable to colloidal ions or charged particles of colloidal size [84].

Consider the following process:

$$Fe(CN)_6^{3-}(aq) + e^-(m) \rightleftharpoons Fe(CN)_6^{4-}(aq) \qquad (1.1)$$

Such an equilibrium was established by first preparing a solution containing both potassium hexacyanoferrate (II), $K_4Fe(CN)_6$, and

potassium hexacyanoferrate(III), $K_3Fe(CN)_6$ dissolved in water and then inserting an electrode made of platinum or other inert metal into the solution (Figure 1.1). Equilibrium is established at the surface of the electrode and involves the two dissolved anions and the electrons in the metal electrode.

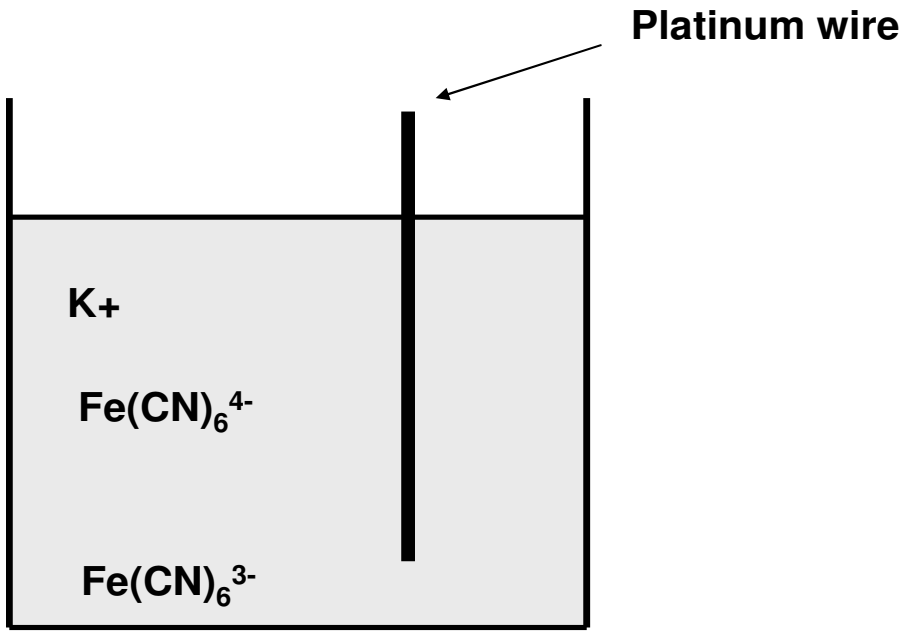

Figure 1.1: A platinum wire immersed into an aqueous solution containing both ferrocyanide and ferricyanide [84].

The establishment of equilibrium implies that the rate of at which $Fe(CN)_6^{4-}$ gives up electrons (become oxidized) to the metal wire or electrode is exactly balanced by the rate at which electrons are released by the wire to the $Fe(CN)_6^{3-}$ anions (become reduced). Once this dynamic equilibrium is established, no further change occurs. Also, the net number of electron that are transferred in one direction or another is infinitesimally small, such that the concentrations of $Fe(CN)_6^{4-}$ and $Fe(CN)_6^{3-}$ are not measurably changed from their values before the electrode is introduced into the solution.

1.2.1.2 Electrochemical equilibrium: Electron transfer at the electrode-solution interface

Considering the equation below:

$$Fe(CN)_6^{3-}(aq) + e^-(m) \rightleftharpoons Fe(CN)_6^{4-}(aq) \qquad (1.2)$$

Transfer of electrons between the metal electrode and the solution phase is a function of the energy levels associated with the species involved in the potential determining equilibrium. For example for the system represented in Equation 1.2 above, the electronic structure of the metal involves electronic conduction 'bands' in which the electrons are free to move throught the solid, binding the (metal) cations rigidly together. The energy levels in these bonds filled up to an energy maximum known as the Fermi level. On the other hand, the energy level associated with the solution phase $Fe(CN)_6^{4-}$ and $Fe(CN)_6^{3-}$ (aq) ions are discrete and relate to an unfilled molecular orbital in $Fe(CN)_6^{3-}$, which gains an electron to form $Fe(CN)_6^{4-}$ [84]. Figure 1.2 shows that before electron transfer takes place between the electrode and the solution, the Fermi level is higher than the vacant orbital in the $Fe(CN)_6^{3-}$ ion thus making it energetically favourable for electrons to leave the Fermi level and join the $Fe(CN)_6^{3-}$ species converting them to $Fe(CN)_6^{4-}$ ions. This energy difference is the driving force of the electron transfer in the system. As this electron transfer proceeds, positive charge builds up on the electrode (metal) and corresponding negative charge in the solution phase therefore creating an electrical double layer. Correspondingly, the electronic energy level in the metal becomes lower while that in the solution phase becomes higher. A situation is reached where the Fermi level lies in between the energy levels of the two ions, so that the rate at which electrons leave the electrode and reduced $Fe(CN)_6^{3-}$ ions equals the rate at which electrons join

the metal from the $Fe(CN)_6^{4-}$ ions which becomes oxidized. At this equilibrium point, there is a charge separation between the electrode and the solution, and this is the origin of the electrode potential established on the metal.

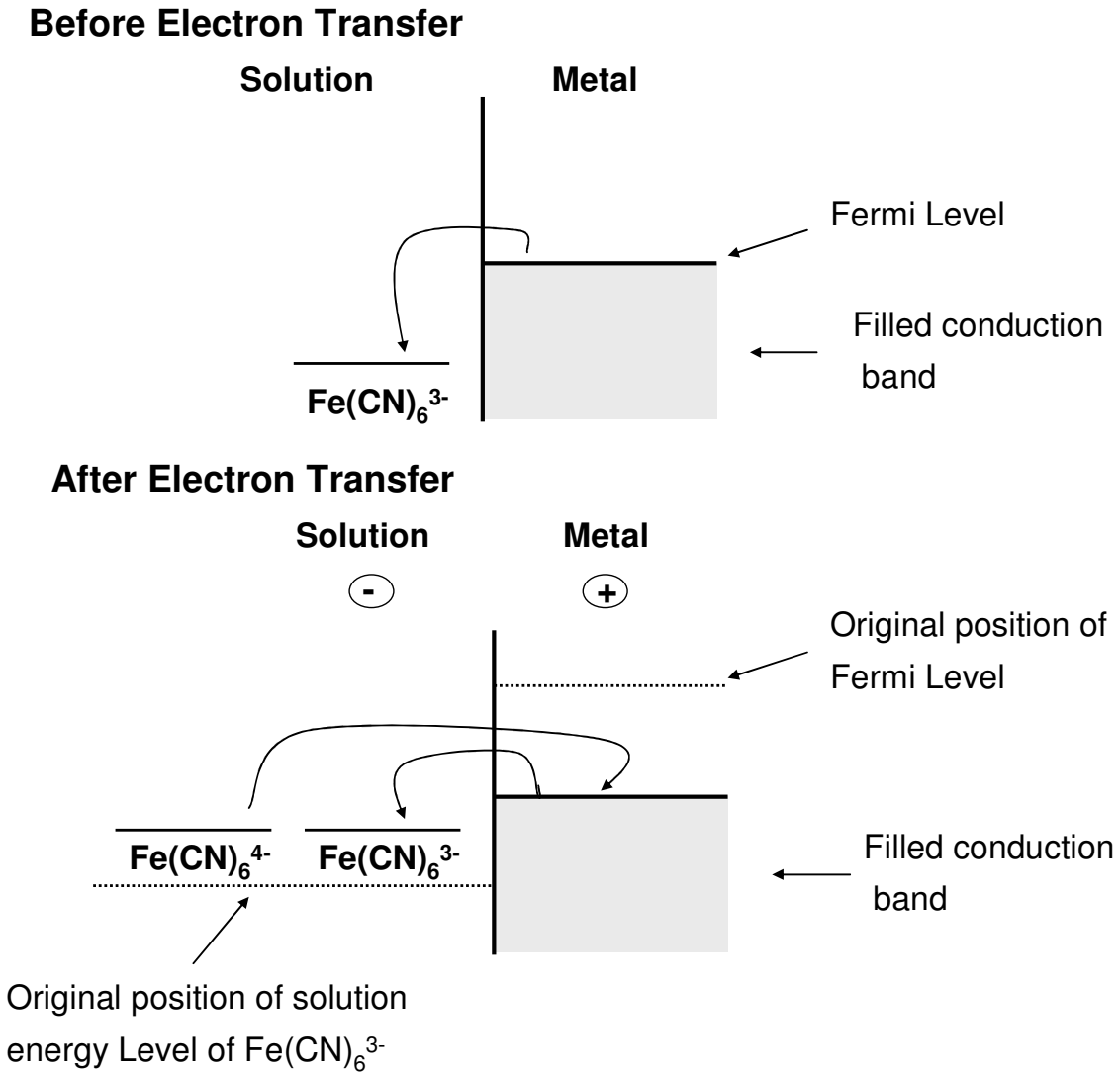

Figure 1.2: The energy of electrons in the ions in solution and in the metal wire [84].

1.2.1.3 Classification of electrochemical techniques

Electrochemical techniques can either be 'bulk' or 'interfacial' technique. Bulk techniques are based on the phenomena that occur in the solution itself while interfacial techniques are based on the events occurring at the electrode-

solution interface. Interfacial technique is sub-divided into potentiometric and voltammetric methods. Voltammetric technique can either be divided into controlled-potential and controlled-current methods. Controlled-potential techniques have advantages such as high sensitivity and selectivity, protable and low cost instrumentation. It allows for potential controlled while the current is measured. Examples include voltammetry and chronoamperometry.

1.2.1.4 Faradaic and non-Faradaic processes

The objective of controlled-potential electroanalytical experiments is to obtain a current response which is related to the concentration of the target analyte. This objective is accomplished by monitoring the transfer of electron(s) during the redox process of the analyte:

$$\mathbf{O} + ne^- \rightleftharpoons \mathbf{R} \qquad (1.3)$$

where O and R are the oxidized and the reduced forms, respectively, of the redox couple. These reactions are called Faradaic process as electrons are transferred across the electrode-solution interface. Non-Faradaic process on the other hand arises where there is no charge transfer across the electrode-solution interface. Processes such as adsorption and desorption can occur, and the structure of the electrode-solution interface can change with changing potential or solution composition. The Non-Faradaic process can be governed by 'transient current' when the potential, electrode area, or solution composition changes.

1.2.1.5 The electrochemical cell

Electrochemical cells in which faradaic currents are flowing are classified as either *galvanic* or *electrolytic* cells. A *galvanic cell* is one in which reactions occur spontaneously at the electrodes

when they are connected externally by a conductor (Figure 1.3a). These cells are often employed in converting chemical energy into electrical energy. Galvanic cells of commercial importance include *primary (nonrechargeable) cells* (e.g., the Leclanche Zn-MnO_2 cell), *secondary (rechargeable) cells* (e.g., a charged Pb-PbO_2 storage battery), and *fuel cells* (e.g., an H_2-O_2 cell). An *electrolytic cell* is one in which reactions are effected by the imposition of an external voltage greater than the open-circuit potential of the cell (Figure 1.3b). These cells are frequently employed to carry out desired chemical reactions by expending electrical energy. Commercial processes involving electrolytic cells include electrolytic syntheses (e.g., the production of chlorine and aluminum), electrorefining (e.g., copper), and electroplating (e.g., silver and gold). The lead-acid storage cell, when it is being "recharged," is an electrolytic cell [85].

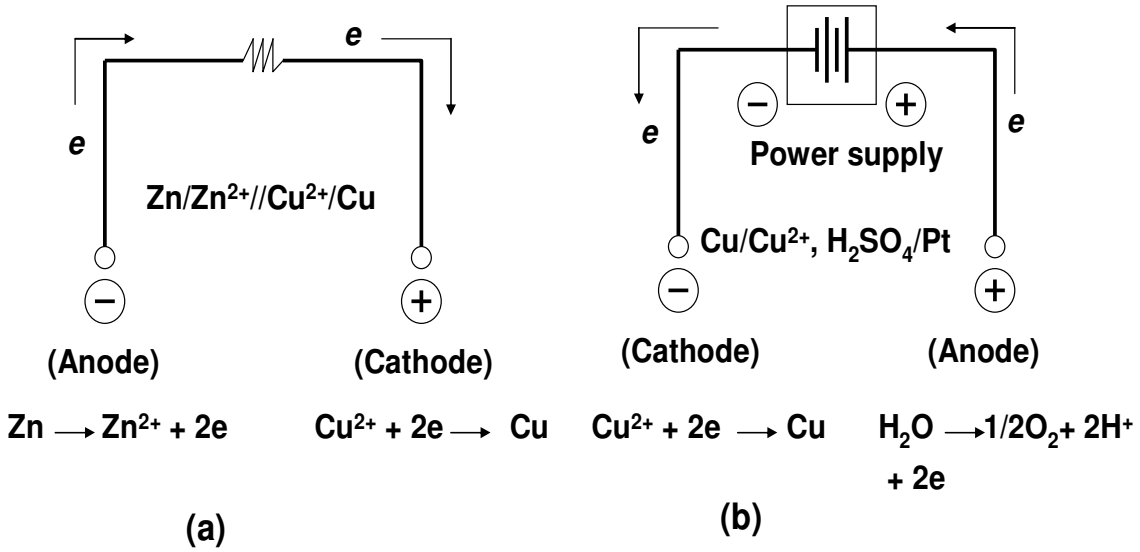

Figure 1.3: (a) Galvanic and (b) electrolytic cells [85].

1.2.1.6 Mass transport processes

In an electrochemical cell, mass transport is a process which governs the net movement of ions, charge or neutral species across the electrode-electrolyte interface. It is considered as mass transfer of an electroactive species in an electrolyte near the electrode. The

mass transport process can be in form of **diffusion, migration** or **convection**. The three mass transport processes are summarised in Figure 1.4.

(a) Diffusion

Diffusion is a spontaneous movement under the influence of concentration gradient, that is, the process in which there is movement of a substance from an area of high concentration of that substance to an area of lower concentration, aimed at minimising concentration differences [86]. If the potential at an electrode oxidizes or reduces an analyte, its concentration at the electrode surface will be lowered, and therefore, more analyte moves to the electrode from the bulk of the solution, which makes it the main current-limiting factor in voltammetric process.

Although migration carries the current in the bulk solution during electrolysis, diffusion should also be considered because, as the reagent is consumed or the product is formed at the electrode, concentration gradient between the vicinity of the electrodes and the electroactive species arise. Under some circumstances, the flux of electroactive species to the electrode is due almost completely to diffusion.

(b) Migration

Migration is the type of charge transport involving movement of charged particles along an electrical field (i.e., the charge is carried through the solution by ions according to their transference number [86]. Controlled-potential experiments require a supporting electrolyte to decrease the resistance of a solution and eliminate electromigration effects to maintain a constant ionic strength. To eleiminate or suppress electromigration, addition of excess or large concentration of inert salt such as KCl is used this work. In analytical applications, the presence of a high concentration of

supporting electrolyte which is hundred times higher than the concentration of electroactive ions means that the contribution of examined ions to the migrational transport is less than one percent.

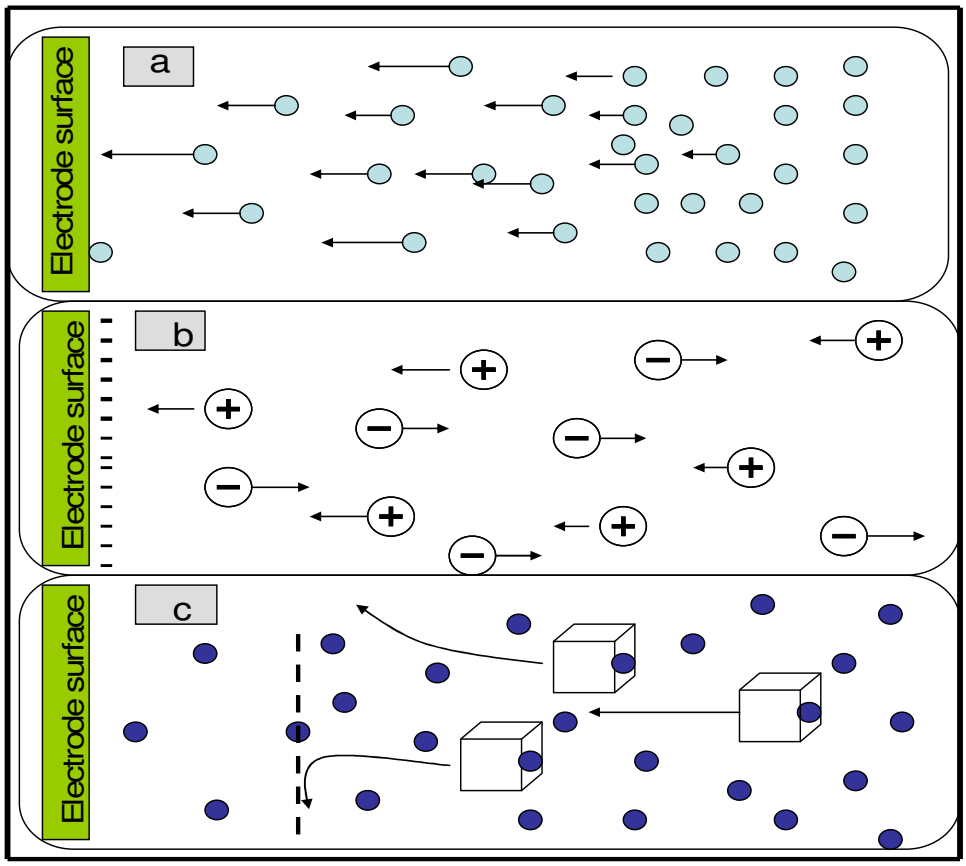

Figure 1.4: The three modes of mass transport process: (a) Diffusion, (b) Migration and (c) Convection [86].

Then it can be assumed that the transport of the examined species towards the working electrode is by diffusion only. Migration of electroactive species can either enhance or diminish the current flowing at the electrode during reduction or oxidation of cations. It helps reduce the electrical field by increasing the solution conductivity, and serves to decrease or eliminate sample matrix effects. The supporting electrolyte ensures that the double layer remains thin with respect to the diffusion layer, and it establishes a uniform ionic strength throughout the solution. However, measuring the current under mixed migration-diffusion conditions may be an

advantage in particular electrochemical and electroanalytical situation.

(c) Convection

It is the transport of charges to the electrode by a gross physical movement; such as fluid flow occurs by stirring or flowing the solution and by rotating or vibrating the electrode (i.e., forced convection) or because of density gradient (i.e., natural convection) [86]. The effect is eliminated during voltammetry experiment by maintaining the cell under quiet and stable condition.

1.3 Voltammetric Techniques

This section gives a brief overview of the electrochemical techniques employed in this study. Electrochemistry involves the measurement of potential (potentiometry) or current response (voltammetry). This study focused on current measurement (voltammetry) and therefore before the different voltammetry techniques used are discussed, it is imperative to understand the concept of the word **voltammetry**.

Voltammetry is a category of electroanalytical methods used in analytical chemistry and various industrial processes. In voltammetry, information about an analyte is obtained by measuring the current as the potential is varied [87,88]. Voltammetry experiments investigate the half cell reactivity of an analyte. Most experiments control the potential (volts) of an electrode in contact with the analyte while measuring the resulting current (amperes) [85]. To conduct such an experiment requires three electrodes (Figure 1.5). The *working* electrode, which makes contact with the analyte, must apply the desired potential in a controlled way and facilitate the transfer of electrons to and from the analyte. A second electrode acts as the other half of the cell. This second electrode must have a known potential with which to gauge the potential of the working electrode, furthermore it must balance the electrons added or removed by the working electrode. While this is a viable setup, it has a number of shortcomings. Most significantly, it is extremely difficult for an electrode to maintain a constant potential while passing current to counter redox events at the working electrode. To solve this problem, the role of supplying electrons and referencing potential has been divided between two separate electrodes. The *reference* electrode is a half cell with a known reduction potential. Its only role is to act as reference in measuring and controlling the working electrodes potential and at

no point does it pass any current. The *auxiliary* electrode passes all the current needed to balance the current observed at the working electrode. To achieve this current, the *auxiliary* will often swing to extreme potentials at the edges of the solvent window, where it oxidizes or reduces the solvent or supporting electrolyte. These electrodes, the *working*, *reference*, and *auxiliary* make up the modern three electrode system.

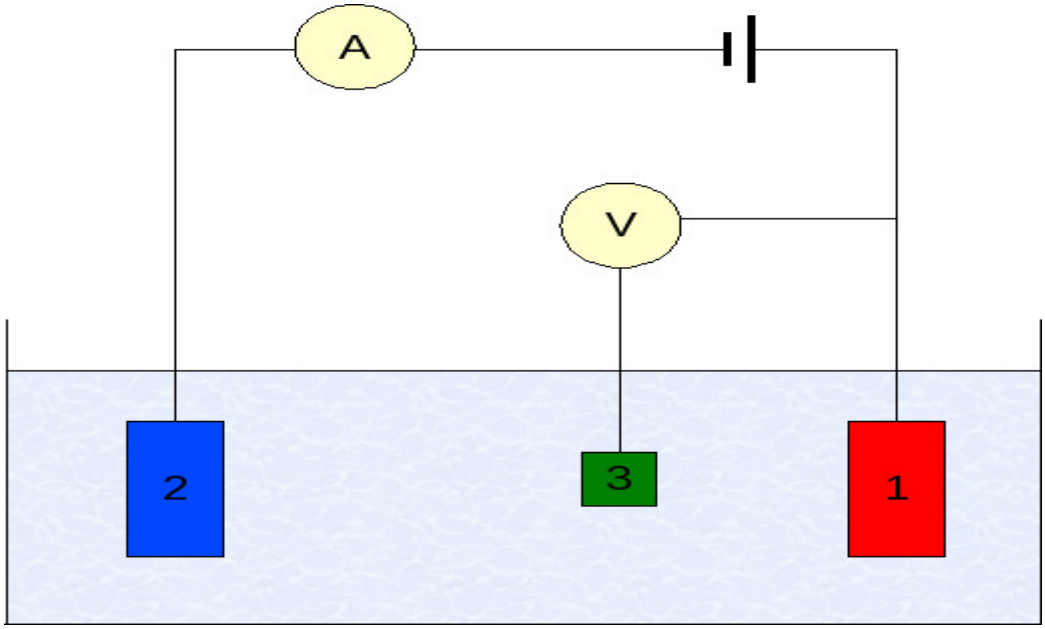

Figure 1.5: Three electrode set-up: (1) working electrode (2) auxillary electrode (3) reference electrode [89].

1.3.1 Types of voltammetry

1.3.1.1 Cyclic voltammetry

Cyclic voltammetry (CV) is the most widely used electrochemical technique. The technique can be used to study electron transfer mechanisms in reactions including providing information on the reversibility, kinetics, and formal reduction and oxidation potentials of a system [85]. The CV experimental set-up consist of a working electrode which can be gold, platinum, glassy carbon etc., a reference electrode against, which the potential is measured against and can be standard calomel electrode (SCE) or

silver|silver chloride (Ag|AgCl) and counter electrodes such as platinum wire can be used. During the CV experiment, the solution is kept stationary and is therefore not stirred in order to avoid movement of ions to the electrode surface by mechanical means.

In a cyclic voltammetry experiment, the potential of an electrode is cycled from a starting potential, E_i to a final potential, E_f (the potential is also called the switching potential) and then back to E_i, (Figure 1.6). The potential at which the peak current occurs is known as the peak potential, E_p. At this potential, the redox species has been depleted at the electrode surface and the current is diffusion limited. The magnitude of the Faradaic current, I_{pa} (anodic peak current) or I_{pc} (cathodic peak current), is an indication of the rate at which electrons are being transferred between the redox species and the electrode. The electron transfer process during cyclic voltammetry experiment can be classified as follows: (i) reversible process (ii) irreversible process and (iii) quasi-reversible process.

A **reversible process** obeys the Nernst reaction in which the electron transfer is rapid, allowing the assumption that the concentration of both the oxidized (O) and the reduced species (R) are in a state of equilibrium (Equation 1.4). Figure 1.6 shows a typical CV for a reversible process. The electroactive species are stable and so the magnitudes of I_{pc} and I_{pa} are equal and they are proportional to the concentrations of the active species. ΔE (E_{pa}-E_{pc}) should be independent of the scan rate, ν but in practice ΔE slightly increases with ν, this is due to the solution resistance, R_s between the reference and working electrodes [90].

$$\mathbf{O} + ne^- \rightleftharpoons \mathbf{R} \qquad (1.4)$$

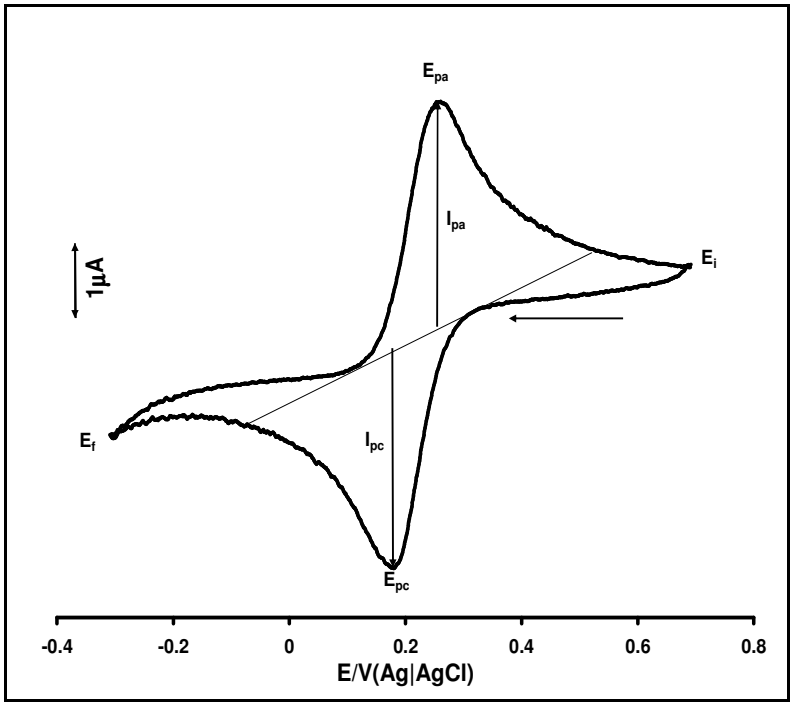

Figure 1.6: Typical cyclic voltammogram for a reversible process.

For a reversible process, the half-wave potential ($E_{1/2}$) equals the formal potential ($E^{o'}$) and are related to the standard potential (E^{o}) as follows (Equation 1.5):

$$E_{1/2} = E^{o'} = E^{o} + \frac{RT}{2F}\ln\frac{[O]}{[R]} \qquad (1.5)$$

where R = gas constant, T = temperature (K), F = Faraday's constant (96485 $Cmol^{-1}$), [**O**] = concentration of oxidized species (mol L^{-1}), [**R**] = concentration of reduced species (mol L^{-1})
The formal redox potential, $E^{o'}$ can be calculated from Equation 1.6:

$$E^{o'} = \frac{E_{pa} + E_{pc}}{2} \qquad (1.6)$$

where E_{pa} = anodic peak potential, E_{pc} = cathodic peak potential

The number of electron transferred in a reversible process can be calculated from Equation 1.7:

$$\Delta E = E_{pc} - E_{pa} = \frac{RT}{nF} \qquad (1.7)$$

At 25 °C, $\Delta E = \frac{0.059V}{n}$ (1.8)

where n = number of electrons transferred, other symbols as in Equation 1.5. At 25°C, the peak current of a reversible process is given by the Randles-Sevcik Equation, 1.9

$$I_p = (2.69x10^5)n^{3/2}[O]A(D\nu)^{1/2} \qquad (1.9)$$

where I_p = peak current (A), A = electrode area (cm^{-2}), D = diffusion coefficient ($cm^2\ s^{-1}$), ν= scan rate ($V\ s^{-1}$).
Using the Randles-Sevcik Equation (1.9), a linear plot of I_p vs. $\nu^{1/2}$ is obtained for a planar diffusion [91,92] to the electrode surface. Deviation from linearity indicates the presence of chemical reaction involving either the oxidized, reduced or both species.

For an **irreversible process**, only forward oxidation or reduction peak is observed but at times with a weak reverse peak, Figure 1.7. This process is usually due to slow electron exchange or slow chemical reactions at the electrode surface [93]. Nernst equation is not applicable in this case since the rate of electron transfer is insufficient to maintain surface equilibrium and thus the oxidized [O] and reduced [R] species are not at equilibrium. The peak current, I_p for irreversible process is given by Equation 1.10.

$$I_p=(2.99x10^5)n[(1-\alpha)n]^{1/2}AC(D\nu)^{½} \qquad (1.10)$$

where α is the rate of electron transfer, C is the concentration of the active species in mol cm^{-3} and the other symbols already defined under Equation 1.9. For a totally irreversible system, ΔE_p is calculated from Equation 1.11:

$$\Delta E_p = E^{o'} - RT/\alpha nF[0.78 - In(k^o/D^{1/2})In(\alpha nF\nu/RT)^{1/2}] \qquad (1.11)$$

k^o = heterogeneous electron transfer constant (cms^{-1}). The rest of the symbols are as in above and they are listed in the Table of symbols.

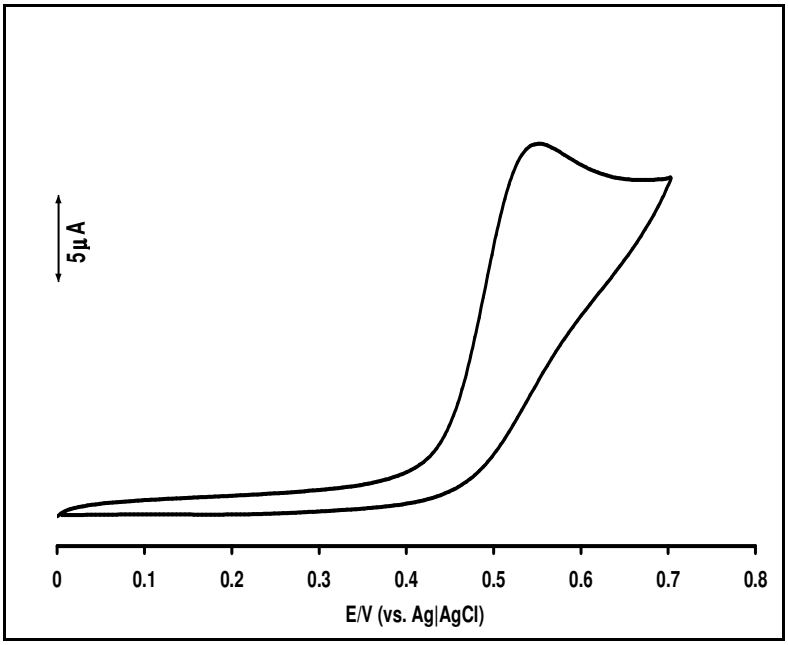

Figure 1.7: Typical Cyclic voltammogram for an irreversible process.

Quasi-reversible process is intermediate between reversible and irreversible systems. The current due to quasi-reversible processes is controlled by both mass transport and charge transfer kinetics [86,94]. The process occurs when the relative rate of electron transfer with respect to that of mass transport is insufficient to maintain Nernst equilibrium at the electrode surface. For quasi-reversible process, I_p increases with

$u^{1/2}$ but not in a linear relationship and ΔE > 59/n mV increases with increasing u.

1.3.1.2 Square wave voltammetry

Exceptional versatility is found in a method called *square wave voltammetry* (SWV), which was invented by Ramaley and Krause [95], but has been developed extensively in recent years by the Osteryoungs and their coworkers [96,97]. This is a differential technique in which potential waveform composed of a symmetrical square wave of constant amplitude superimposed on a base staircase potential (Figure 1.8) [85,86,98]. It is the plot of the difference in the current measured in forward (i_f) and reverse cycle (i_r), plotted against the average potential of each waveform cycle. In this technique, the peak potential occurs at the $E_{1/2}$ of the redox couple because the current function is symmetrical around the potential [96,99].

The scan rate of a square wave voltammetry experiment is given by the Equation 1.12:

$$\nu = f.\Delta E_s \qquad (1.12)$$

Where f is the frequency (Hz) and ΔE_s is the potential size. The main advantages of SWV are excellent peak separation, high sensitivity and ability to eliminate capacitive charging current compared with cyclic voltammetry or the differential pulse voltammetry.

1.3.1.3 Linear sweep voltammetry (LSV)

Linear sweep voltammetry (LSV) is a voltammetric method where the current at a working electrode is measured while the potential between the working electrode and a reference electrode is swept linearly in time (Figure 1.9). Oxidation or reduction of

species is registered as a peak or trough in the current signal at the potential at which the species begins to be oxidized or reduced [85]

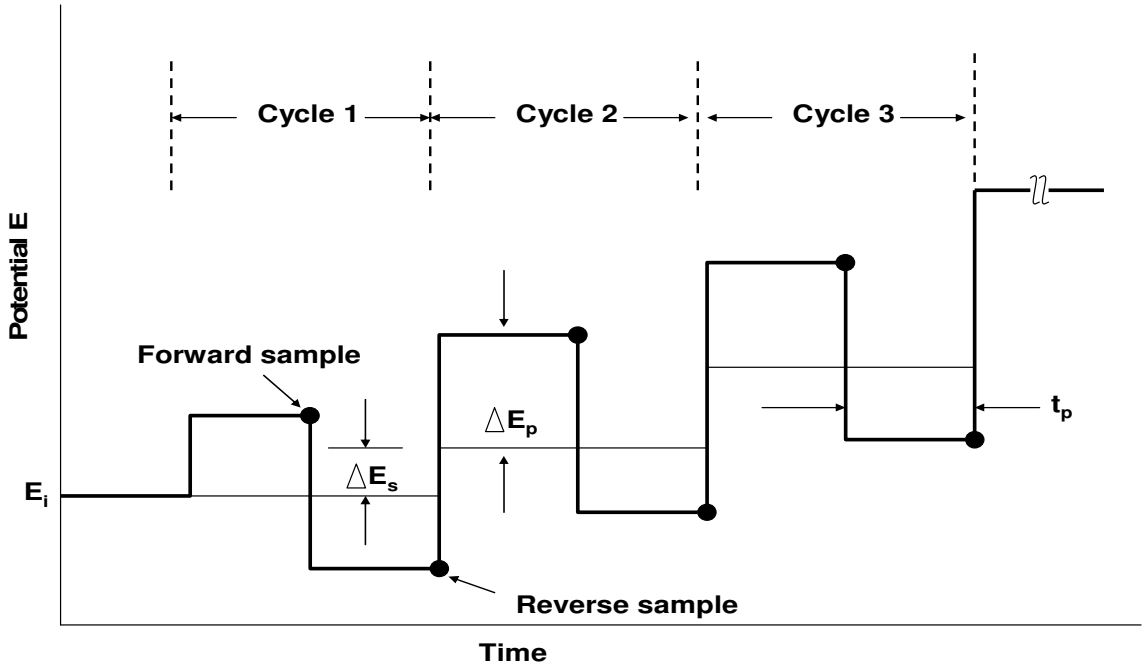

Figure 1.8: Waveform and measurement scheme for square wave voltammetry. Shown in bold is the actual potential waveform applied to the working electrode. The light intervening lines indicate the underlying staircase onto which the square wave can be regarded as having been superimposed. In each cycle, a forward current sample is taken at the time indicated by the solid dot, and a reverse current sample is taken at the time marked by the shaded dot [85].

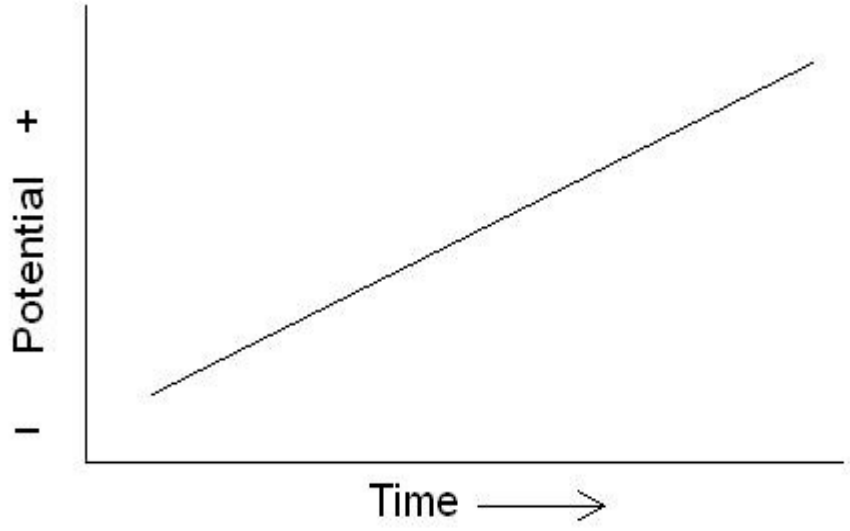

Figure 1.9: Linear potential sweep

1.3.1.4 Rotating disk electrode

The *rotating disk electrode* (RDE) provides an efficient and reproducible mass transport, and hence the analytical measurement can be made with high sensitivity and precision. The convective nature of the electrode results in very short response time [86]. The detection limits of the electrode can be lowered via periodic changes in the rotation speed, and isolation of small mass-transport-dependent currents from simultaneously flowing surface-controlled background currents. The electrode consists of a disk imbedded in a rod of an insulating material. The rod is attached to a motor directly by a chuck or by a flexible rotating shaft or pulley arrangement and is rotated at a certain frequency, / (revolutions per second). The more useful descriptor of rotation rate is the angular velocity, ω (s^{-1}), where $\omega = 2\pi rf$. Electrical connection is made to the electrode by means of a brush contact. During experiment, the current flux of the analyte is induced towards the electrode. The limiting current (for a reversible system) is thus proportional to the square root of the angular velocity by the *Levich equation* (Equation 1.13):

$$i_{l,c} = 0.62nFAD_0^{2/3}\omega^{1/2}\nu^{-1/6}C_0 \qquad (1.13)$$

where $i_{l,c}$ is the diffusion-limited currents, *n* is the number of electrons transferred, and other symbols are defined above and are listed on the list of symbols.

1.3.1.5 Chronoamperometry

It is an electrochemical technique in which the potential of the working electrode is stepped, and the resulting current from faradic processes occurring at the electrode (caused by the potential step) is monitored as a function of time (Figure 1.10). In the waveform

(Figure 1.10), the current response followed the working electrode potential being stepped from an initial potential at which the oxidized (reduced) species is stable in solution, to the first step potential where a redox reactions occurred forming the reduced (oxidized) species and held at this value for the time duration (for a single potential experiment) or stepped to a second potential where it is held for the duration of the second step time.

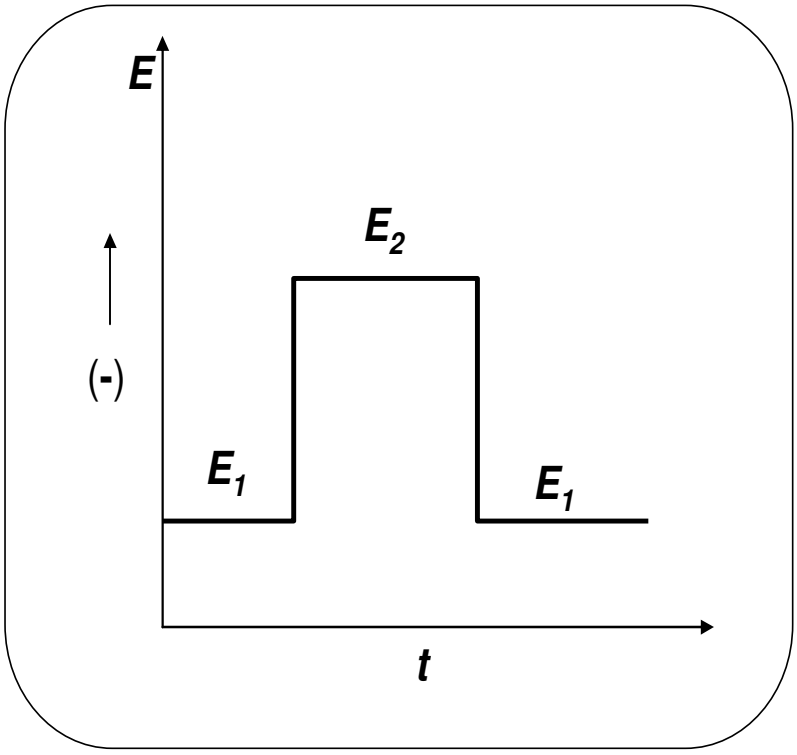

Figure 1.10: Typical waveform for a double potential step chronoamperometry [85].

Limited information about the identity of the electrolyzed species can be obtained from the ratio of the peak oxidation current versus the peak reduction current. However, as with all pulsed techniques, chronoamperometry generates high charging currents, which in this case, decay exponentially with time. To measure the faradic current (the current that is proportional to the concentration of the analyte), current in the last 70-80% of each scan is integrated (when charging current has dissipated). Most commonly

investigated with a three electrode system. Since the current is integrated over relatively longer time intervals, chronoamperometry gives a better signal to noise ratio in comparison to other amperometric technique [85,87]. For a current-time dependent relationship (Cottrell equation; Equation 1.14) for a linear diffusion controlled process [85,86], the diffusion coefficient (D) can be estimated from the slope of the plot of I versus $t^{-1/2}$.

$$I = \frac{nFAD^{1/2}C}{\pi^{1/2}t^{1/2}} \qquad (1.14)$$

All symbols are as in above and they are listed in the list of symbols. Also using the relationship in Equation 1.15 [85,86] where I_{cat} and I_{buff} are the currents in the presence and absence of analyte, respectively; C is the analyte bulk concentration, k is the catalytic rate constant ($M^{-1}s^{-1}$) and t is the elapsed time (s), the catalytic rate constant K can be obtained from the plots of I_{cat}/I_{buff} vs. $t^{1/2}$.

$$\frac{I_{cat}}{I_{buff}} = \pi^{1/2}(kCt)^{1/2} \qquad (1.15)$$

1.3.1.6 Galvanostatic charge discharge technique

This is an electrochemical measuring technique for electrochemical analysis or for the determination of the kinetics and mechanism of electrode reactions based on the control of the current flowing through the system. The method consists of placing a constant current pulse upon an electrode and measuring the variation of the resulting current through the solution. This is called the galvanostatic method for measuring the rate of an electrochemical reaction. The potentiostatic is constituted by

applying a potential pulse while observing the variation of the rate as a function of time (Figure 1.11). The technique is usually used to investigate the charging and the discharging process of electrochemical capacitors [100,101].

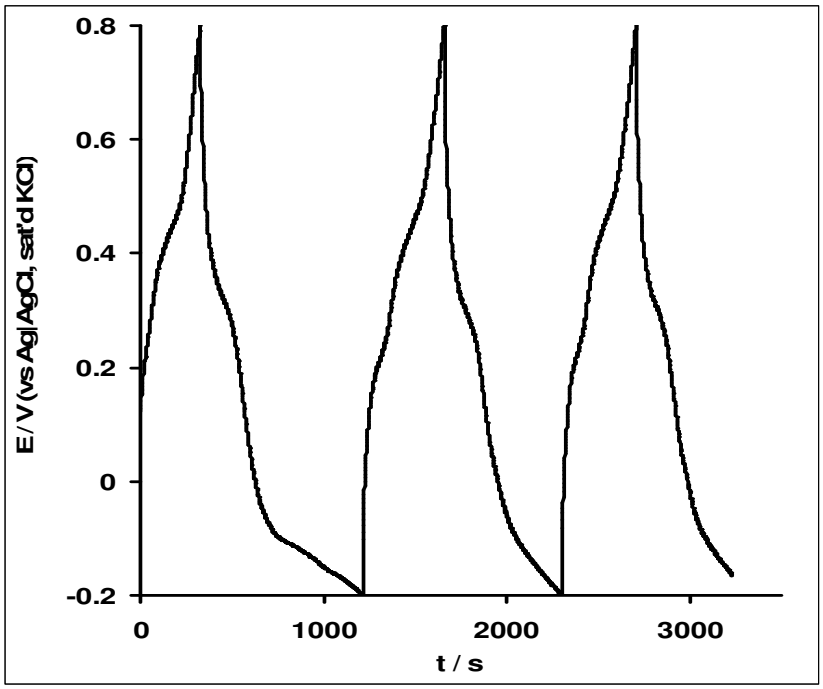

Figure 1.11: Typical galvanostatic charge-discharge curve.

1.3.1.7 Electrocatalysis using voltammetry

The electrocatalysis process studied in this project using the voltammetric techniques already discussed above mainly involves electron transfer between the analyte and the electrode surface. The mechanism involve is briefly described in scheme 1.1. In this work, the catalyst (M or MO) on the CNT platforms become oxidized in the electrolyte. The oxidized catalyst interacts with the analyte which are mostly in their reduced state. Electron transfer process takes place leading to the oxidation of the analyte while at the same tme; the catalyst is simultaneously reduced and regenerated for further catalysis.

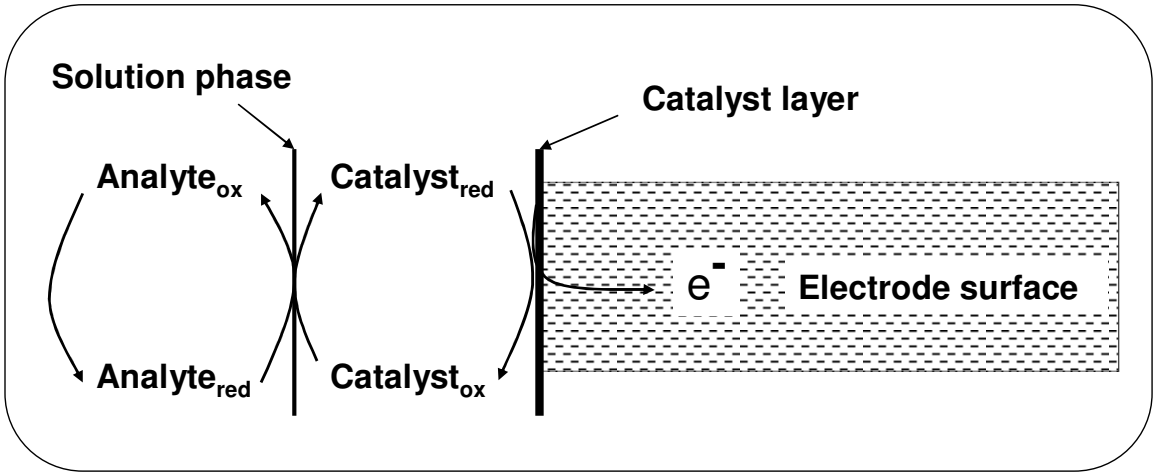

Scheme 1.1: Schematic diagram showing electrocatalytic process at modified electrode [86].

1.4 Electrochemical Impedance Spectroscopy (EIS)

Electrochemical impedance spectroscopy (EIS) is a relatively new and powerful method of characterizing many of the electrical properties of materials and their interfaces with electronically conducting electrodes. It may be used to investigate the dynamics of bound or mobile charge in the bulk or interfacial regions of any kind of solid or liquid material: ionic, semiconducting, mixed electronic–ionic and even insulators (dielectrics) [102]. It is also used to explore the properties of porous electrodes, and for investigating passive surfaces [103]. EIS technique has been shown to be effective for probing the redox and structural features of a surface-confined species [104]. Other advantages include: (i) rapid acquisition of data such as ohmic resistance, capacitance, inductance, film conductivity, as well as charge or electron transfer at the electrode-film interface, (ii) the ability to obtain accurate, reproducible measurement, (iii) the capacity of the system to remain at equilibrium due to use of low amplitude-sinusoidal voltage (~ 5 mV), (iv) capability to adapt for various applications and (v) characterize interfacial properties in the absence of redox reactions.

1.4.1 Basics of impedance spectroscopy

Impedance is measured by applying a sinusoidal potential *V (t)*, of small amplitude to an electrochemical cell and measuring resultant sinusoidal current *I (t)*, through the cell [105-108]. The applied sinuisodal potential and current are represented as a function of time. These measurements are done over a suitable frequency range and the results can be related to the physical and chemical properties of the material [105-108]. The relationship is shown in Equation 1.16:

$$Z = \frac{V(t)}{I(t)} \qquad (1.16)$$

where $V(t)$ is the sinusoidal applied voltage at time t, $V(t) = V_o \sin \omega t$ where V_0 is the maximum potential applitude, ω is the radial frequency (in rad.s^{-1}) and can be related to frequency f *(Hz)* as $\omega = 2\pi f$. At the same frequency as the applied sinusoidal potential, the current response $I(t)$ is also sinusoidal but with a shift in phase, $I(t) = I_o \sin(\omega + \theta)$, where I_o is the maximum current applied and θ is the phase shift by which the voltage lags the current (Figure 1.12a) [105]. Therefore, impedance is a vector quantity where the quantity $Z = V/I$ represents the magnitude and θ represent the direction (Figure 1.12b). The complex notation of impedance is shown in Equation 1.17.

$$Z = Z' + jZ'' = Z_{real} + jZ_{imaginary}. \qquad (1.17)$$

where Z' and Z'' are the real and imaginary parts of the impedance respectively and j is a complex number [105].

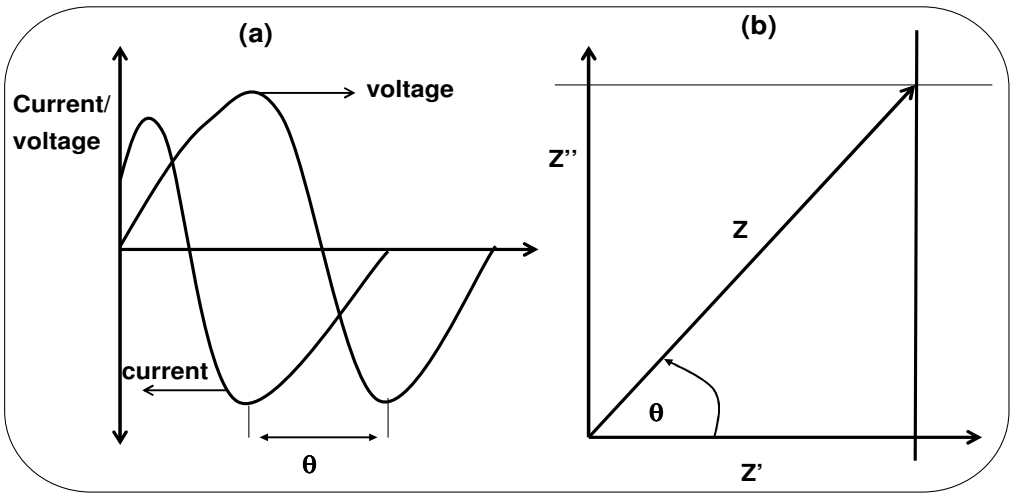

Figure 1.12: (a) Applied sinusoidal voltage and resulting sinusoidal current response. (b) Vector representation of real Z' and imaginary Z'' of impedance Z [105].

1.4.2 Application and data presentation

Impedance measurements include both the electrical resistance and resistance due to morphological state of the materials. EIS has been used to monitor the whole procedure in preparing modified electrodes, which could provide useful information for each step and be used for probing the changes of the surface modification. The impedance data are fitted to an equivalent circuit using the FRA software package for complex non-linear least squares calculations based on the EQUIVCRT programme. Simple electrical elements such as resistors and capacitors in the circuit measure resistance and capacitance respectively during the electrochemical process [102-105,108-111]. The resistance in the circuit is an indication of the electrical conductivity of the electrolyte and the constant phase element (*CPE*) results from the charge which is in excess at the electrode-electrolyte interface. Ideal Randles equivalent circuit involves double layer (C_{dl}) (Figure 1.13a). It incorporates various contributions to the interfacial barrier behaviour; these factors are the resistance of electrolyte (R_s), the charge transfer resistance (R_{ct}), double-layer capacitance (C_{dl}) and Warburg impedance (Z_w). Modified Randles circuit uses *CPE* in place of C_{dl} as illustrated in Figure 1.13b. The impedance of *CPE* is defined as

$$Z_{CPE} = \frac{1}{[Q(j\omega)^n]} \qquad (1.18)$$

where Q is the frequency-independent constant relating to the surface electroactive properties, ω is the radial frequency, the exponent n arises from the slope of log Z vs log f (and has values $-1 \leq n \leq 1$). If $n = 0$, the CPE behaves as a pure resistor; $n = 1$, *CPE* behaves as a pure capacitor, $n = -1$, *CPE* behaves as an

inductor; while n = 0.5 corresponds to Warburg impedance (Z_w) which is associated with the domain of mass transport control arising from the diffusion of ions to and from the electrode|solution interface. Generally speaking, *CPE* has been known to occur via several factors notably (i) the nature of the electrode (e.g., roughness and polycrystallinity), (ii) distribution of the relaxation times due to heterogeneities existing at the electrode/electrolyte interface, (iii) porosity and (iv) dynamic disorder associated with diffusion [112]. Most times, *CPE* represents the real and practical situations experienced during electrochemical impedance experiment as compared to C_{dl}.

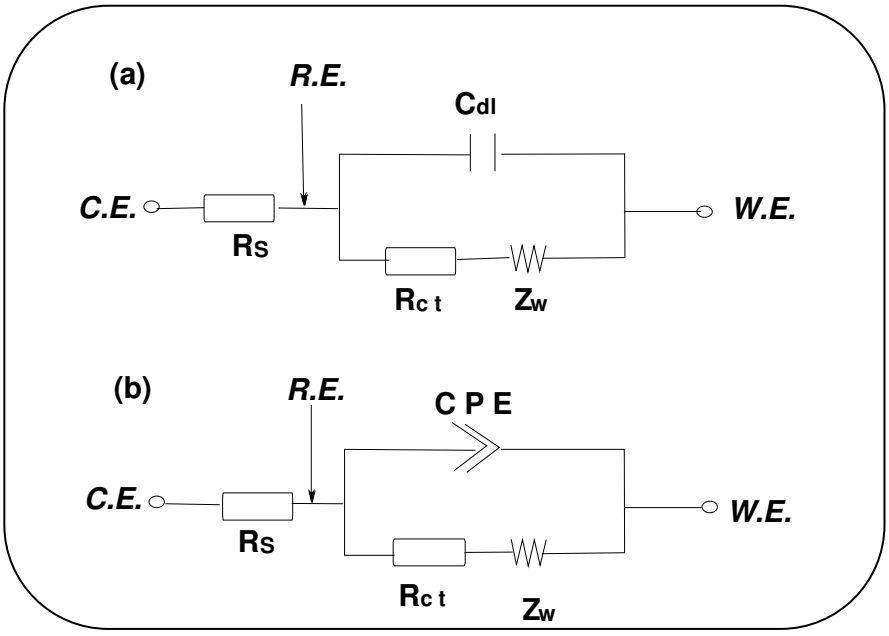

Figure 1.13: (a) Typical Randles equivalent circuit for an ideal electrochemical system. (b) Modified Randles equivalent circuit for real, practical situation.

Apart from the normal and modified Randles circuit, several other circuit models have been used in the fitting of the impedance data in this study. Some include an inductance (L). Inductive behaviour takes place when the Faradaic current is governed by the occupation of an intermediate state [113-115]. The inductive behaviour can be attributed to factors such (1) instrumental

artefacts, or (2) the inductance of the electrode, or (3) the inductance of the connecting wires [116]. The curve obtained from the impedance fitting is called the Nyquist plot, which is imaginary impedance versus the real impedance ($-Z_{\text{imaginary}}$ versus Z_{real}) (Figure 1.14a). It includes a semicircular part and a linear part. The semicircular part at higher frequencies corresponds to the electron-transfer-limited process and its diameter is equal to the electron transfer resistance (R_{ct}), which controls the electron transfer kinetics of the redox probe at the electrode interface. Meanwhile, the linear part at lower frequencies corresponds to the diffusion process.

All the obtained spectra were first subjected to the Kramaers-Kronig (K-K) test. The main essence of the K-K test is simply to check whether the measured impedance spectra comply with the assumptions of the well known K-K transformation, viz (i) that the impedimetric response is only related to the excitation signal; (ii) that the impedimetric response is linear (or the perturbation is small, e.g., <10mV, for non-linear systems; (iii) that the system does not change with time, say due to ageing, temperature changes, non-equilibrium conditions, etc; and (iv) that the system is finite for all values of ω, including zero and infinity [117,118]. Failure of the K-K test, signified by a large value of pseudo χ^2 is usually an indication that no good fit can be obtained using the electrical equivalent circuits' methods. It should be noted that aside from visual inspection of goodness of the fitting lines, two accurate ways to establish how well the modeling functions reproduce the experimental data sets are the relative error estimates (in %) and chi-square functions (χ^2) [119], which is the sum of squares of the relative residuals (i.e., sum of the real and imaginary χ^2), easily obtained from the K-K test.

Generally, a bare electrode should exhibit an almost straight line for the Nyquist plot (Figure 1.14a) because electrochemical

reactions at such electrode surfaces are expected to be mass diffusional limiting electron-transfer processes [102-105,117]. For a modified electrode, the Nyquist plot shows characteristic semi-circle pattern due to barrier to the interfacial electron transfer (Figure 1.14b). The interfacial barrier behaviour has been described by Randles equivalent circuit (Figure 1.13a). The R_{ct} value is influenced by the film thickness and the nature of the films on the electrodes. The R_{ct} is the domain of kinetic control and it is proportionally related to the diameter of the semi-circle of the Nyquist plot. In some systems the reaction rate might be controlled by transport phenomenon and this effect needs to be taken into consideration. The measured impedance can be explained based on its relationship with the Warburg impedance (Z_w) as described above.

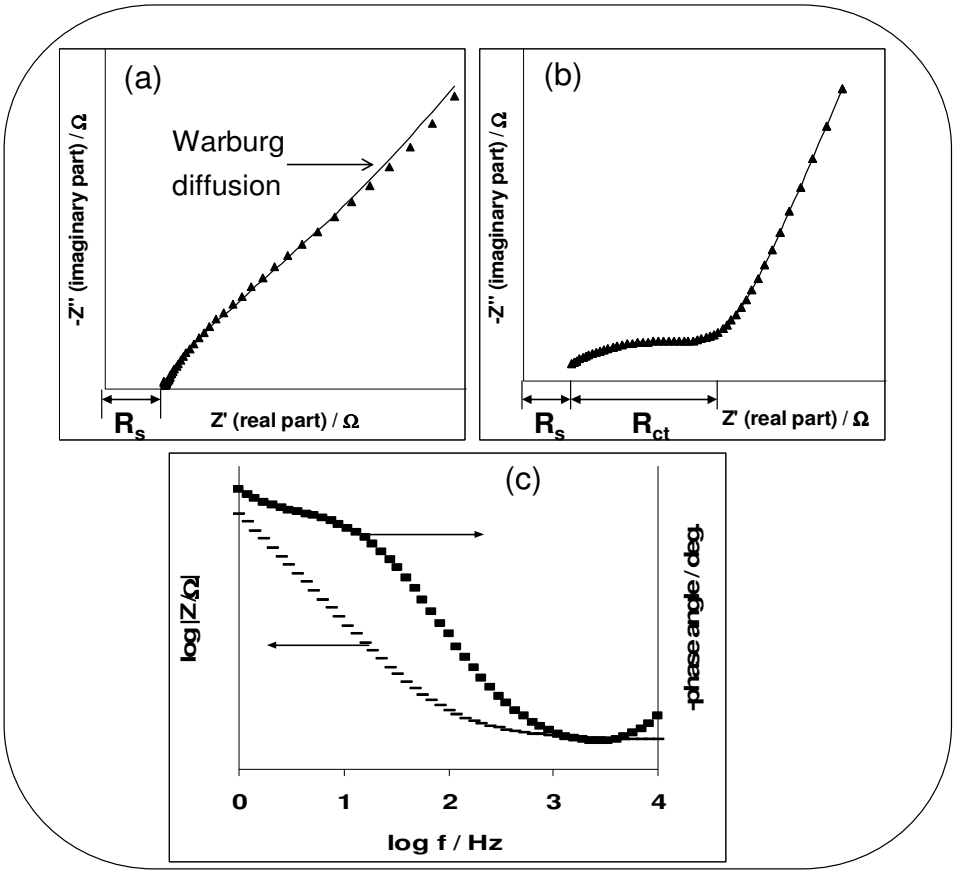

Figure 1.14: Typical Nyquist plot for (a) bare and (b) modified electrode. (c) is the corresponding Bode plots.

Another important plot obtained from the EIS experiment is the Bode plots (Figure 1.14c) [102-105,117]. Bode plots is the plot of phase angle (θ) versus the logarithm of the frequency (log *f*), or the logarithm of impedance magnitude (log *Z*) versus the logarithm of the frequency (log *f*). The plot provides information about the capacitive properties of a modified electrode. From the plot phase angle (θ) versus log *f*, the peak height represented the capacitive nature of the electrode while the phase angle and the frequency values gives an idea of the relaxation process of the electrode|solution interface. Slope obtained from the plot of log *Z* versus log f also described the capacitive behaviour of the system. An ideal capacitive behaviour requires a phase angle of 90^0 and a slope value of – 1.0.

1.5 Chemically Modified Electrodes

A chemically modified electrode (CME) is an electrode surface coated with a thin film of selected conducting materials for the purpose of improving the chemical, electrochemical, optical, electrica, and electron transfer properties of the film in a rational, chemically designed manner [120].

The desired redox reaction at the bare electrode using voltammetric techniques such as CV and SWV often involves slow transfer kinetics and therefore occurs only at an appreciable rate only at potential substantially higher than its thermodynamic redox potential. Such reactions can be catalysed by attaching to the surface a suitable electron-transfer mediator. The function of the mediator is to fascilitate the charge transfer between the analyte and the electrode. In most cases, the mediated reaction sequence (e.g. for a reduction process) can be described by equations below.

$$M_{ox} + ne^- \longrightarrow M_{red} \qquad (1.19)$$

$$M_{red} + A_{ox} \longrightarrow M_{ox} + A_{red} \qquad (1.20)$$

where M represents the mediator and A the analyte. Hence, the electron transfer takes place between the electrode and mediator and not directly between the electrode and analyte. The net results of this electron shuttling are a lowering of the over-voltage to the formal potential of the mediator and an increase in current density. The efficiency of the electrocatalytic process depends also upon the actual distance between the bound redox site and the surface (since electron-transfer rate decreases exponentially when the electron-tunneling distance is increased).

For the determination of surface concentration of the electroactive material, Equation (1.21) or Equation (1.22) for a surface confined species was employed, where I_p (μA) is directly proportional to the scan rate, ν (Vs^{-1}) [84-86].

$$\Gamma = \frac{Q}{nFA} \tag{1.21}$$

$$I_p = \frac{n^2 F^2 A \Gamma \nu}{4RT} \tag{1.22}$$

where Γ = total surface coverage by electroactive species Q = quantity of charge in coulombs, the rest of the symbols have their usual meaning.

1.5.1 Carbon Electrodes

Carbon electrodes (such as the glassy carbon, carbon paste, highly oriented pyrolytic graphites, basal plane pyrolytic graphite and edge plane pyrolytic graphites electrodes) have long been recognised as versatile and supporting platforms for electrocatalysis and electrochemical sensing due to their numerous advantages such as low cost, chemical inertness and wide potential window in most electrolyte solutions over the precious metal electrodes (e.g gold, platinum, aluminium, silver copper). Among this carbon based electrodes, edged plane pyrolytic graphite electrode (EPPGE) have been reported to have a better catalytic and reactivity which is solely due to edge plane sites/defects (Figure 1.15) which are the key to fast heterogeneous charge transfer [121].

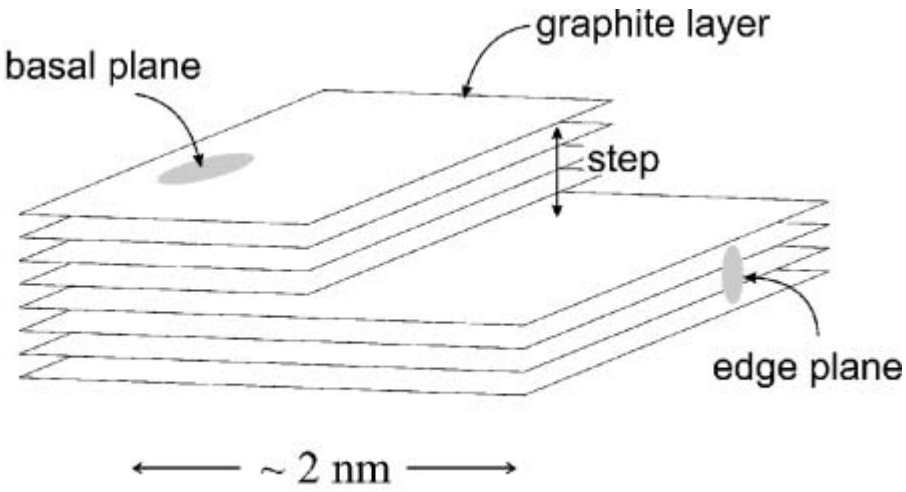

Figure 1.15: Pyrolytic graphite plate showing the basal and the edge plane sites [121].

For example, the electrochemical oxidation of homosteine in 0.1 M phosphate buffer solution was studied at boron-doped diamond (BDD), glassy carbon (GC), EPPG and BPPG electrodes and a CNT film modified BPPG electrode. While no appreciable oxidation waves seen in the potential range studied for the other electrodes, the EPPG electrode exhibited a large and easily quantifiable signature at *ca* + 0.66 V (*vs.* SCE) demonstrating a significant reduction in the overpotential in comparison with the other commonly used electrode substrate while also exhibiting an enhanced signal-to-noise ratio [122]. EPPG electrode has also been explored for the detection of nitrogen dioxide. Its response was compared with that of BDD, BPPG and GC electrodes. For the three later electrodes, no Faradaic waves were observed in contrast to the well-defined signal seen at the EPPG electrode [123]. Other application of EPPG electrode includes the detection of NADH [124], chlorine [125], halides [126], ascorbic acid [127], cathodic stripping voltammetry of manganese [128] and anodic stripping voltammetry of silver [129]. This outstanding property of EPPG electrode over other carbon based electrodes has made it the best choice for the studies reported in this work. It is well known that

the slow electron transfer behaviour at the bare electrode can be improved upon by surface modification with electron transfer mediators such as CNTs and redox active metal catalyst. These surface modifiers substantially enhance the electrochemical response at the bare electrode.

1.5.2 Carbon nanotubes modified electrodes

Carbon nanotubes occur in two main types: single-walled carbon nanotubes (SWCNTs) which consist of single rolled-up graphite sheet or single graphite tube with a diameter of approximately 1 nm and multi-walled carbon nanotubes (MWCNTs), which consist of several sheets of graphites rolled into concentric tubes with various lengths and diameters [130].

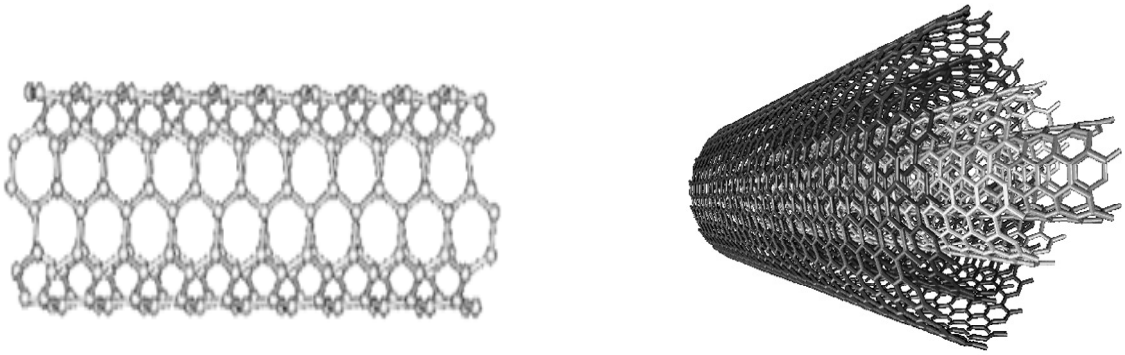

(a) (b)

Figure 1.16: Structure of (a) SWCNT and (b) MWCNT.

Carbon nanotubes are generated by arc evaporation [131], laser ablation [132], pyrolysis [133], and electronic methods [134]. Ijima and co-workers also showed that the synthetic yield of SWCNT preparation can be improved by adding cobalt or other transition metals such as nickel, iron, and molybdenum, with the graphite in the arc vaporisation process [135]. Properties of CNTs

have been widely investigated and SWCNTs possess important mechanical, thermal, photochemical and electrical properties [136] which are industrially useful. MWCNTs contain several SWCNTs in their structure and, therefore, possibly have analogous physicochemical properties to those corresponding to SWCNTs. These nanomaterials are robust and stiff but flexible and they have been reported as the strongest of all the synthetic fibres [136]. Materials containing CNTs may, however, be strong enough to build spacecrafts, space elevators, artificial muscles, and land and sea vehicles [136]. SWCNTs can conduct twice the electricity of copper, making these materials excellent electrical conductors, and may also be used to improve rechargeable batteries and fuel cell production [136]. Its presence on the surface of bare electrodes such as glassy carbon [137], graphite [138], carbon fiber [139], gold [140], and platinum (Pt) electrodes [141] has enhanced their electrical properties tremendously.

Several authors have reported the excellent electrocatalytic properties of nanotubes in the redox behaviour of different molecules and bio-molecules. There are reports on the advantages of CNTs modified electrodes on the electrocatalytic response of hydrazine [142], glucose [143], dihydronicotinamide adenine dinucleotide (NADH) [144], dopamine [145], nitric oxide [146], ascorbic acid [147], hydrogen peroxide [148]. Thus CNTs-modified electrodes have shown interesting catalytic properties toward electrochemical processes. Studies have shown that carbon nanotubes provided a large surface for metal deposition on electrodes and thus provided a synergistic relationship for an improve electron transfer between the base electrode and the CNT-M hybrids [16,69]. However, the extent and the mechanism for the electron transfer of the CNT-M or CNT-MO modified electrodes are not clearly understood. Therefore, this study investigated some of this rection mechanism using different electrochemical techniques

and the information provided is discussed in Chapter 3 to 9. It must be noted that electrodes modified with carbon nanotubes have increased surface areas and adsorption efficiency compared to other common electrodes, and exhibit intriguing ability to enhance the electrochemical responses of several organic molecules [149, 150], thus making them more favourable as electrode materials for the type of investigation reported in this work compared to other common electrodes.

1.5.3 Metal and metal oxides nanoparticles

The use of metal nanoparticles for electrode preparation is no longer news in the field of electro-analytical chemistry. Several methods have been developed for making metal and metal oxides nanoparticles: (1) electrodeposition [151], electropolymerisation [152], self-assembled monolayers (SAM) [153], Sol-gel technique [154], photolytic reduction [155], radiolytic reduction [156], sonochemical method [157], solvent extraction reduction [158], microemulsion technique [159], polyol process [160] and alcohol reduction [161]. Some of these methods are employed for electrode modification with the NPS and are discussed later. The synthesis and electrocatalytic behaviour of these important metals and their oxides towards sensing of biological and environmentally important molecules forms the subject of discussion in this thesis.

1.5.4 Electrocatalytic behaviour of carbon nanotubes-metal nanocomposite modified electrodes

Electrochemical detection of biological and environmental analytes using metal and metal oxide modified electrode was found very cheap and convenient over other methods of determination. Not only that, metal and metal oxides have been used to modify

electrodes for use as electrocatalysts and sensors [65,66,162-166]. These materials act as electron mediators, increasing the rate of electron transfer at the electrode-solution interface and also lowering the over-potentials for redox processes. The modification introduces some chemical and electrochemical properties which the bare electrodes do not posses. Electrocatalysis can be observed by comparing the CV of an analyte on modified electrode with that on bare electrodes; higher catalytic current, I_p and a shift to less positive peak potential in the CV of the former compared to the latter is an indication of electrocatalytic oxidation of the analyte. Typical example of electrocatalysis is shown in Figure 1.17.

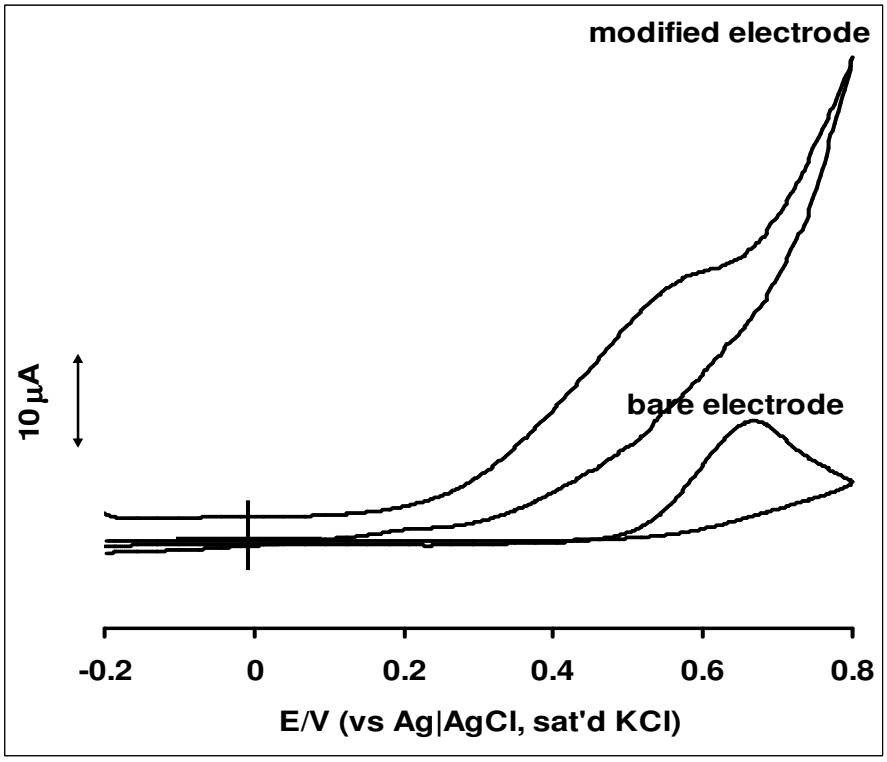

Figure 1.17: Cyclic voltammogram showing electrocatalytic process of an analyte on the bare and modified electrode.

Research on the possible applications of CNTs decorated with metal nanoparticles, particularly nickel, cobalt, and iron is beginning to receive some attention in electrochemistry especially in catalysis, supercapacitor an as an electron transfer mediator on

electrode surface [162-168]. Further to CNT-metal nanoparticles investigated in this work is the decoration of CNT with Prussian blue nanoparticles. Prussian blue (PB) is an iron cyanide complex with the molecular formula $Fe_4(III)[Fe(II)(CN)_6]_3$. It is used as an electron-transfer mediator due to its excellent electrocatalytic properties and has found applications in electrochromic devices [169], nanomagnetic [170], biomedical [171], molecular sieves [172], catalysis [150] and in solid-state batteries [173]. It was reported that electrodes modified with PB nanoparticles demonstrate a significantly decreased background, resulting in improved signal-to-noise ratio [174]. Several methods have been employed for PB preparation [175,176] but PB prepared by chemical deposition was considered to be more stable in a wider pH range [177]. CNT-PB modified electrodes have been used for the detection of many biomolecules including hydrogen peroxide [177], glucose [178], haemoglobin [179], oxygen [180], and NADH [181]. However, to the best of my knowledge, this is the first time the analyte reported in this work will be studied on CNT-PB modified electrode.

1.5.4.1 Nickel and nickel oxide carbon nanotubes modified electrodes

For many decades, nickel was regarded as a potentially toxic element, since its concentration in various foods was higher than that needed for living organisms. More recently, it is now considered a possible essential element for plants, although deficiencies can occur under certain circumstances. Not only that, the element either as pure metal or as nanoparticles has found uses in the area of electrochemistry as sensors for different compounds in food, water and other component of the environment. It is interesting to know that nickel nanoparticles have been used as sensor for both biological and chemical analyte. Pure nickel

electrodes and nickel-coated electrodes find various applications in the field of electroanalytical chemistry. Nickel electrodes can be used for electrochromic devices [182], alkaline batteries [183] and as electrocatalysts [184]. It has been reported that sensor having nickel as its working electrode reduces material cost and affords good long-term stability [185].

There are many literature on the used of nickel modified electrode for the catalysis of many organic and inorganic molecules such as nitrite (NO_2^-) [65,66]; acetaminophen [186]; dopamine [187]; glucose [188]; ethanol [189]; sulphite (SO_3^{2-}) [190]; sulphide (S^{2-}) [191]; chlorate ion (ClO^{4-}) [192]; methanol [193]; insulin [154]; phenol [194]; hydrogen peroxide [195]; ascorbic acid [188]; amino acids [115]; acethycholine [196]; thiocyanate ions [197]; thiosulphite ion [167]; hydrazine [198]; thiols [199] etc. but research reports on the use of nickel or nickel oxide nanoparticles as electrode modifier for the same purpose were very sketchy. However, recently, due to the advent of nanoscience and nanotechnology, some of these molecules are detected using electrode modified with nickel nanoparticles. Applications of nickel and nickel oxide nanoparticles modified electrodes as sensors in electrochemistry include: the electrochemical detection of acetaminophen (ACOP) on the carbon coated nickel magnetic nanoparticles modified glassy carbon electrode (C–Ni/GCE) [186]. The C–Ni/GCE has been applied successfully to the simultaneous determination of ACOP, dopamine (DA) and ascorbic acid (AA) in their mixture [186]. Nanostructured nickel based ethanol sensors have been developed by sputtering technique for ethanol sensing [200] Performance was increased using this technique. Shibli et al. [21] developed electrochemical sensor by electroplating nano nickel oxide reinforced nickel on graphite substrate. The modified electrode showed good sensing performance with a response time as low as 8 s during sensing and estimation of acetylcholine.

Glucose oxidase (GOx) was successfully co-deposited on nickel-oxide (NiO) nanoparticles at a glassy carbon using electrodeposition technique and the biosensor shows excellent electrocatalytical response to the oxidation of glucose with fast amperometric response when ferrocenmethanol was used as an artificial redox mediator [162]. Electrocatalytic oxidation and determination of hydrazine on nickel hexacyanoferrate (NiHCF) nanoparticles-modified carbon ceramic electrode (CCE) have been reported [167]. Electrocatalytic reduction of hydrogen peroxide (H_2O_2) on the self-immobilized cytochrome c on the electrodeposited NiO NPs modified glassy carbon electrode (Cyt c/NiO NPs/GC) has been studied [168].

Catalytic reduction of H_2O_2 on horseradish peroxidase/nickel oxides nanoparticles/glassy carbon (HRP/NiO NPs/GC) electrode had been reported [201]. Other literature reports on the catalytic application of Ni and NiO NPs are summarised in Table 1.1. While most of the modified electrode reported on the Table employed the catalytic activities of Ni and NiO nanopartilces as composite with other materials, the relationship between CNT/M or CNT/MO as simple and cheap electrode materials for catalysis was not given much attention. Thus, this study was basically aim at investigating the effect of the synergistic behaviour of the nanocomposite formed between the M or MO nanoparticles and CNT on the catalysis of some analyte. The effect will be discussed under Chapter 3.

Table 1.1: Electrocatalytic oxidation of some analytes on nickel and nickel oxide modified electrode.

Modified Electrodes	Fabrication method	Analyte	Medium	Ep (Volt)	LOD	Ref
C-Ni/GCE	Drop-dry	ACOP	BR buffer	0.569	0.60 µM	186
C-Ni/GCE	Drop-dry	ACOP/DA/AA	BR buffer	0.52 / 0.348 /0.164	2.3/1.2/4.1µM	200
GOx/NiO/GCE	Electrodeposition	Glucose	PBS/MeOH	0.25	24.0 µM	162
NiHCF/CCE	Electrodep/Dip Dry	Hydrazine	PBS	0.52	8.0 µM	167
Cytc/NiO NPs/GC	Electrodep / SAM	H_2O_2	PBS	- 0.25	-	168
HRP/NiO NPs/GC	Electrodeposition	H_2O_2	PBS	- 0.30	123.0 µM	201
Hb/NiO/GCE	Electrodeposition	H_2O_2	PBS	-0.25	0.63 µM	202
Cat/NiO/GCE	Electrodeposition	H_2O_2 / NO_2^-	PBS	-0.45 /-0.55	0.60 µM	203
$NiCo(OH)_2$/ITO	Electrodeposition	Urea	KOH	0.50	-	22
Ga/NiO/GCE	Electrodeposition	Insulin	PBS	0.65	22.0 pM	204
Co-Ni/C	Electrodeposition	O_2	KOH	0.65	-	205
Ni-P-C	Electrodeposition	H_2	NaOH	-	-	206
Mb/NiO NPs/GC	Electrodeposition	H_2O_2	PBS	- 0.25	75.0 µM	207
GC/NiOx/CB	Electrodep/dip-dry	H_2O_2	PBS	- 0.27	1.67.0 µM	208
GC/NiOx/TH	Electrodep/Dip dry	H_2O_2	PBS	- 0.27	0.36 µM	208
CoNiFe/GCE	Electrodeposition	H_2	NaOH	-	-	209
Pt/NiO composite	Mixing/Drop dry	CH_3OH	H_2SO_4	0.53	-	210
CholOxNiNP/MWCNT/GC	Electrodeposition	Cholesterol	PBS	- 0.20	1.0 µM	211

NCGC	Electrodeposition	Fructose	NaOH	0.35	0.98 μM	151
Ni/Ti	Dip-Dry	Cyclohexanol	NaOH	0.43	-	212
MWCNTs/NMN	Electrodep/Drop Dry	Methane	NaOH	0.4	-	213
PtRuNi/C	Drop dry	CO / CH_3OH	H_2SO_4	0.53 / 0.50	-	214
Ni/Pt/Ti/Al_2O_3	Sputtering	CH_3CH_2OH	KOH	0.61		215

HCF: hexacyanoferrate nanoparticles; **CCE:** carbon ceramic electrode; **Hb:** Hemoglobin **GCE:** glassy carbon electrode;**BR:** mixture of H_3PO_4/boric acid/H2SO4; **ACOP:** Acetaminophen; **FerMeOH:** Ferrocenemethanol; **ITO:** indium tinoxide electrode; **Cyt c:** cytochrome c; **NPs:** nanoparticles; **Mb:** myoglobin; **HRP:** horseradish peroxidase; **CholOx:** Cholesterol oxidase; **NC:** nano-structured Ni(II)–curcumin film; **NMN:** nickel hydroxide nanoparticles modified nickel electrode.

1.5.4.2 Iron and iron oxide carbon nanotubes modified electrodes

Applications of nanosized magnetic particles have received considerable attention in biotechnology and medicine for their novel properties [216,217]. Up to date, the application of magnetic nanoparticles have stretched to various areas including magnetic recording, magnetic fluids [218], immobilization of proteins [219], detection of DNA hybridization [220], drug delivery catalytic reactions [216]. Iron is a versatile element and can form several phases with different oxidation states and structures such as shown below [221].

$$FeO \leftrightarrow FeO \leftrightarrow Fe_3O_4 \leftrightarrow \gamma\text{-}Fe_2O_3 \leftrightarrow \alpha\text{-}Fe_2O_3 \leftrightarrow FeOOH \quad (1.23)$$

Magnetite (Fe_3O_4), maghemite (γ-Fe_2O_3), and hematite (α-Fe_2O_3) are probably the most common out of the many oxides form in which iron oxides exist in nature [222].

Some of the catalytic works of iron nanocomposite modified electrodes have been reported. For example, Siswana et al. [223] reported that nanoparticles of iron (II) phthalocyanine (nanoFePc) impregnated on a carbon paste electrode (nanoFePc-CPE) revealed interesting electrocatalytic behaviour towards amitrole; pure catalytic diffusion-controlled process, with high Tafel slope suggesting strong binding of amitrole with nanoFePc catalyst. A carbon–iron nanoparticle modified glassy carbon electrode (CIN-GCE) has been developed for the determination of calcium dobesilate (CD) in pharmaceutical formulations with improved sensitivity and better reproducibility [224]. The electrocatalytic behaviour of an iron-cobalt carbon nanocomposite modified GCE electrode (FeCo/CNT/GCE) towards H_2O_2 reduction was studied [225]. Methanol oxidation in aqueous solution using FePt alloy nanoparticles modified glassy carbon electrode have been investigated. The modified electrode has strong catalytic oxidation of methanol in aqueous environment

compared with the bare GCE [226]. Mamuru and Ozoemena [72] reported that the nano iron pthalocyanine (nanoFePc) modified electrode exhibited enhanced electrocatalytic properties towards the detection of thiocyanate and nitrite in aqueous solutions compared to the bulk FePc counterpart. Gangeri et al. [227] compared the electrocatalytic activities of Pt/CNT and Fe/CNT on Nafion membrane electrode for fuel cell oxidation of CO_2. Their study indicated that Fe/CNT shows a better behavior than Pt/CNT (although a faster deactivation) in the conversion of carbon dioxide to liquid fuels, particularly isopropanol. Carbon-coated iron nanoparticles (CIN, a new style fullerence related nanomaterial) modified glassy carbon electrode (CIN/GCE) has been developed for the determination of uric acid (UA) [175]. The highly electrocatalytic activity of CNT/nano-Fe_3O_4 coated electrodes toward not only the reduction but also the oxidation of hydrogen peroxide have been reported [176]. Table 1.2 summarises other related literature reports.

Table 1.2: Electrocatalytic oxidation of some analytes on iron and iron oxide modified electrode.

Modified Electrodes	Fabrication method	Analyte	Medium	Ep (V)	LOD	Ref
nanoFePc-EPPGE	Drop-dry	SCN^- / NO_2^-	PBS	0.96	-	72
nanoFePc-CPE	Chemical Mixing	Amitrole	PBS/Na_2SO_4	0.42	3.62 nM	223
FeCo/CNT/GCE	Drop-dry	H_2O_2	KHphthalate	- 0.69	-	225
FePt/GCE	Drop-dry	CH_3OH	H_2SO_4	0.64	-	226
Fe/CNT/CC/Nafion membrane	Drop-dry/hot-pressing	CO_2	$KHCO_3$	-	-	227
CIN/GCE	Drop-dry	Uric acid	PBS	0.425	0.15 µM	163
Nano-Fe_2O_3/CPE	Chemical mixing	H_2O_2	H_3PO_4/H_3BO_3/ CH_3COOH	-0.56	$2x10^{-5}$ M	164
FeTMAPP/MWCNT/Au	SAM	O_2	PBS	- 0.25	0.38 µM	177
ssCT-DNA/CH-Fe_3O_4/ITO	Drop-dry	Nucleic-Acid	PBS	0.15	2.5ppb	228
Ur-GLDH/CH-Fe_3O_4/ITO	Dip-dry	Urea	PBS	0.18	0.5mg/dL	74
GOx/CH–Fe_3O_4/ITO	Dip-dry	Glucose	PBS	0.25	-	229
Fe_3O_4 MNPs	-	Phenol/ Anniline	PBS	-	-	230
Fe_3O_4@AuNPs/HS$(CH_2)_6$Fc/CPE	SAM	Dopamine	PBS	0.38	0.64 µM	231
IgGs/CH–Fe_3O_4/ITO	Drop-dry	Ochratoxin-A	PBS	0.45	$0.5ngdL^{-1}$	232
CNT/Fe_3O_4/CTS/GOx/PG	Magnetic loading / Drop-dry	Glucose	PBS	-	-	233
CNT/nano-Fe_3O_4/PG	Magnetic loading / Drop-dry	H_2O_2	PBS	- 0.36	-	234
Hb/CIN-CH/GCE	Drop-dry.	H_2O_2	PBS	0.50	1.2 µM	235
Nano-Fe-BDD	Electrodeposition	Trichloroacetate	NH_4F	-1.50	-	236
Nano-Fe-Pd	Chemical mixing	Lindane/ atrazine	CH_3OH	-	$0.1\ \mu gl^{-1}$	237

MMPs: magnetic nanoparticles; **nanoFePc-CPE:** nano iron phthalocyanine carbon paste electrode; **GNP/MWNTs-FeTMAPP-Au:** gold nanoparticles multi wall carbon nanotubes iron-5,10,15,20-tetrakis[aaaa-2-trismethylammoniomethyl-phenyl]porphyrin modified gold electrode; **FeCo/CNT/GCE:** iron –cobalt nanocomposite modified glassy carbon electrode; **ssCT-DNA/CH-Fe_3O_4/ITO :** single standard *calf thymus* deoxyribose nucleic acid (ssCT-DNA) - chitosan (CH)-iron oxide (Fe3O4) nanoparticles based hybrid nanobiocomposite indium tin oxide modified electrode; **CC:** carbon cloth; **Ur-GLDH/CH-Fe_3O_4/ITO:** Urease and glutamate dehydrogenase co-immobilized iron oxide nanoparticles-chitosan (CH) based nanobiocomposite film modified indium-tinoxide (ITO) glass plate; **GOx/CH–Fe3O4/ITO:** glucose oxidase-chitosan-iron oxide nanobiocomposite indium tinoxide electrode; **Fe3O4@AuNPs/HS(CH2)$_6$Fc/CPE:** 6-ferrocenylhexanethiol (HS(CH2)6Fc) functionalized iron oxide at gold nanoparticles films on carbon paste electrode; **IgGs/CH–Fe3O4/ITO:** immunoglobulin antibodies chitosan–iron oxide nanoparticles-indium–tin oxide (ITO) electrode; **CNT/Fe3O4/CTS/GOx/PG:** carbon nanotubes-iron oxide nanocomposite-chiotsan-immobilised glucose oxidase-plexiglas plate; **CIN/GCE:** Carbon-coated iron nanoparticles modified glassy carbon electrode.

1.5.4.3 Cobalt and cobalt oxide carbon nanotubes modified electrodes

Pure cobalt nanoparticles (2–20 nm) are of great research interest due to its unusual phenomena (quantum effects) and industrial applications [238,239]. They are used materials for magnetic, fluids, optoelectronics and in data storage applications [238-240]. Cobalt atoms has been largely employed for preventing the formation of less electroactive β phase of $Ni(OH)_2$ nanoparticles during electrode modification. Furthermore, the inclusion of Co^{3+} also increases the hydroxide conductivity shifting the redox peaks of $Ni(OH)_2$ to less positive potentials [241]. On the other hand, cobalt oxide films are composed of nanosized metal oxide particles, and have been intensively investigated in recent years for their use in processes such as energy storage system [242], electrochromic thin films [243], magnetoresistive devices [244] and heterogeneous catalysis [245].

Studies using Co and cobalt oxides (CoxOy) decorated electrodes for biological and environmental sensing have been reported [165,166,246-248]. Electrodes decorated with cobalt oxide nanoparticles without CNTs for sensing properties have also been studied [19,249]. Few studies using CNT-Co modified electrodes have been carried out [250-254], for example, Yang *et al.* [252] used chemically prepared cobalt hexacyanofferate nanoparticles-CNT-chitosan modified electrode (CoNP-CNT-CHIT) for glucose detection. Recently, Shen *et al.* [253] reported Pt-Co nanoparticles supported on single-walled carbon nanotubes (SWCNTs-Pt-Co) obtained via chemical process for methanol oxidation. Also, Zhao *et al.* [254] made the composite by chemical reduction of cobalt salt in CNT solution and the electrode, containing other metals as composite shows good electrocatalysis towards methanol oxidation. Other literature reports include: glassy carbon and gold electrodes modified cobalt oxide nanoparticles for electrocatalytic processes using

different organic molecules such as glucose [255], cysteine [256], propylamine [257], hydroquinone [258] and methanol [259] as model compounds [217]. Cobalt oxide/FAD composite modified GC electrode shows excellent catalytic activity for nitrite reduction at reduced over potential [19]. Novel cobalt oxide nanoparticles based sensor for the detection of trace amount of As^{3+} ion in aqueous solution has been developed. The modified electrode shows excellent catalytic activity toward arsenic oxidation at wide pH range [217]. Electrocatalytic reduction of hydrogen peroxide and oxygen at GC electrode modified with haemoglobin (Hb) and cobalt oxide nanoparticles have been reported [77]. Other works reported in literature are summarised in Table 1.3.

Table 1.3: Electrocatalytic oxidation of some analytes on cobalt and cobalt oxide modified electrode.

Modified Electrodes	Fabrication	Analyte	Medium	Ep (V)	LOD	Ref
Co-Ni/C	Drop-dry	O_2	KOH	0.65	-	218
FeCo/CNT/GCE	Drop-dry	H_2O_2	KHthalate	- 0.69	-	225
FAD/CoOx/GCE	Electrodeposition	NO_2^-	PBS	-0.45	0.20 µM	19
GC/CoOx	Electrodeposition	As^{3+} ion	PBS	0.80	11.0 nM	217
Hb-CoOx/GCE	Electrodeposition	H_2O_2	PBS	-0.55	0.50 µM	77
SWCNT-Co-EPPGE	Electrodeposition	NO_2^-	PBS	0.88	5.61 µM	79
Pt-Co/C	Drop-dry	CH_3OH	KOH	-0.35	-	260
$NiCo(OH)_2$/ITO	Electrodeposition	Urea	KOH	0.50	-	165
GC/CoOx	Electrodeposition	H_2O_2	PBS	0.85	0.4 nM	261
CHM-GCE	Electrodeposition	Cysteine	NaOH	0.60	85.2 µM	262
CoNP–CNT–CHIT	Drop-dry	H_2O_2	PBS	- 0.20	-	263
CoNP–CNT–CHIT-GOx	Drop-dry	Glucose	PBS	- 0.20	5.0 µM	263
GOD–NanoCoPc/PGE	Drop-dry	Glucose	PBS	0.55	5.0 µM	264
NanoCoPc/PGE	Drop-dry	H_2O_2	PBS	0.58	-	264
CoNP/MWCNT/GCE	Drop-dry	Thioridazine	PBS	0.55	$5.0x10^{-8}$ M	265
Co_3O_4/C	Chemical Mixing	H_2O_2 / O_2	NaOH	- 0.2	-	266
CoHCF nanotubes	Electrodeposition	Ascorbicacid/ Dopamine	PBS	0.04/ 0.22	1.2 µM	267
PtCo/Ebonex	Electrodeposition	O_2	KOH	> 1.50	-	268
LOD–NanoCoPc/GCE	Drop-dry	AscorbicAcid (lactate)	PBS	0.50	-	269

CHM-GC: cobalt hydroxide nanoparticles modified glassy carbon electrode; **GOD–NanoCoPc/PGE:** glucose oxidase nano cobalt phthalocyanine modified pyrolytic graphite electrode; **SSF:** stainless steel foils; **LOD–NanoCoPc/GCE:** lactase oxidase nano cobalt phthalocyanine composite modified glassy carbon electrode.

1.5.5 Supercapacitive behaviour of carbon nanotubes metal oxides

The CNT/MO nanocompoiste investigated in this work are characterised by charging or capacitive current in the electrolytes. Therefore, it becomes imperative to establishing the charge storage properties of these materials as a potential source for energy generation. The study is important especially in response to the increasing demands for clean energy technologies, where supercapacitors are considered to be the most promising energy storage and power output technologies [270] for portable electronics, electric vehicles, and renewable energy systems. Supercapacitors fill the gap between batteries and conventional dielectric capacitors and have considerable potential for use in high power applications [271]. The amount of energy stored is usually small and can be delivered instantaneously, making supercapacitor devices able to provide pulsed high power rather than high amount of energy [272]. Supercapacitors or electrochemical capacitors are basically classified into two types depending on the nature of the charge-storage mechanism [273]: double-layer and pseudocapacitors. Double-layer capacitors stores charges through nonfaradaic processes while the pseudocapacitors are through faradaic process. In the former, charge separation (ions, or ions and electrons) arises at interfaces between solids and ionic solutions, especially at colloids, metal electrodes, and semiconductors, giving rise to the so-called double-layer [101] (Figure 1.18). The charge difference (Δq) gives rise to a corresponding potential build up ΔV across the interface, thus resulting in a capacitance $C = \Delta q/\Delta V$ or $d(\Delta q)/d(\Delta V)$ which is referred to as the 'double-layer' capacitance [101].

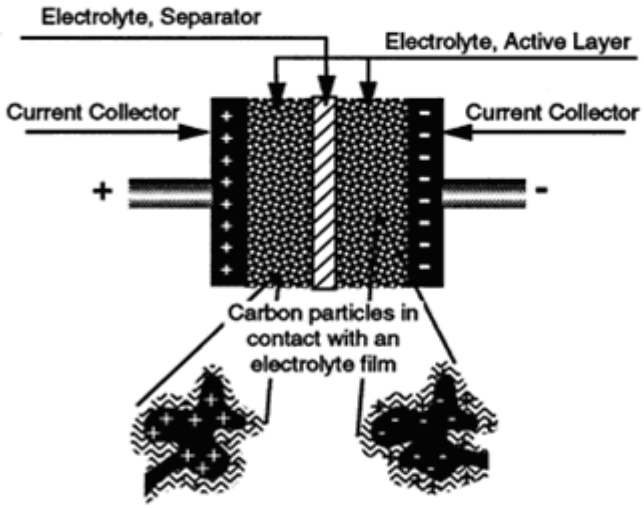

Figure 1.18: Principle of single-cell double-layer capacitor showing charge separation and storage at current collectors.

Electrochemical redox supercapacitors consist of electroactive materials with several oxidation states and their high capacitance and energy characteristics have been investigated [274]. Several materials such as the redox active metals, transition metal oxides [275-277] and conducting polymers [278] with various oxidation states have been used for this supercapacitor type. RuO_2 is well known as a good metal oxide in supercapacitors because of its high specific capacitance values (740 F g^{-1}) [279], from a three electrode system. However, its application is limited because of its disadvantages such as the high cost and toxic nature. In the quest for an alternative sources, researchers have explored the charge storage properties of different materials such as anhydrous cobalt–nickel oxides [280], MnO_2 or MnOx [273,281], NiO [282], Co_3O_4 [283], and Fe_3O_4 [284] as inexpensive alternatives to RuO_2. Thus, the need for other transition metal and metal oxides and their composites which are user- and environmentally friendly, providing a sufficiently high power and energy, and can be made available at a relatively cheap price for commercial application cannot be overemphasised.

NiOx is preferred material for supercapacitor applications [286-287]. Researchers have been actively engaged in the synthesis of NiOx film of high surface area, uniform and ordered meso- or nano-porous network by using available physical and chemical methods to obtain superior capacitive performance [286, 287]. The surface area and morphology which can enhance ion transfer in the pore system and the active material–electrolyte interfacial area, is considered as the boosting factor. Furthermore, nickel oxide is easily available and possesses a high specific capacitance that is comparable with carbon materials [288]. For example, the performances of the electrochemical double layer capacitor from nickel acetate/polyacrylonitrile-based Ni/C nanocomposite fibers with different mass ratios have been evaluated. The results show that the introduction of a proper proportion of nickel into carbon could enhance both specific capacitance and electrochemical stability of the nickel/carbon composite electrodes [289]. In another study, composite electrodes for electrochemical supercapacitors were fabricated by impregnation of slurries of the manganese dioxide nanofibers and multiwalled carbon nanotubes (MWCNTs) into porous nickel foam current collectors. It was demonstrated that MWCNT improved electrochemical performance of the electrodes by forming a secondary conductivity network within the nickel foam cells [290]. Porous nickel oxide/multiwalled carbon nanotubes (NiO/MWNTs) composite material was synthesized and its electrochemical behaviour was studied. The composite shows an excellent cycle performance at a high current and keeps capacitance retention of about 89% over 200 charge/discharge cycles [291]. Recently, nickel oxide ordered mesoporous carbons (NiO-OMC) have drawn great interest due to the application as electrochemical double-layer capacitor. Results showed that NiO nanoparticles embedded inside the mesoporous carbon particles enhances its capacitive behaviour

[292]. Lee et al. [293] reported the synthesis of novel mesostructured of NiO/C composite with NiO nanoparticles studded in the wall of mesoporous carbon. Such novel structure was important for the mass-transfer process in the electrode reaction, consequently, resulting in a large specific capacitance

Other works using the electrochemical properties of Ni and NiO nanocomposite materials as energy storage devices in supercapacitors have been reported [294-297]. Most of the studies reported above were carried out in basic medium probably due to the interaction of the OH^- ions (nucleophile) with the Ni^{2+} ion. Thus, this work focused on establishing the supercapacitive behaviour of the synthesised NiO nanoparticles in acidic and neutral media which could be better or alternative electrolyte to the presently explored alkaline medium.

Fe_3O_4 is another recently discovered inexpensive electrode material, exhibiting pseudocapacitance with alkali sulfites and sulfates electrolytes, but is very sensitive to the electrolyte anion species and the dispersion of the oxide crystallites [298]. These behaviours suggest a different capacitance mechanism from that of either RuO_2 or MnO_2. Wang et al. [299] have investigated the capacitance mechanisms of Fe_3O_4 capacitor in Na_2SO_3, Na_2SO_4, and KOH aqueous solutions by various analysis methods. Kuo's group [300] have studied and reported the supercapacitive behaviour of MFe_2O_4 (M = Mn, Fe, Co, or Ni) and similar crystal structures to Fe_3O_4.The capacitance with $MnFe_2O_4$ as pseudocapacitive electrode materials decreased by ~18% during the first 1000 cycles and then remained unchanged throughout 3000 cycles. They attributed the good cycling stability to the very small volume variation. Chen et al. [296] reported the electrochemical properties of nanosized $Ni_3(Fe(CN)_6)_2(H_2O)$ prepared by simple co-precipitation method, using cyclic voltammetry (CV), constant charge/discharge tests and electrochemical impedance spectroscopy (EIS). Chen et al. [301]

studied the supercapacitive behaviour of Fe_3O_4 film deposited on stainless steel in 1 M Na_2SO_3 solution at different scan rate using cyclic voltammetry experiment. The Fe_3O_4 film demonstrated pseudocapacitive properties. Other reports on the supercapacitive properties of Fe and FexOy nanoparticles materials in different electrolytes have been reported [302,297]. Just like NiO NPs, the integration of Fe_xO_y nanoparticles with CNT and its supercapacitive behaviour (especially in acidic medium) on carbon electrode such as BPPGE have not been given much attention. Therefore, this work provides information on the findings in both acidic and neutral medium using the electrode or cell system described and reported in Chapter 2 and 10.

Chen et al. [297] reported the application of nano-sized insoluble iron, cobalt and nickel hexacyanoferrates (Mhcf) for supercapacive purpose. Cyclic voltammogram and constant charge-discharge in 1 M KNO_3 showed different electrochemical capacitive performance due to the different types of the second metal. In another study, a high specific capacitance (508 Fg^{-1}) was obtained for cobalt sulphide nanowire (CoS) in 3 M KOH which is very competitive with the best supercapacitor material, RuO_2 (720 – 760 Fg^{-1}) but its cost is remarkably lower than RuO_2 [303]. Wang et al. [299] prepared a thin-film electrode with a Co/Al nanocomposite that gave specific capacitance of 2500 F cm^{-3} (833 Fg^{-1}) in 6 M KOH electrolyte and a good high-rate capability to show the best performance when used as an electrode in thin-film supercapacitors (TFSCs). Yu et al. [304] synthessied cuspate deltoid cobaltous oxide (CoO) crystallites and investigated its supercapacitive property in 2 M KOH. The cyclic voltammetry results indicate that the CoO shows acceptable capacitive behavior with specific capacitance of about 88 Fg^{-1}. Zheng et al. [305] reported that the galvanostatic electrochemical results of CoO-doped mesoporous NiO nanoplatelets in 5 M KOH indicated much-improved specific capacity and better

reversible stability than that of the pure NiO porous nanoplatelets and CoO-doped NiO microparticles.

1.5.6 Electrode modification techniques

Various techniques can be used to modify electrodes. These techniques include:

1.5.6.1 Electrodeposition

It is a plating process that uses electrical current to reduce cations of a desired material from a solution and coat a conductive object with a thin layer of the material, such as a metal [201-205]. Both the anode and the cathode components are immersed in a solution called an electrolyte containing one or more dissolved metal salts as well as other ions that permit the flow of electricity. A rectifier supplies a direct current to the anode, oxidizing the metal atoms that comprise it and allowing them to dissolve in the solution.

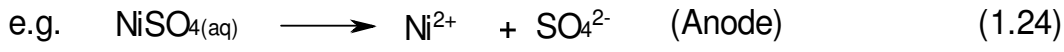

At the cathode, the dissolved metal ions in the electrolyte solution are reduced at the interface between the solution and the cathode, such that they "plate out" onto the cathode.

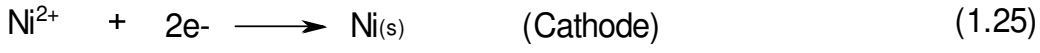

The rate at which the anode is dissolved is equal to the rate at which the cathode is plated, vis-a-vis the current flowing through the circuit. The metal oxide can also be deposited by repetitive cycling (Figure 1.19) the metal in phosphate buffer solution. Unlike electropolymerisation, a polymer is not formed and the first cycle is almost similar to the subsequent scans.

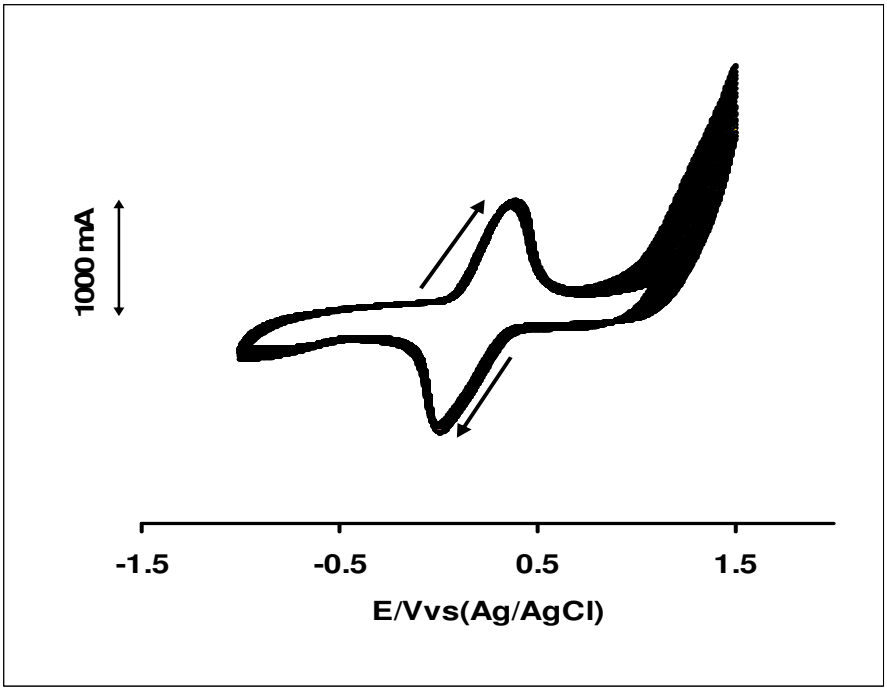

Figure 1.19: Repetitive cyclic voltammograms of an electrode modified with metal oxides film.

This method along side with the drop-dried electrode modification procedures are the major techniques used in this study because of their simplicity, and the advantage of setting a constant deposition potentials which guide against variation in the amount of nanomaterials deposited on the electrode from one experiment to another. The surface concentration of the deposited nanomateria, were obtained using Equations (1.20) or Equation (1.21) above. A well formed M/CNT and MO/CNT have a surface coverage concentration of about approximately 10^{-9} to 10^{-8} mol cm^{-2}.

1.5.6.2 Electropolymerisation

Electropolymerisation is the most efficient method of depositing polymer films on electrodes. Electropolymerisation process involves the repetitive voltammetric scanning of the solution of the modifier monomers at the electrode surface within a specific potential window [203,211]. This can be oxidative or

reductive voltammetric scanning in which the monomer forms radicals which combine to form polymers on electrodes. It is a reproducible process and also it is possible to control the film thickness by varying the conditions for polymerisation process such as time, scan rate, potential range and the type of electrolytes. Various conducting surfaces such as metals, metal oxides and carbon based electrodes can be used as the depositing surface. Many works have been done using electropolymerization for the deposition of thick layer of metal oxides and hydroxides [203,211].

1.5.6.3 Dip-dry

It involves the immersion of an electrode in solution of a catalyst or a modifier for a period of time to allow for surface adsorption of the material. The electrode is later withdrawn and the solvent is allowed to dry [167,208,212].

1.5.6.4 Drop-dry

The electrode is modified by placing few drops of the catalyst or modifier on its surface and allowing the solvent to dry off [114,200,214].

1.5.6.5 Spin-coating

It involves evaporation of solution of a modifier from electrode surface by high speed rotations using centrifugal force. Example is the modification of indium tin oxide substrate with xerogel oxide film by spin-coating a viscous gel [306].

1.5.6.6 Composite technique:

It is a process of impregnating the buck electrode material with a chemical modifier [307].

1.5.6.7 Sol-gel method

The sol-gel process is a wet-chemical technique (a.k.a. chemical solution deposition) widely used recently in the fields of materials science and ceramic engineering. Typical precursors are metal alkoxides and metal chlorides, which undergo various forms of hydrolysis and polycondensation reactions to give metal oxides. Sol-gel derived materials have diverse applications in optics, electronics, energy, space, (bio)sensors, medicine (e.g., controlled drug release), reactive material and separation (e.g., chromatography) technology [308].

1.5.6.8 Self-assmbled-monolayers

It is the formation of highly ordered molecular assemblies formed by the adsorption of molecules from solution directly onto the surface of an appropriate substrate (Figure 1.20). SAM technique has a number of advantages which include simplicity, reproducibility and formation of highly ordered and stable monolayers which are chemically bound onto electrodes [177,231].

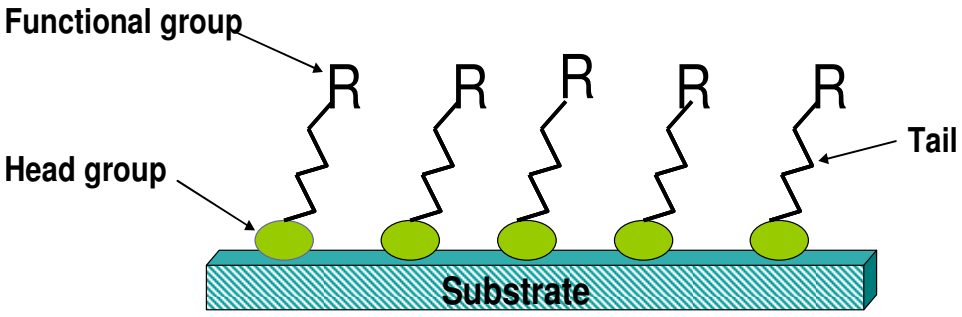

Figure 1.20: Typical SAM modified electrode showing formation of monolayer.

1.5.6.9 Langmuir- Blodgett technique

Langmuir-Blodgett (LB) technique is a method of depositing crystalline films one molecular layer at a time, by dipping the

substrate into water containing a polymer that forms a single layer of molecular chains on the surface. This layer is then transferred from the water to the substrate. The dipping can be repeated to create an ordered multilayer film that does not require poling to orient the molecules. The main advantages of this method are large-scale defect-free areas, very short preparation time, and very neat products [309].

1.5.6.10 Chemical vapour deposition

Chemical vapor deposition (CVD) is a chemical process used to produce high-purity, high-performance solid materials. The process is often used in the semiconductor industry to produce thin films. In a typical CVD process, the water (substrate) is exposed to one or more volatile precursors, which react and/or decompose on the substrate surface to produce the desired deposit. Frequently, volatile by-products are also produced, which are removed by gas flow through the reaction chamber [310].

1.6 Nanoscience in Electrochemistry

In electrochemistry, the use of bare electrodes for electrochemical detection of species has a number of limitations, such as low sensitivity and reproducibility, the slow electron transfer reaction, low stability over a wide range of solution composition and high over-potential at which the electron transfer process occurs. In the face of some of these challenges, the quest for a plausible way of fabricating an efficient sensor of significant advantages and applications in food, industries and environment has lead to the advent of nanoscience and nanotechnology applications. Thus, the chemical modification of inert substrate electrodes with redox active thin film offers significant advantages in the design and development of chemical sensor and biosensors.

The development of nanoscience and nanotechnology has been increasing very fast along the last years and nanostructured materials have raised a remarkable attention due to their unique properties provoked by quantum size effects [311] or due to the great superficial area achieved by nanostructures, largely employed in solar cells [312], electrochromic devices [313], catalysis [314] sensors and biosensors [315,316]. Nanoscience involves the study of materials on the nanoscale level between approximately 1 and 100 nm [317] and involves study of how to control the formation of two- and three-dimensional assemblies of molecular scale building blocks into well-defined nanostructures or nanomaterials [318]. In general, these nanoparticles (NPs) can be categorised into carbon-based materials such as fullerenes and carbon nanotubes and inorganic nanoparticles including the ones based on metal oxides (zinc oxide, iron oxide, titanium dioxide and cerium oxide etc), metals (gold, silver and iron) and quantum dots (cadmium sulfide and cadmium selenide) [319]. Other metals of wide application in the area of electrochemistry and nanoscience include nickel, cobalt, zinc, copper, aluminium, platinum, titanium etc. NPs differ from

larger materials in that the number of atoms at the surface and their physical properties are different from those of bulk materials [320]. Properties associated with the bulk materials are averaged properties, such as density, resistivity and magnetisation and the dielectric constant. Critically, however, many properties of these materials change over at the NP scale [321]. These differences arise from the small size and large number of surface atoms of the particles and related effects.

1.7 Langmuir Isotherm Adsorption Theory

Many electrochemical phenomena and processes are to a great extent influenced by different adsorption processes. Of prime importance is the adsorption on the electrode surface of components of the electrolyte solution, as well of those participating in the electrode reaction, or those "inert" components that do not participate. Depending on the nature of the system, the adsorption process can be either reversible or irreversible. In the first case adsorption equilibrium exists between the particles adsorbed on the adsorbent's surface and the particles in the electrolyte (or in any other phase contacting with the adsorbent). After removing the substance from the electrolyte, adsorbed particles leave the surface and enter into the electrolyte. In the case of an irreversible adsorption, the adsorbed particles remain at the surface even if their concentration in the bulk phase drops to zero. In this case the adsorbed particles can be removed from the surface only by means of a chemical reaction (e.g., their oxidation by oxygen) or by a displacement process during the adsorption of other substances. Processes of physical adsorption are often reversible, wheras processes of chemisorption are mostly irreversible. A convenient parameter for quantitative estimates of adsorption which is of the monolayer type is the degree of surface coverage (θ) defined by the relation [322]:

$$\theta = \frac{A_j}{A_j^o} \qquad (1 \geq \theta \geq 0) \qquad (1.26)$$

A_j is the amount of species of the adsorbed substance j (adsorbate) per unit area of the true surface area of the electrode, A_j^o is limiting adsorption value when the surface is covered completely by particles of a given substance (i.e., at full monolayer coverage). By

convention, adsorption is regarded as insignificant when θ<0.1, and as significant when θ>0.5.

The adsorption of a component *j* in a given system depends on temperature *T* and on the component's concentration, $C_{V,j}$, in the bulk phase. The overall adsorption equation can be written as $A_j = f(T, C_{V,j})$ where *f* is the activity coefficient. The relation between adsorption and the adsorbate's bulk concentration (or pressure, in the case of gases) at constant temperature is called the *adsorption isotherm*; the relation between adsorption and temperature at constant concentration is called the *adsorption isobar*. From the shape of the adsorption isotherms, the adsorption behaviour can be interpreted. In the case of monolayer adsorption, the isotherms are usually written in the form $\theta_j = f(C_{V,j})$.

At higher values of θ, when the number of free sites on the surface diminishes, one often observes relations of the form:

$$\theta = BC_V\ (1 + BC_V) \quad \text{or} \quad \theta\,(1-\theta) = BC_V \qquad (1.27)$$

Where *B* is the adsorption coefficient (units: dm^3mol^{-1}). At low values of the bulk concentration ($BC_V << 1$), the degree of surface coverage is proportional to this concentration, but at high values it tends toward a limit of unity. The rate of adsorption is proportional to the bulk concentration and to the fraction 1- θ of vacant sites on the surface: $v_a = k_a(1-\theta)$, while the rate of desorption is proportional to the fraction of sites occupied: $v_d = k_d\theta$. In the steady state these two rates are equal. With the notation $k_a/k_d = B$, Equation (1.26) was obtained [322]. In 1918, Irving Langmuir derived this equation and based it on four assumptions: (1) The surface of the adsorbent is uniform (homogenous). That is, all the adsorption sites are equivalent and have the same heat of adsorption and hence, the same adsorption coefficient *B*. (2) Adsorbed molecules do not interact. (3) All adsorption occurs

through the same mechanism and adsorption is reversible. (4) At the maximum adsorption, only a monolayer is formed: molecules of adsorbate do not deposit on other, already adsorbed, molecules of adsorbate, only on the free surface of the adsorbent [322]. These four assumptions are seldom all true: there are always imperfections on the surface, adsorbed molecules are not necessarily inert, and the mechanism is clearly not the same for the very first molecules to adsorb to a surface as for the last. The Langmuir isotherm is nonetheless the first choice for most models of adsorption, and has many applications in surface kinetics and thermodynamics.

The Langmuir adsorption equation has also been derived for less ideal situations, involving quasi- and irreversible adsorbing electroactive molecules with different strenghths of adsorption of the reactant and products as [98,323-325]:

$$\theta = \frac{BC}{(1+BC)} \tag{1.28}$$

Here θ is the ratio of the surface coverage of the analyte Γ of analyte at concentration C to its maximum surface concentration Γ_{max} (i.e, $\theta = \Gamma / \Gamma_{max}$). Therefore,

$$\frac{C}{\Gamma} = \frac{I}{B\Gamma_{max}} + \frac{C}{\Gamma_{max}} \tag{1.29}$$

Assuming that the stripping peak current is proportional to the surface concentration of the analyte, Equation 1.29 can be re-written as:

$$\frac{C}{I_p} = \frac{I}{BI_{p,max}} + \frac{C}{I_{p,max}} \qquad (1.30)$$

A plot of C/I_p versus C gives a linear relationship. From the slope and the intercept of the line, the adsorption equilibrium constant B is obtained. The standard free energy change due to adsorption of the analyte can be evaluated from the relationship:

$$\Delta G^o = -RT\ln B. \qquad (1.31)$$

This theory and equations are applied in this work for evaluating the extent of adsorption of the analytes investigated, especially DEAET and hydrazine on the modified electrodes.

1.8 Microscopy and Spectroscopy Techniques

1.8.1 Microscopy

Microscopy is the technical field of using microscopes to view samples or objects. There are three well-known branches of microscopy, optical, electron and scanning probe microscopy. Optical and electron microscopy involve the diffraction, reflection, or refraction of electromagnetic radiation/electron beam interacting with the subject of study, and the subsequent collection of this scattered radiation in order to build up an image. This process may be carried out by wide-field irradiation of the sample (e.g transmission electron microscopy) or by scanning of a fine beam over the sample (e.g. scanning electron microscopy). Scanning probe microscopy involves the interaction of a scanning probe with the surface or object of interest [326].

1.8.1.1 Scanning Electron Microscope (SEM)

A scanning electron microscope (SEM) is a powerful microscope that images the sample surface by scanning it with a high-energy beam of electrons in a raster scan pattern. The electrons interact with the atoms that make up the sample producing signals that contain information about the sample's surface topography, composition and other properties such as electrical conductivity [326]. Applications include failure analysis, identification of fracture modes and origins, physical and chemical characterization of surfaces, microstructural analysis, corrosion damage and pitting, nanoscience, particle analysis and foreign materials. Figure 1.21 represents the SEM image of a modified electrode.

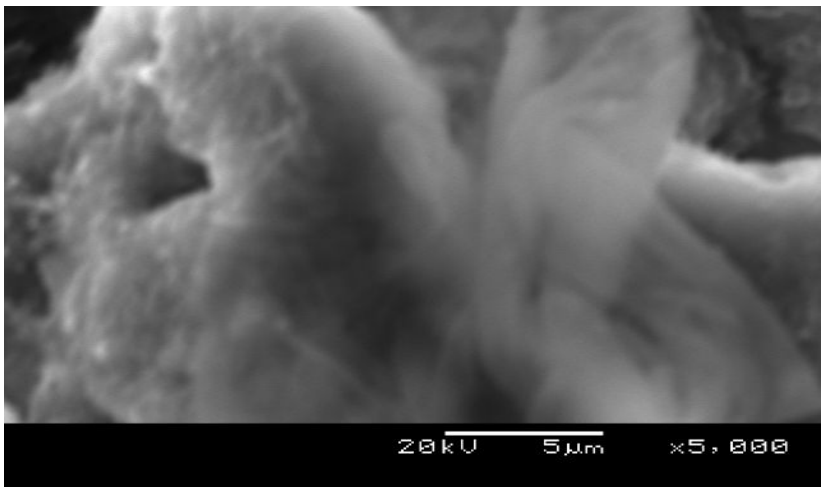

Figure 1.21: A Typical SEM Image showing formation of metal oxide nanoparticles film on modified electrode.

1.8.1.2 Transmission electron microscope (TEM)

Transmission electron microscopy (TEM) is a microscopy technique whereby a beam of electrons is transmitted through an ultra thin specimen, interacting with the specimen as it passes through. An image is formed (e.g., Figure 1.22) from the interaction of the electrons transmitted through the specimen; the image is magnified and focused onto an imaging device, such as a fluorescent screen, on a layer of photographic film, or to be detected by a sensor such as a CCD camera. TEM forms a major analysis method in a range of scientific fields, in both physical and biological sciences. TEMs find application in cancer research, virology, materials science as well as pollution and semiconductor research [327].

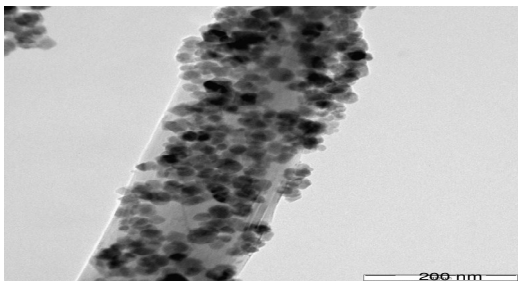

Figure 1.22: A Typical TEM Image of CNT decorated with metal nanoparticles.

1.8.1.3 Atomic force microscope

The atomic force microscope (AFM) or scanning force microscope (SFM) is a very high-resolution type of scanning probe microscope, with demonstrated resolution of fractions of a nanometer, more than 1000 times better than the optical diffraction limit. AFM is one of the foremost tools for imaging, measuring and manipulating matter at the nanoscale. The information is gathered by "feeling" the surface with a mechanical probe. Piezoelectric elements that facilitate tiny but accurate and precise movements on (electronic) command enable the very precise scanning.

The AFM consists of a microscale cantilever with a sharp tip (probe) at its end that is used to scan the specimen surface (Figure 1.23). The cantilever is typically silicon or silicon nitride with a tip radius of curvature on the order of nanometers. When the tip is brought into proximity of a sample surface, forces between the tip and the sample lead to a deflection of the cantilever according to Hooke's law. Typically, the deflection is measured using a laser spot reflected from the top surface of the cantilever into an array of photodiodes. A feedback mechanism is employed to adjust the tip-to-sample distance to maintain a constant force between the tip and the sample. The AFM can be operated in a number of modes, depending on the application. In general, possible imaging modes are divided into static (also called Contact) modes and a variety of dynamic (or non-contact) modes where the cantilever is vibrated [328].

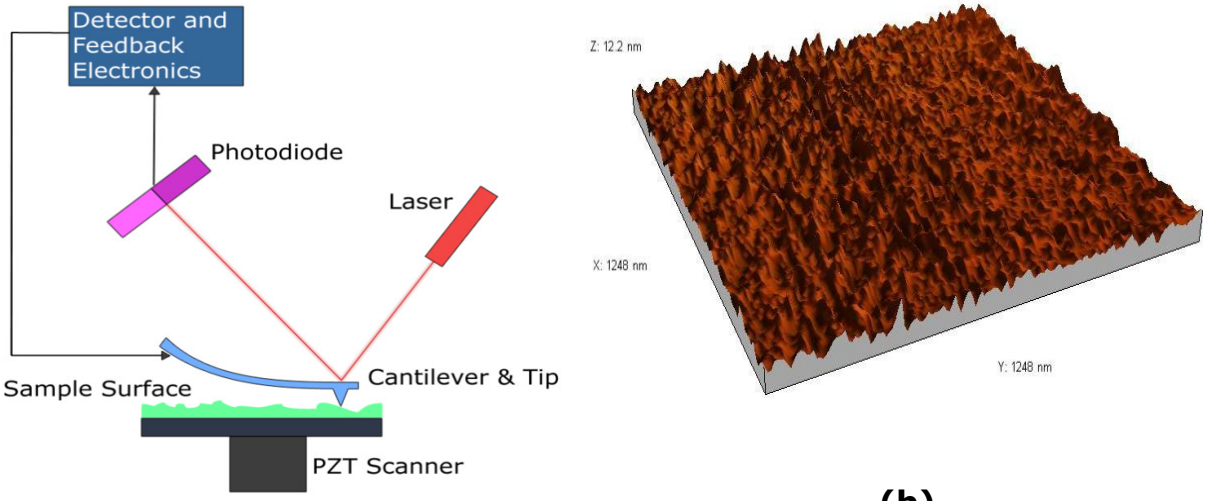

(a) **(b)**

Figure 1.23: (a) Atomic force microscope block diagram. (b) AFM three dimentional (3D) image of a nanomaterial growth on a modified electrode [328].

1.8.2 Spectroscopy

Spectroscopy is the study of the interaction between radiation and matter as a function of wavelength, frequency or energy which is usually in the form of photon of light and represented as $E = hv$ where h is the Planck constant. A plot of the response as a function of wavelength—or more commonly frequency—is referred to as a spectrum.

1.8.2.1 Energy dispersive X-ray spectroscopy (EDS)

Energy dispersive X-ray spectroscopy (EDS) is an analytical technique used for the elemental analysis or chemical characterization of a sample (Figure 1.24). As a type of spectroscopy, it relies on the investigation of a sample through interactions between electromagnetic radiation and matter, analyzing X-rays emitted by the matter in response to being hit with charged particles. The characteristic X-rays of an element's atomic structure to be identified is unique and can be separated from other [329,330].

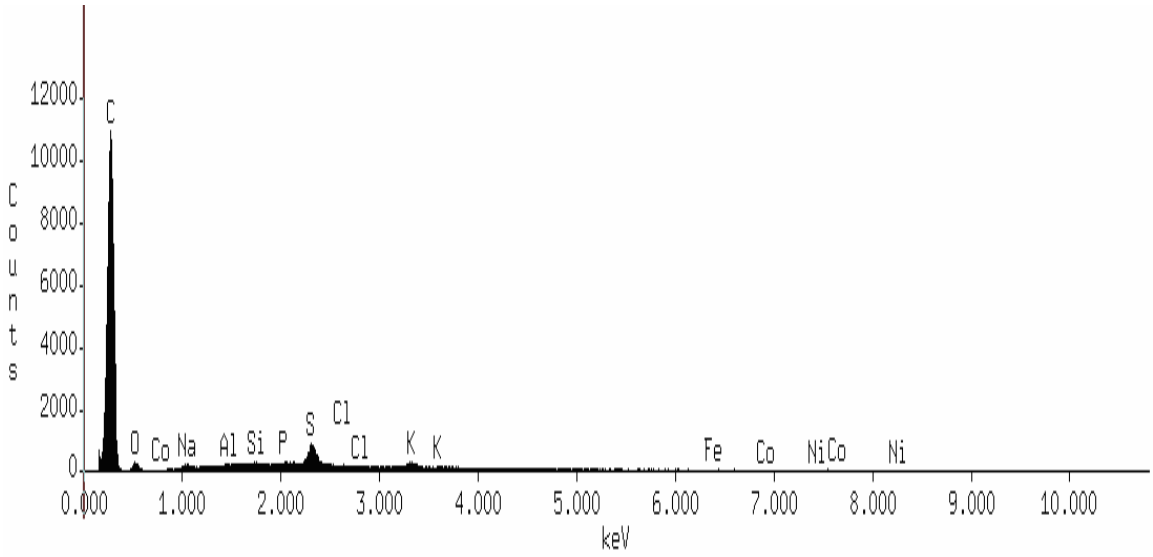

Figure 1.24: EDX profile of a material showing the possible elemental composition.

1.8.2.2 X-ray photoelectron spectroscopy

X-ray photoelectron spectroscopy (XPS) is a quantitative spectroscopic technique that measures the elemental composition, empirical formula, chemical state and electronic state of the elements that exist within a material (Figure 1.25). XPS spectra are obtained by irradiating a material with a beam of aluminium or magnesium X-rays while simultaneously measuring the kinetic energy (KE) and number of electrons that escape from the top 1 to 10 nm of the material being analyzed. XPS is routinely used to analyze inorganic compounds, metal alloys, semiconductors, polymers, elements, catalysts, glasses, ceramics, paints, papers, inks, woods, plant parts, make-up, teeth, bones, medical implants, bio-materials, viscous oils, glues, ion modified materials and many others [331].

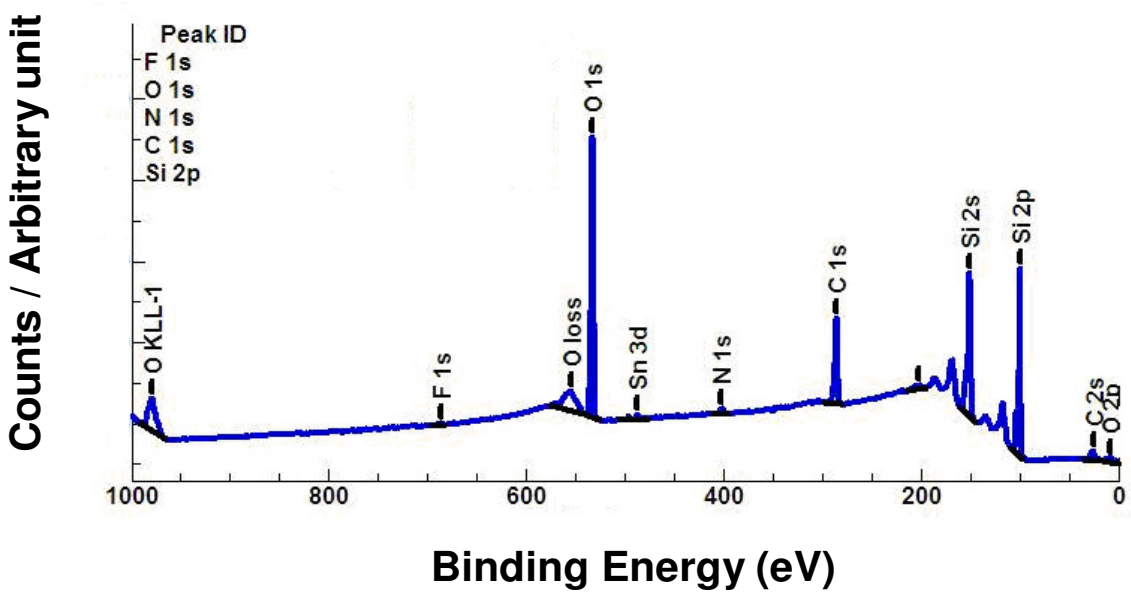

Figure 1.25: Wide scan XPS spectrum showing the present elements.

1.8.2.3 X-ray diffraction spectroscopy

X-ray diffraction finds the geometry or shape of a molecule using X-rays. X-ray diffraction techniques are based on the elastic scattering of X-rays from structures that have long range order. Single-crystal X-ray diffraction is a technique used to solve the complete structure of crystalline materials, ranging from simple inorganic solids to complex macromolecules, such as proteins. Powder diffraction (XRD) is a technique used to characterize the crystallographic structure, crystallite size (grain size), and preferred orientation in polycrystalline or powdered solid samples. Powder diffraction is commonly used to identify unknown substances, by comparing diffraction data against a database maintained by the International Centre for Diffraction Data [332]. Figure 1.26 showed the X-ray diffraction pattern formed when X-rays are focused on a crystalline material and a typical XRD spectrum obtained.

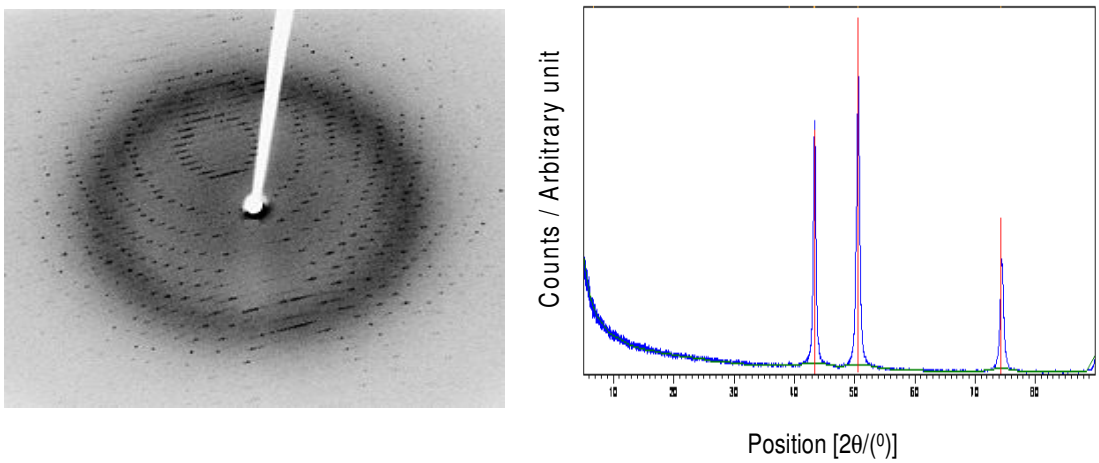

Figure 1.26: (a) X-ray diffraction pattern formed when X-rays are focused on a crystalline material (b) XRD spectrum of synthesised metal nanoparticles showing identified peaks of the metal at different 2θ position [332].

1.8.2.4 Infrared spectroscopy

Infrared (IR) spectroscopy is a well known analytical technique which deals with the infrared region of the electromagnetic spectrum. It can be used to identify compounds or investigate sample composition. Figure 1.27 presents an IR apparatus showing the different components. Infrared spectroscopy exploits the fact that molecules have specific frequencies at which they rotate or vibrate corresponding to discrete energy levels (vibrational modes). These resonant frequencies are determined by the shape of the molecular potential energy surfaces, the masses of the atoms and, by the associated vibronic coupling. Infrared spectroscopy is widely used in both research and industry as a simple and reliable technique for measurement, quality control and dynamic measurement. It is of especial use in forensic analysis in both criminal and civil cases, enabling identification of polymer degradation for example. It is perhaps the most widely used method of applied spectroscopy [346].

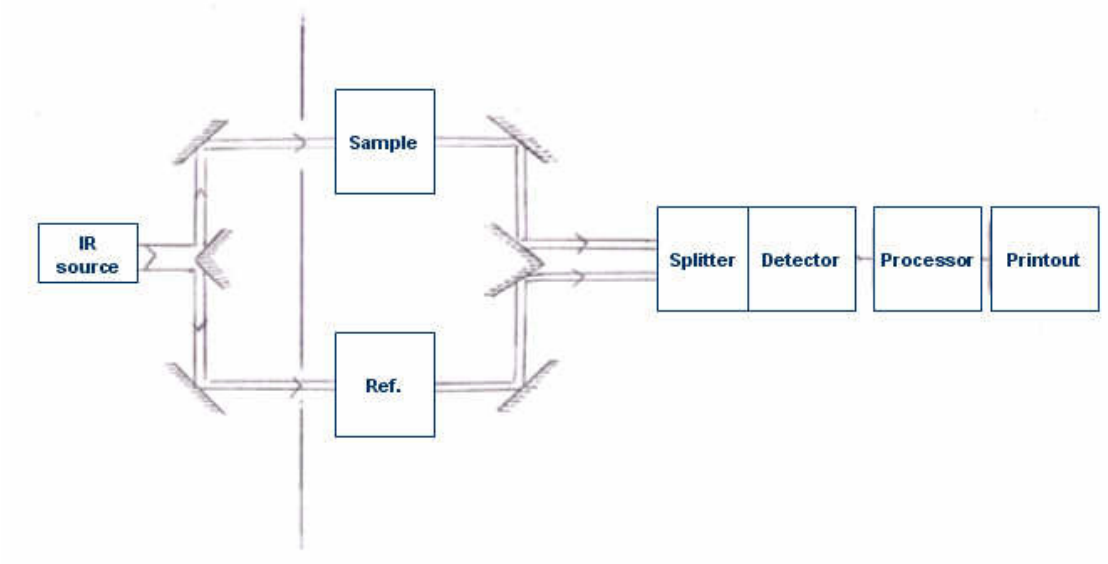

Figure 1.27: IR spectroscopy apparatus [333].

1.8.2.5 Ultraviolet-visible spectroscopy

Ultraviolet-visible spectroscopy (UV-Vis) involves the spectroscopy of photons in the UV-visible region. The absorption in the visible ranges directly affects the color of the chemicals involved. In this region of the electromagnetic spectrum, molecules undergo electronic transitions. Absorption of photons of light measures transitions from the ground state to the excited state. UV/Vis spectroscopy is routinely used in the quantitative determination of solutions of transition metal ions and highly conjugated organic compounds [333, 334].

1.9 Overview of Analytical Probes Used in this Work

1.9.1 Hydrazine

Electro-oxidation of hydrazine (N_2H_4) on carbon surfaces has continued to receive significant research interests [36 - 45] due to the extensive applications of hydrazine and its derivatives in a plethora of areas relating to chemical industry, military, agriculture and pharmaceuticals. Hydrazine is regarded an important anodic material for fuel cell and used for zero-emission fuel cells, it is also used as a fuel in high energy-energy propellant in rockets and spacecrafts by the military and aerospace industries [41,335]. On the negative side, hydrazine and its methyl derivatives have been implicated as potential carcinogens, mutagens and hepatotoxic substances that could cause liver and kidney damages [336]. Also, in 2003, hydrazine was implicated in terrorist incident [337]. It could be said therefore that it is this dual purpose of hydrazine as useful materials in several applications such as fuel cell development and as hazardous substances that underpins the need to investigate its electro-oxidative behaviour at low cost and easily available carbon electrodes.

Despite huge literature on the electro-oxidation of hydrazine on carbon based electrodes [36-45], the use of carbon nanotubes decorated with metal nanoparticle is limited. Hitherto, all attention on CNT-supported metal nanoparticles, as evident in the recent review by Wildgoose *et al*. [338], has been directly only on metals such as Pt, Pd, Ru, Ag and Au. It has also been constantly reported that HiPCo, MWCNTs and SWCNTs are inherently contaminated with iron nanoparticles thus explaining why "electrocatalysis" observed on such CNT-based carbon electrodes [339-342] for certain analytes, including hydrazine [340] are/could be strongly influenced by the iron nanoparticle impurities. More recently, however, Kruusma *et al.* [340] demonstrated that HiPCo SWCNTs contain

residual iron oxide impurities which dominated their electrochemical activity towards the detection of hydrogen peroxide and hydrazine. Given the ability of iron impurities in CNTs to influence electro-oxidation of hydrazine [340], it could be interesting to explore the electrochemical response of metal-decorated SWCNTs ('deliberate metal impurification') towards the electro-oxidation of hydrazine and this form part of the investigation carried out in this study. To the best of my knowledge, no consideration has been given to this type of investigation, especially with nickel and iron nanoparticles which have been established to be the major impurities of SWCNTs.

1.9.2 Diethylaminoethanethiol

Chemical warfare agents are toxic chemical substances used by terrorists with the intention to kill, injure or incapacitate their perceived enemies. Under the provisions of the Chemical Weapons Convection [343], such agents are regarded as the "poor man's atomic bomb because of the low cost and the low technology required to develop them [343]. It is known that about 70 different chemicals have been used or stockpiled as chemical weapon agents during the 20th and 21st century. Notable of these agents are the so-called V-type (i.e., VE, VG, VM and VX) nerve agents [343,344]. The V-type nerve agents are considered more dangerous because they are more persistent, do not easily evaporate into a gas, and therefore present primarily a contact hazard to man. One of the main thiol hydrolysis products (Equation 1.32) of the V-type nerve agents is the 2-diethylaminoethanethiol (DEAET) [344].

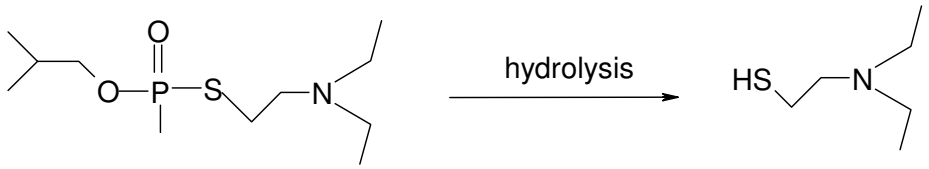

(1.32)

R-VX

Diethylaminoethanethiol(DEAET)

2-diethylaminoethanethiol (DEAET) is a thiol compound, a well known degradation product of the V-type nerve agent [343-345]. Since, DEAET is more stable in the aqueous environment than its parent Russian analogue of the V-type nerve agent, called R-VX (i.e.,*O*-isobutyl-*S*-(2-diethylaminoethyl)methylphosphonothioate), it serves as one of the excellent models for electrochemical detection and interrogation of the behaviour of the R-VX nerve agent or thiol compounds at electrode surface. Although several methods including chromatography, mass spectrometry and electrochemistry are common for the detection of thiols, the use of such analytical methods for the detection of the hydrolysis products of V-type nerve agents is still hugely unexplored. Few reports involving electrophoresis [346,347] and electrochemical techniques [28,106,107,348] have emerged for the detection of DEAET. Some of the reported techniques are fraught with some notable drawbacks such as the employment of unstable enzyme materials, time-consuming electrode preparation involving chemical pre-treatments and derivatizations. Also, electrochemical oxidation of thiols at conventional electrodes occurs at very high potential, thus the need for chemically modified electrodes cannot be overemphasised. Therefore, this study explored the detection of DEAET on CNT-metal nanocomposite platform. The study also represent the first time the catalytic behaviour of this nanocomposite on EPPG electrode will be investigated. To the best of my knowledge, there has been no report on the use of electrodes modified with nickel nanoparticle-decorated carbon nanotubes for the detection of degradation products of V-type nerve agents. Indeed, compared to transition metals, nickel is not a popular redox-mediator in electroanalysis. But it was observed previously that surface-confined nickel micropowder (ca. 17 – 60 mm range) immobilized on basal plane pyrolytic graphite electrode showed good electrocatalytic response towards DEAET

1.9.3 Nitrite

Nitrite ion is important as it is commonly used as an additive in some foods [349]. Other uses include color fixative and preservation in meats, manufacturing diazo dyes, in the textile industry, photography, manufacture of rubber chemicals, fertilizers in agriculture [350] and medicinal agents (used as a vasodilator [351], bronchodilator [352], intestinal relaxant [353]. It can be formed as a result of the degradation of some fertilizers and corrosion inhibitor [354]. Nitrite is one of the major components of waste water from nuclear power production [355] and is involved in the bacterial process known as the nitrogen cycle [356]. It also plays important physiological roles in the form of NO, for example, as an intra- and messenger, a neurotransmitter, and an immune system mediator [349]. Nitrite promotes corrosion when dissolved in water and is also classified as an environmentally hazardous species because of its toxicity [357]. The ions can interact with amines to form carcinogenic nitrosamines [358].

Due to the importance of nitrite in the environmental sciences and in food chemistry, a large number of analytical methods have been used to determine nitrite ions, including spectrophotometry [359-362], chromatography [363] and electrochemical methods [364-366] in recent years but with some shortcomings such as interference by other ions and complicated sample pre-treatment process, unsuitability for on-site monitoring and inability for detoxification. Electrochemical methods offer useful alternative since they allow a faster and precise analysis [59,367,368]. In order to tackle this problems, devices which are simple, inexpensive, stable and having the potential for the detoxification of these molecules are highly in demand. Electrochemical devices fall into this category, therefore electrocatalytic oxidation of nitrite on CNT/M or CNT/MO EPPGE modified electrode is reported in this study for the first time.

1.9.4 Dopamine

Dopamine (DA) is a biological molecule formed as a result of the decarboxylation of 3, 4- dihydroxy phenylalanine. It acts as a neurotransmitter in both the central and peripheral nervous system. Dopamine level can be as high as 50 nmol/g in the mammalian central nervous system in a region of the brain known as the "caudate nucleus" [182]. Low concentration of this compound in the extra cellular fluid of the caudate nucleus or its complete depletion has been associated with a disease called Parkinson's disease in which the patient suffers ability to having control over his movement [183]. Other diseases resulting from the abnormal metabolism of dopamine include epilepsy, senile dementia and HIV infection [185, 369,370]. Thus, it becomes imperative that the fabrication of a sensor that will determine the presence of this molecule in human fluid should be the focus of neuro-scientist. More importantly, because of the interfering effect of this molecule with other biological molecules such as ascorbic acid (AA) and uric acid (UA), fabrication of a very sensitive and selective analytical sensor has been a major challenge in its detection.

Several analytical techniques have been used in the past for DA detection but each with one disadvantage or the other. Electrochemical methods have also been employed with the use of different electrodes as sensors such as nanostructure material in polymer matrix (e.g. gold nanoparticles on polymer matrix) [371,372], GC/ Nafion/ NanoPt [372], carbon nanotube [183,373], ordered mesoporous carbon [183,374], carbon ionic liquid [183,375] and so on are among several carbon based materials that have been used for the electrochemical determination and separation of DA and AA. Generally, the electrochemical techniques have proven to be the more effective analytical method for determination of biological molecules including DA and AA. However, despite the success of the different electrochemical

technique used so far, there is a need for an effective, efficient, simple and low cost sensor that will selectively determine DA in the presence of AA and UA in biological fluid. Therefore, in this study, an iron oxide carbon nanotubes modified electrode (EPPGE) was fabricated. The electrode conveniently detects DA in the presence of 1000 times AA concentration.

References

1. P.G. Wiles, J. Abrahamson, *Carbon* 6 (1978) 341.

2. S. Iijima, *Nature* 354 (1991) 56.

3. M. Majumder, N. Chopra, R. Andrews, B.J. Hinds, *Nature* 438 (2005) 930.

4. R.H. Baughman, A.A. Zakhidov, W.A. de Heer, *Science* 297 (2002) 787.

5. J.J. Davis, R.J. Coles, H. Allen, O. Hill., *J. Electroanal Chem.* 440 (1997) 279.

6. H. Luo, Z. Shi, N. Li, Z. Gu, Q. Zhuang, *Anal Chem*. 73 (2001) 915.

7. J.M. Nugent, K.S.V. Santhanam, A. Rubio, P.M. Ajayan, *Nano Lett.* 1 (2001) 87.

8. S.J. Tans, A.R.M. Verschueren, C. Dekker, *Nature* 393 (1998) 49.

9. C. Liu, Y.Y. Fan, M. Liu, H.T. Cong, H.M. Cheng, M.S. Dresselhaus, *Science* 286 (1999) 1127.

10. C.Y. Liu, A.J. Bard, F. Wudl, I. Weitz, J.R. Heath, *Electrochem. Solid State Lett.* 2 (1999) 577.

11. J.S. Ye, X. Liu, H.F. Cui, W.D. Zhang, F.S. Sheu, T.M. Lim, *Electrochem. Commun.* 7 (2005) 249.

12. J.J. Gooding, *Electrochim. Acta* 50 (2005) 3049.

13. N.L. Pocard, D.C. Alsmeyer, R.L. McCreery, T.X. Neenan, M.R. Callstrom, *J. Mater. Chem.* 2 (1992) 771.

14. M.Musameh, J.Wang, A.Merkoci, Y. Lin, *Electrochem.Commun.* 4 (2002) 743.

15. Y.-C. Weng, J.F. Rick, T.-C. Chou, *Biosens. Bioelectron.* 20 (2004) 41.

16. A. Salimi, E. Sharifi, A. Noorbakhsh, S. Soltanian, *Biosens. Bioelectron.* 22 (2007) 3146.

17. A.R. Tao, S. Habas, P.D. Yang, *Small* 4 (2008) 310.

18. C.J. Murphy, A.M. Gole, S.E. Hunyadi, J.W. Stone, P.N. Sisco, A. Alkilany, B.E. Kinard, P. Hankins, *Chem. Comm.* 5 (2008) 544.

19. A. Salimi, R. Hallaj, H. Mamkhezri, S. Mohamad, T. Hosaini, J. *Electroanal. Chem.* 619 (2008) 31.

20. X. Zhang, K.-Y. Tsang, K.-Y. Chan, *J. Electroanal. Chem.* 573 (2004) 1.

21. S.M.A. Shibli, K.S. Beenakumari, N.D. Suma, *Biosens. Bioelectron.* 22 (2006) 633.

22. M. Vidotti, M.R. Silva, R.P. Salvador, S.I. C´ordoba de Torresi, L.H. Dall'Antonia, *Electrochim. Acta* 53 (2008) 4030.

23. R.J. Aitken, M.Q. Chaudhry, A.B.A. Boxall, M. Hull, *Occup. Med.* 56 (2006) 300.

24. B. Nowack, T.D. Bucheli, *Environ. Pollut.* 150 (2007) 5.

25. A. Balamurugan, G. Sockalingum, J. Michel, J. Faure, V. Banchet, L. Wortham, S. Bouthors, D. Laurent-Maquin, G. Balossier, *Mater. Lett.* 60 (2006) 3752.

26. N. Laosiripojana, W. Sutthisripok, S. Assabumrungrat, *Chem. Eng. J.* 112 (2005) 13.

27. K.I. Ozoemena, J. Pillay, T. Nyokong, *Electrochem. Commun.* 8 (2006) 1391.

28. J. Pillay, K.I. Ozoemena, *Electrochim. Acta* 52 (2007) 3630.

29. B.S. Sherigara, W. Kutner, F. D'Souza, *Electroanalysis* 15 (2003) 753.

30. A. Salimi, C.E. Banks, R.G. Compton, *Analyst* 129 (2004) 225.

31. V. Selvaraj, M. Alagar, K. Sathish Kumar, *Appl. Cat. B: Environm.* 75 (2007) 129.

32. L. Zhang, Z. Fang, G.-C. Zhao, X.-W. Wei, *Int. J. Electrochem. Sci.*, 3 (2008) 746.

33. M. Yang, Y. Yang, Y. Liu, G. Shen, R. Yu, *Biosens. Bioelectron*, 21 (2006) 1125.

34. D.G. Rickerby, M. Morrison, *Sci. Technol. Adv. Mater.* 8 (2007) 19.

35. J. Pillay, K.I. Ozoemena, *Electrochem. Commun.* 9 (2007) 1816.

36. C. Lin, A.B. Bocarsly, *J. Electroanal. Chem. Interfacial Electrochem.* 300 (1991) 325.

37. H. Razmi-Nerbin, M.H. Pournaghi-Azar, *J. Solid State Electrochem.* 6 (2002) 126.

38. Y-D. Zhao, W.-D. Zhang, H. Chen, Q-M. Luo, *Talanta* 58 (2002) 529.

39. D. Geraldo, C. Linares, Y-Y. Chen, S. Ureta-Zanartu, J.H. Zagal, *Electrochem. Commun.* 4 (2002) 182.

40. M.H. Pournaghi-Azar, R. Sabzi *J. Electroanal. Chem.* 543 (2003) 115.

41. K. Yamada, K. Asazawa, K. Yasuda, T. Loroi, H. Tanaka, Y. Miyazaki, T. Kobayashi, *J Power Sources* 115 (2003) 236.

42. C. Linares, D. Geraldo, M. Paez, J.H. Zagal, *J. Solid State Electrochem.* (2003) 7: 626-631.

43. K.I. Ozoemena, *Sensors* 6 (2006) 874.

44. M. Revenga-Parra, E. Lorenzo, F. Pariente, *Sens. Actuators* B 107 (2005) 678.

45. G.I. Cardenas-Jiron, V. Paredes-Garcia, D. Venegas-Yazigi, J.H. Zagal, M. Paez, J. Costamagna, *J. Phys. Chem.* A 110 (2006) 11870.

46. X. Ji, C.E. Banks, A.F. Holloway, K. Jurkschat, C.A. Thorogood, G.G. Wildgoose, R.G. Compton, *Electroanalysis* 18 (2006) 2481.

47. X. Wang, N. Yang, Q. Wan, X. Wang, *Sens. Actuators* B 128 (2007) 83.

48. D.-M. Zhou, H.-X. Ju, H.-Y. Chen, *J. Electroanal. Chem.*, 408 (1996) 219.

49. M.H. Pournaghi-Azar, R. Ojani, *Talanta* 42 (1995) 1839.

50. H. Razmi, M. Agazadeh, B. Habibi-A, *J. Electroanal. Chem.*, 547 (2003) 25.

51. H. Razmi, A. Azadbakht, Electrochim. Acta 50 (2005) 2193.

52. J.-J. Sun, J.-J. Xu, H.-Q. Fang, H.-Y. Chen, *Bioelectrochem. Bioenergetics* 44 (1997) 45.

53. M. Mazloum-Ardakani, H. Beitollahi, B. Ganjipour, H. Naeimi, M. Nejati, *Bioelectrochem.* 75 (2009) 1.

54. R.K. Shervedani, M. Bagherzadeh, S.A. Mozaffari, *Sens. Actuators B* 115 (2006) 614.

55. L.S. Rocha, H.M. Carapuça, *Bioelectrochem.* 69 (2006) 258.

56. M.A. Kamyabi, Z. Asgari, H. Hosseini Monfared, A. Morsali, *J. Electroanal. Chem.* 632 (2009) 170.

57. M.A. Kamyabi, F. Aghajanloo, *J. Electroanal. Chem.* 614 (2008) 157.

58. J. Lei, H. Ju, O. Ikeda, *J. Electroanal. Chem.* 567 (2004) 331.

59. M.H Pournaghi-Azar, H. Dastangoo, *J. Electroanal. Chem.* 567 (2004) 211.

60. J.L. Manzoori, M.H. Sorouraddin, A.M. Haji-Shabani, *Talanta* 46 (1998) 1379.

61. P. Tau, T. Nyokong, *J. Electroanal. Chem.* 611 (2007) 10.

62. W.S. Cardoso, Y. Gushikem, *J. Electroanal. Chem.* 583 (2005) 300.

63. A. Salimi, H. Mamkhezri, S. Mohebbi, *Electrochem. Commun.* 8 (2006) 688.

64. D. Zheng, C. Hu, Y. Peng, S. Hu, *Electrochim. Acta* 54 (2009) 4910.

65. C. Xia, W. Ning, G. Lin, *Sens. Actuators B* 137 (2009) 710.

66. W.J.R. Santos, P.R. Lima, A.A. Tanaka, S.M.C.N. Tanaka, L.T. Kubota, *Food Chemistry* 113 (2009) 1206.

67. Z. Wang, Q. Liang, Y.Wang, G. Luo, *J. Electroanal. Chem.* 540 (2003) 129.

68. F.H. Wu, G.C. Zhou, X.W. Wei, *Electrochem. Commun.* 4 (2002) 690.

69. R.P. Deo, N.S. Lawrence, J.Wang, *Analyst* 129 (2004) 1076.

70. W. Li, C. Liang, W. Zhou, J. Qiu, Z. Zhou, G. Sun, Q. Xin, *J. Phys. Chem. B* 107 (2003) 6292.

71. Y. Liu, Y-L. Yan, J. Lei, F. Wu, H. Ju, *Electrochem. Commun.* 9 (2007) 2564.

72. S. A. Mamuru, K.I. Ozoemena, *Mat. Chem. Phys.* 114 (2009) 113.

73. A. Kaushik, P.R. Solanki, A.A. Ansarib, B.D. Malhotra, S. Ahmad, *Biochem. Eng. J.* 46 (2009) 132.

74. A. Kaushik, P.R. Solanki, A.A. Ansari, G. Sumana, S. Ahmad, B.D. Malhotra, *Sens. Actuators B* 138 (2009) 572.

75. S. Zhang, X. Zhao, H. Niu, Y. Shi, Y. Cai, G. Jiang, *J. Hazardous Mat.* 167 (2009) 560.

76. F. Moura, G.C. Oliveira, M.H. Araujo, J.D. Ardisson, W.A.A. Macedob, R.M. Lago, *Applied Catalysis A: General* 307 (2006) 195.

77. A. Salimi, R. Hallaj, S. Soltanian, *Biophysical Chem.* 130 (2007) 122.

78. M. Khodzitskiya, L. Lutsevb, S. Tarapova, A. Zamkovojc, A. Stognijd, N. Novitskii, *J. Magnetism Magnetic Materials* 320 (2008) L37.

79. W. Tao, D. Pan, Y. Liu, L. Nie, S. Yao, *Anal. Biochem.* 338 (2005) 332.

80. G. Burgot, F. Auffret, J.L. Burgot, *Anal. Chim. Acta* 343 (1997) 125.

81. A.B. Moreira, H.P.M. Oliveira, T.D.Z. Atvars, I.L.T. Dias, G.O. Neto, E.A.G. Zagatto, L.T. Kubota, *Anal. Chim. Acta* 539 (2005) 257.

82. W. Peng, T. Li, H. Li, E. Wang, *Anal. Chim. Acta* 298 (1994) 415.

83. D.A. Kippen, F. Cerini, L. Vadas, R. St¨ocklin, L. Vu, R.E. Offord, K. Rose, *J. Biol. Chem.* 272 (1997) 12513.

84. R.G. Compton, C.E. Bank , *Understanding Voltammetry*, World Scientific Publishing Co. Pte. Ltd. WC2H 9HE UK, 2007.

85. A.J. Bard, L.R. Faulkner, *Electrochemical Methods: Fundamentals and Applications*, 2nd Ed., John Wiley & Sons, Hoboken NJ 2001.

86. J. Wang, *Analytical Electrochemistry*, VCH Publisher Inc., New York (1994).

87. K. Peter; W.R. Heineman, *Laboratory Techniques in Electroanalytical Chemistry,* Second Edition, Revised and Expanded (2 ed.) CRC. (1996).

88. C.G. Zoski. *Handbook of Electrochemistry*. Elsevier Science (2007).

89. http://en.wikipedia.org/wiki/File:Three_electrode_setup.png (Acessible online, April 5, 2009).

90. P.A. Christenson, A. Hamnet, *Techniques and Mechanisms in Electrochemistry*, 1st ed, Blackie Academic and Professional, London, 1994.

91. J.E.B. Randles, *Trans. Faraday Soc*. 44 (1948) 327.

92. R.S. Nicholson, I. Shain, *Anal. Chem.* 36 (1964) 1351.

93. W.R. Heineman, P.T. Kissinger in *Laboratory Techniques in Electroanalytical Chemistry,* 2nd ed., eds. P.T. Kissinger and W.R. Heineman, Marcel Dekker Inc., New York, 1996.

94. M.L. Foresti, R. Guidelli, L. Nyholm *J. Electroanal. Chem.* 269 (1989) 27.

95. L. Ramaley, M. S. Krause, Jr., *Anal. Chem.* 41 (1969) 1362.

96. J. Osteryoung, *Accts. Chem. Res.* 26 (1993) 77.

97. R.A. Osteryoung, J. Osteryoung, *Phil. Trans. Roy. Soc. London, Ser. A* 302 (1981) 315.

98. J. Wang, D.B. Luo, P.A.M. Farias, J.S. Mahmoud, *Anal. Chem.* 57 (1985) 158.

99. J.G. Osteryoung, R.A. Osteryoung, *Anal. Chem*. 57 (1985) 101A.

100. B.E. Conway, *J. Electrochem.* 138 (1991) 1539.

101. B.E. Conway, V. Birss, J. Wojtowicz, J. of Power Sources 66 (1997) 1.

102. E. Barsoukov, J.R. Macdonald, *Impedance Spectroscopy, Theory, Experiment, and Applications*, 2nd Edn. John Wiley and Sons Inc., New Jersey, 2005.

103. J.R. Macdonald, Ed., *Impedance Spectroscopy Emphasizing Solid Materials and Systems*, Wiley/Interscience, New York, 1987.

104. E. Katz and I. Wilner, *in: Ultrathin Electrochemical Chemo- and Biosensors. Technology and Performance*, V.M. Mirsky Ed. Springer- Verlag, New York, 2004, pp. 68–116, Chapter 4.

105. J.R. Macdonald, W.B. Johnson in : E. Barsoukov, J.R. Macdonald (Eds.), *Impedance Spectroscopy*, 2nd ed., John Wiley and Sons Inc., 2005.

106. K.A. Joshi, M. Prouza, M. Kum, J. Wang, J. Tang, R. Haddon, W. Chen, A. Mulchandani, *Anal. Chem.* 78 (2006) 331.

107. O.V. Shoulga, C. Palmer, *Anal. Bioanal. Chem.* 385 (2006) 1116.

108. Q. He, W. Chen, S. Mukerjee, S. Chen, F. Laufek, *J. Power Sources* 187 (2009) 298.

109. J.J. Feng, J.J. Xu, H.Y. Chen, *J. Electroanal. Chem.* 585 (2005) 44.

110. W. Chen, L.-P. Xu, S. Chen, *J. Electroanal. Chem.* 631 (2009) 36.

111. S. Chen, *J. Electroanal. Chem.* 574 (2004) 153.

112. V. Ganesh, S. Pitchumani, V. Lakshminarayanan, *J. Power Sources* 158 (2006) 1523.

113. J. Bisquert, H. Randriamahazaka, G. Garcia-Belmonte, *Electrochim Acta* 51 (2005) 627.

114. M. Jafarian, M.G. Mahjani, H. Heli, F. Gobal, H. Khajehsharifi, M.H. Hamedi, *Electrochim Acta* 48 (2003) 3423.

115. S. Majdi, A. Jabbari, H. Heli, A.A. Moosavi-Movahedi *Electrochim. Acta* 52 (2007) 4622.

116. Research Solutions & Resources available online at: http://www.consultrsr.com/resources/eis/induct2.htm (accessed 0nline, 24 February 2008).

117. User Manual for Frequency Response Analysis (FRA) for Windows version 4.9, Eco Chemie B.V., Utrecht, The Netherlands, 200 and references therein.

118. B.A. Boukamp, *J. Electrochem. Soc.* 142 (1995) 1885.

119. G. Nurk, H. Kasuk, K. Lust, A. Janes, E. Lust, *J. Electroanal. Chem.* 553 (2003) 1.

120. F. Zhi, X. Lu, Y. Jiandong, X. Wang, H. Shang, S. Zhang, X. Zhongua, *J. Phys. Chem. C* 113 (2009) 13166.

121. Craig E. banks, R.G. Compton, *Analyst* 131 (2006) 15.

122. R.R. Moore, C.E. Banks, R.G. Compton, *Analyst* 129 (2004) 755.

123. C.E. Banks, A. Goodwin, C.G.R. Heald, R.G. Compton, *Analyst*, 130 (2005) 280.

124. C.E. Banks, R.G. Compton, *Analyst* 130 (2005) 1232.

125. E.R. Lowe, C.E. Banks, R.G. Compton, *Anal. Bioanal. Chem.*, 382 (2005) 1169.

126. E.R. Lowe, C.E. Banks, R.G. Compton, *Electroanalysis*, 17 (2005) 1627.

127. F. Wantz, C.E. Banks, R.G. Compton, *Electroanalysis*, 17 (2005) 1529.

128. C.M. Welch, C.E. Banks, S. Komorsky-Lovric, *Croat. Chim. Acta* (in press).

129. F. Wantz, C.E. Banks, R.G. Compton, *Electroanalysis* 17 (2005) 655.

130. G. Gao, *Nanostructures and nanomaterials. Synthesis, Properties & Applications.* London: Imperial College Press; 2004.

131. T.W. Ebbesen, *Ann. Rev. Mater. Sci.* 24 (1994) 235.

132. M. Paradise, T. Goswami, Mater. Des. 28 (2007) 1477.

133. M. Endo, K. Takeuchi, S. Igarashi, K. Kobori, M. Shiraishi, H.W. Kroto, J. Phys. Chem. Solids 54 (1993) 1841.

134. W.K. Hsu, J.P. Hare, M. Terrones, H.W. Kroto, D.R.M. Walton, P.J.F. Harris, *Nature* 377 (1995) 687.

135. S. Arepalli, P. Nikolaev, W. Holmes, B.S. Files, *Appl. Phys. Lett.* 78 (2001) 1610.

136. S. Ijima, T. Ichihashi, *Nature* 363 (1993) 603.

137. Rubianes, G.A. Rivas, *Electrochem. Commun.* 9 (2007) 480.

138. F. Valentini, A. Amine, S. Orlanducci, M.L. Terranova, G. Palleschi, *Anal. Chem.* 75 (2003) 5413.

139. N. Maleki, A. Safavi, F. Tajabadi, *Anal. Chem.* 78 (2006) 3820.

140. R.S. Chen, W. Huang, H.Tong, Z. Wang, J. Cheng, *Anal. Chem.* 75 (2003) 6341.

141. A. Abbaspour, A. Izadyar, *Talanta* 71 (2007) 887.

142. H. R. Zare, N. Nasirizadeh, F. Chatraei, S. Makarem, *Electrochim. Acta* 54 (2009) 2828.

143. J. Wang, M. Musameh, *Analyst* 11 (2003) 1382.

144. M. Musameh, J. Wang, A. Merkoci, Y. Lin, *Electrochem. Commun.* 4 (2002) 743.

145. Z. Wang, Q. Liang, Y. Wang, G. Luo, *J. Electroanal. Chem.* 540 (2003) 129.

146. F.H. Wu, G.C. Zhou, X.W. Wei, *Electrochem. Commun.* 4 (2002) 690.

147. H. Luo, Z. Shi, N. Li, Z. Gu, Q. Zhuang, *Anal. Chem.* 73 (2001) 915.

148. J. Wang, M. Mosameh, Y. Lin, *J. Am. Chem. Soc.* 125 (2003) 2408.

149. G. Selvarani, S.K. Prashant, A.K. Sahu, P. Sridhar, S. Pitchumani, A.K. Shukla, *J. Power Sources* 178 (2008) 86.

150. K.C. Pan, C.S. Chuang, S.H. Cheng, Y.O. Su, *J. Electroanal. Chem.* 501 (2001) 160.

151. M.Y. Elahi, M.F. Mousavi, S. Ghasemi, *Electrochim. Acta* 54 (2008) 490.

152. S. Griveau, J. Pavez, J.H. Zagal, F. Bedioui, *J. Electroanal. Chem.* 497 (2001) 75.

153. Y. Liu, Y.-L. Yan, J. Lei, F. Wu, H. Ju, *Electrochem. Commun.* 9 (2007) 2564.

154. A. Salimi, M. Roushani, B. Haghighi, S. Soltanian, Biosens. Bioelectron. 22 (2006) 220.

155. S. Remita, M. Mostafavi, M.O. Delcourt, Radiat. Phys. Chem. 47 (1996) 275.

156. J.H. Hodak, A. Henglein, M. Giersig, G.V. Hartland, *J. Phys. Chem. B* 104 (2000) 11708.

157. Y. Mizukoshi, K. Okitsu, Y. Maeda, T.A. Yamamoto, R. Oshima, Y. Nagata, *J. Phys. Chem. B* 101 (1997) 7033.

158. M. Brust, M.Walker, D. Bethell, D.J. Schiffrin, R.Whyman, *J. Chem. Soc. Chem. Commun.* 7 (1994) 801.

159. K. Osseo-Asare, F.J. Arriagada, *Ceram. Trans.* 12 (1990) 3.

160. L.K. Kurihara, G.M. Chow, P.E. Schoen, *Nanostruct. Mater.* 5 (1995) 607.

161. H.H. Huang, X.P. Ni, G.L. Loy, C.H. Chew, K.L. Tan, F.C. Loh, J.F. Deng, G.Q. Xu, *Langmuir* 12 (1996) 909.

162. M. Yang, J. Jiang, Y. Lu, Y. He, G. Shen, R. Yu, *Biomaterials* 28 (2007) 3408.

163. S. Wang, Q. Xu, G. Liu, *Electroanalysis* 20 (2008) 1116.

164. J. Hrbac, V. Halouzka, R. Zboril, K. Papadopoulos, T. Triantis, *Electroanalysis* 19 (2007) 1850.

165. M. Vidotti, M.R. Silva, R.P. Salvador, S.I. Cordoba de Torresi, L.H. Dall'Antonia, *Electrochim. Acta* 53 (2008) 4030.

166. C. Ding, F. Zhao, M. Zhang, S. Zhang, *Bioelectrochem.* 72 (2008) 28.

167. A. Abbaspour, A. Khajehzadeh, A. Ghaffarinejad, *J. Electroanal. Chem.* 631 (2009) 52.

168. A.B. Moghaddam, M.R. Ganjali, R. Dinarvand, T. Razavi, A. A. Saboury, A.A. Moosavi-Movahedi, Parviz Norouzi, *J. Electroanal. Chem.* 614 (2008) 83.

169. P.R. Somani, S. Radhakrishnan, *Mater. Chem. Phys.* 77 (2003) 117.

170. M. Taguchi, K. Yamada, K. Suzuki, O. Sato, Y. Einaga, *Chem. Mater.* 17 (2005) 4554.

171. D.M. DeLongchamp, P.T. Hammond, *Adv. Funct. Mater.* 14 (2004) 224.

172. M. Pyrasch, A. Toutianoush, W.Q. Jin, J. Schnepf, B. Tieke, *Chem.Mater.* 15 (2003) 245.

173. M. Jayalakshimi, F. Scholz, *J. Power Sources* 87 (2000) 212.

174. F. Qu, A. Shi, M. Yang, J. Jiang, G. Shen, R. Yu, *Anal. Chimic Acta* 605 (2007) 28.

175. S.J. Nakanishi, G.T. Lu, , H.M. Kothari, E.W. Bohannan, J.A. Switzer, *J. AM. Chem. Soc.* 125 (2003) 14998.

176. J.M. Zen, P.Y. Chen, A.S. Kumar, *Anal. Chem.* 75 (2003) 6017.

177. S. Han, Y. Chen, R. Pang, P. Wan, *Ind. Eng. Chem. Res.* 46 (2007) 6847.

178. W. Zhao, J.J. Xu, C.G. Shi, H.Y. Chen. *Langmuir* 21 (2005) 9630.

179. Y. Xian, Y. Zhoua, Y. Xian, L. Zhouc, H. Wang , L. Jin, *Anal. Chimic. Acta* 546 (2005) 139.

180. Y. Miao, J. Chen, X. Wu, J. Miao, *Colloids Surfaces A*: *Physicochem. Eng. Aspects* 295 (2007) 135.

181. A-M Gurban, T. Noguer, C. Bala, L. Rotariu, *Sens. Actuat. B* 128 (2008) 536.

182. S. Thiagarajan, S. Chen, *Talanta* 74 (2007) 212.

183. G. Xu, M. Xu, J. Zhang, S. Kim, Z. Bae, *Bioelectrochem*. 72 (2007) 87.

184. O. Hornykiewicz, S.J. Kish, *Adv. Neurol.* 45 (1986) 19.

185. X. Cao, L. Luo, Y. Ding, X. Zou, R. Bian, *Sens. Actuator* 129 (2007) 941.

186. S. Wang, F. Xie, R.-F. Hu, (2006). *Sens. Actuators* B 123 (2007) 495.

187. G.-R. Xu, M.-L. Xu, J.-M. Zhang, S. Kim, Z.-U. Bae, *Bioelectrochem.* 72 (2008) 87.

188. A. Salimi, M. Roushani, *Electrochem. Commun.* 7 (2005) 879.

189. Y.C. Weng, J.F. Rick, T.C. Chou, *Biosens. Bioelectron.* 20 (2004) 41.

190. A. Salimi, M. Roushani, R. Hallaj, *Electrochim. Acta* 51 (2006) 1952.

191. D. Giovanelli, N.S. Lawrence, S.J. Wilkins, L. Jiang, T.G.J. Jones, R.G. Compton, *Talanta* 61 (2003) 211.

192. M.R. Ganjali, P. Norouzi, F. Faridbod, M. Yousefi, L. Naji, M. Salavati-Niasari, *Sens. Actuators B* 120 (2007) 494.

193. Z.-H. Wang, L.-L. Zhang, K.-Y. Qiu, *J. Power Sources* 161 (2006) 133.

194. J. Obirai, F. Bedioui, T. Nyokong, *J. of Electroanal. Chem.* 576 (2005) 323.

195. Y.Y. Liao, T.C. Chou, *Electroanalysis* 12 (2000) 55.

196. S. Lin, T.-C. Chou, *J. Electrochem. Soc.* 152 (2005) H53.

197. H.A. Zamani, F. Malekzadegan, M.R. Ganjali, *Anal. Chim. Acta* 555 (2006) 336.

198. S.J. Richard, S. Prabakar, S. Narayanan, *J. Electroanal. Chem.* 617 (2008) 111.

199. E.F. Perez, L.T. Kubota, A.A. Tanaka, G. De Oliveira Neto *Electrochim. Acta* 43 (1998) 1665.

200. Y.-C. Weng, J.F. Rick, T.-C. Chou, *Biosens. Bioelectron.* 20 (2004) 41.

201. A. Mohammadi, A.B. Moghaddam, M. Kazemzad, R. Dinarvand, J. Badraghi, *Mat. Sc. Eng. C* 29 (2009) 1752.

202. A. Salimi, E. Sharifi, A. Noorbakhsh, Saied Soltanian, *Electrochem. Commun.* 8 (2006) 1499.

203. A. Salimi, E. Sharifi, A. Noorbakhsh, S. Soltanian, *Biophys. Chem.* 125 (2007) 540.

204. A. Salimi, A. Noorbakhash, E. Sharifi, A. Semnani, *Biosens. Bioelectron.* 24 (2008) 792.

205. J. Ahmed, S. Sharma, K.V. Ramanujachary, S.E. Lofland, A.K. Ganguli, *J. Coll. Interf. Sci.* 336 (2009) 814.

206. R.K. Shervedani, A.R. Madram, *INTERN. J. HYDROGEN ENERGY* 33 (2008) 2468.

207. Abdolmajid Bayandori Moghaddam, Mohammad Reza Ganjali, Rassoul Dinarvand, Sara Ahadi, Ali Akbar Saboury, *Biophys. Chem.* 134 (2008) 25.

208. Abdollah Noorbakhsh, Abdollah Salimi, *Electrochim. Acta* 54 (2009) 6312.

209. M. Jafarian, O. Azizia, F. Gobal, M.G. Mahjani, *International Journal of Hydrogen Energy* 32 (2007) 1686.

210. YuLin Min, YouCun Chen, YingGuo Zhao, Chao Chen, *Mat. Lett.* 62 (2008) 4503.

211. M. Yang, Y. Yang, F. Qu, Y. Lu, G. Shen, R. Yu, *Anal. Chim. Acta* 571 (2006) 211.

212. Q. Yi, W. Huang, J. Zhang, X. Liu, L. Li, *J. Electroanal. Chem.* 610 (2007) 163.

213. J. Qiao, S. Tang, Y. Tian, S. Shuang, C. Dong, M.M.F. Choi *Sens. Actuat. B* 138 (2009) 402.

214. M.V. Martı´nez-Huerta, S. Rojas, J.L. Go´mez de la Fuente, P. Terreros, M.A. Pen, J.L.G. Fierro, *Appl. Cat. B: Environmental* 69 (2006) 75.

215. Y.C. Weng, J.F. Rick, T.C. Chou, *Biosens. Bioelectron.* 20 (2004) 41.

216. S.H. Huang, M.H. Liao, D.H. Chen, *Biotechnol. Prog.* 19 (2003) 1095.

217. L. Josephson, J.M. Perez, R. Weissleder, *Angew. Chem. Int. Ed.* 40 (2001) 3204.

218. Z.H. Wang, C.J. Choi, B.K. Kim, J.C. Kim, Z.D. Zhang, *Carbon* 41 (2003) 1751.

219. L.M. Rossi, A.D. Quach, Z. Rosenzweig, Anal. Bioanal. Chem. 380 (2004) 606.

220. M. Pumera, M.T. Castaneda, M.I. Pividori, R. Eritja, A. Merkoci, S. Alegret, *Langmuir* 21 (2005) 9625.

221. R.W. Cornell e, U. Schwertmann, *The Iron Oxides*, VCH, Weinheim, 1996.

222. R.M. Cornell, U. Schwertmann, *The Iron Oxides: Structure, Properties, Reactions, Occurrences and Uses*, second ed. Wiley-VCH, Weinheim, 2003.

223. M. Siswana, K.I. Ozoemena, T. Nyokong, *Talanta* 69 (2006) 1136.

224. S. Wang, Q. Xu, X. Zhang, G. Liu, *Electrochem. Commun.* 10 (2008) 411.

225. P Yuan, H.-Q. Wu, H.-Y. Xu, D.-M. Xu, Y.-J. Cao, X.-W. Wei, *Mat. Chem. Phys.* 105 (2007) 391.

226. M. Wen, H. Qi, W. Zhao, J. Chen, L. Li, Q. Wu, *Coll. Surf. A: Physicochem. Eng. Aspects* 312 (2008) 73.

227. M. Gangeri, S. Perathoner, S. Caudo, G. Centi, J. Amadou, D. Begin, C. Pham-Huu , M.J. Ledoux , J.-P. Tessonnier, D.S. Su, R. Schlogl, *catalysis Today* 143 (2009) 57.

228. J. Wang, G. Liu, A. Merkoçi, *Anal. Chim. Acta* 482 (2003) 149.

229. A. Kaushika, R. Khana, P.R. Solankia, P. Pandeya, J. Alamb, S. Ahmadb, B.D. Malhotra, *Biosens. Bioelectrtn.* 24 (2008) 676.

230. S. Zhang, X. Zhao, H. Niu, Y. Shi, Y. Cai, G. Jiang, *J. Hazard. Mat.* 168(2009) 1.

231. J.-D. Qiu, M. Xiong, R.-P. Liang, H.-P. Peng, F. Liu, *Biosens. Bioelectron.* 24 (2009) 2649.

232. A. Kaushik, P.R. Solanki, A.A. Ansari, S. Ahmad, B.D. Malhotra, *Electrochem. Commun.* 10 (2008) 1364.

233. S. Qu, J. Wang, J. Kong, P. Yang, G. Chen, *Talanta* 71 (2007) 1096.

234. H.-L. Zhang, X.-Z. Zou, G.-S. Lai, D.-Y. Han, F. Wang, *Electroanalysis* 19 (2007) 1869.

235. H.-L. Zhang, X.-Z. Zou, G.-S. Lai, D.-Y. Han, F. Wang, *Electroanalysis* 19 (2007) 1869.

236. V. Saez, J. Gonzalez-Garcia, M.A. Kulandainatha, F. Marken, *Electrochem. Commun.* 9 (2007) 1127.

237. S.H. Joo, D. Zhao, *Chemosphere* 70 (2008) 418.

238. H. Gleiter, *Prog. Mater. Sci.* 33 (1989) 223.

239. J.P. Chen, C.M. Sorensen, K.J. Klabunde, G.C. Hadjipanayis, *Phys. Rev. B* 51 (1995) 11527.

240. K. Tanabe, *Mater. Lett.* 61 (2007) 4573.

241. S.I.C. deTorresi, K. Provazi, M. Malta, R.M.Torresi, *J. Electrochem. Soc.* 148 (2001) A1179.

242. V. Srinivasan, J.W. Weidner, *J. Power Sources* 108 (2002)15.

243. L.D. Kadam, S.H. Pawar, P.S. Patil, *Mater. Chem. Phys.* 68 (2001) 280.

244. H. Okabe, J. Akimitsu, T. Kubodera, M. Matoba, T. Kyomen, M. Itoh, Phys*. B Condens. Matter*. 378–380 (2006) 863.

245. J. Tyczkowski, R. Kapica, J. Lojewska, *Thin Solid Films* 515 (2007) 6590.

246. E. Villagra, F. Bedioui, T. Nyokong, J.C. Canales, M. Sancy, M.A. Paez, J. Costamagna, J.H. Zagal, *Electrochim. Acta* 53 (2008) 4883.

247. N. Sehlotho, S. Griveau, N. Ruille, M. Boujtita, T. Nyokong, F. Bedioui, *Mater. Sci. Eng.* C, 28 (2008) 606.

248. J. Arguello, H.A. Magosso, R. Landers, Y. Gushikem, *J. Electroanal. Chem.* 617 (2008) 45.

249. A. Salimi, H. Mamkhezri, R. Hallaj, S. Soltanian, *Sens. Actuators*, B 129 (2008) 246.

250. M.D. Abad, J.C. Sánchez-López, A. Berenguer-Murcia, V.B. Golovko, M. Cantoro, A.E.H. Wheatley, A. Fernández, B.F.G. Johnson, J. Robertson, *Diamond Relat. Mater.* 17 (2008) 1853.

251. Z. Dong, K. Ma, J. He, J.Wang, R. Li, J. Ma, *Mater. Lett.* 62 (2008) 4059.

252. M. Yang, J. Jiang, Y. Yang, X. Chen, G. Shen, R. Yu, *Biosens. Bioelectron.* 21 (2006) 1791.

253. J. Shen, Y. Hu, C. Li, C. Qin, M. Ye, *Electrochim. Acta* 53 (2008) 7276.

254. H. Zhao, L. Li, J. Yang, Y. Zhang, *Electrochem. Commun.* 10 (2008) 1527.

255. I.G. Casella, M.R. Guascito, *J. Electroanal. Chem.* 476 (1999) 54.

256. I.G. Casella, M. Gatta, *J. Electroanal. Chem.* 534 (2002) 31.

257. I.G. Casella, *J. Electroanal. Chem.* 520 (2002) 119.

258. L.F. Fan, X.Q. Wu, M.D. Guo, Y.T. Gao, *Electrochim. Acta* 52 (2007) 3654.

259. M. Jafarian, M.G. Mahjani, H. Heli, F. Gobal, H. Khajehsharifi, M.H. Hamedi, *Electrochim. Acta* 48 (2003) 3423.

260. Xin Zhang, Kwok-Ying Tsang, Kwong-Yu Chan, *J. Electroanal. Chem.* 573 (2004) 1.

261. A. Salimi, R. Hallaj, S. Soltanian, H. Mamkhezri, *Anal. Chim. Acta* 594 (2007) 24.

262. M. Hasanzadeh, G. Karim-Nezhad, N. Shadjou, M. Hajjizadeh, B. Khalilzadeh, L. Saghatforoush, M.H. Abnosi, A. Babaei, S. Ershad, *Anal. Biochem.* 389 (2009) 130.

263. M. Yang, J. Jiang, Y. Yang, X. Chen, G. Shen, R. Yu, *Biosens. Bioelectron.* 21 (2006) 1791.

264. K. Wang, J.-J. Xu, H.-Y. Chen, *Biosens. Bioelectron.* 20 (2005) 1388.

265. S. Shahrokhiana, M. Ghalkhania, M. Adeli, M.K. Amini, *Biosens. Bioelectron.* 24 (2009) 3235.

266. D. Cao, J. Chao, L. Sun, G. Wang, *J. Power Sources* 179 (2008) 87.

267. Y. Shi, B. Zhou, P. Wu, K. Wang, C. Cai, *J. Electroanal. Chem.* 611 (2007) 1.

268. E. Slavcheva, V. Nikolova, T. Petkova, E. Lefterova, I. Dragieva, T. Vitanov, E. Budevski, *Electrochim. Acta* 50 (2005) 5444.

269. K. Wang, J.-J. Xu, H.-Y. Chen, *Sens. Actuators* B, 114 (2006) 1052.

270. B.E. Conway, *Electrochemical SuperCapacitors*, Kluwer Academic/Plenum Publishers, New York, 1999.

271. M. Winter, R. J. Brodd, *Chem. Rev*. 104 (2004) 4245.

272. C. Peng, S. Zhang, D. Jewell, G.Z. Chen, *Prog. Nat. Sci.* 18 777 (2008).

273. T. Shinomiya, V. Gupta, N. Miura, *Electrochim. Acta* 51 (2006) 4412.

274. C-M Huang, C-H Hu, K-H Chang, J-M Li, Y-F Li, *J. Electrochem. Soc.* 156 (2009) A667.

275. P. Ghosh, S. Mahanty, R.N. Basu, *J. Electrochem. Soc.* 156 (2009) A681.

276. M. S. Wu, H-H. Hsieh, *Electrochim. Acta* 53 (2008) 3427.

277. V. Srinivasan, J.W. Weidner, *J. Electrochem. Soc.* 147 (2000) 880.

278. M. D. Ingram, H. Staesche, K. S. Ryder, *J. Power Sources* 129 (2004) 107.

279. C-H Hu, K-H Chang, M-C lin, and Y-T Wu, *Nano. Letters* 6 (2006) 2690.

280. Z. Fan, J. Chen, K. Cui, F. Sun, Y. Xu, and Y. Kuang, *Electrochim. Acta* 52 (2007) 2959.

281. S. Devaraj, N. Munichandraiah, *J. Electrochem. Soc.* 154 (2007) A80.

282. K.W. Nam, K.B. Kim, *J. Electrochem. Soc.* 149 (2002) A346.

283. L. Cao, M. Lu, H.L. Li, *J. Electrochem. Soc.* 152 (2005) A871.

284. S.Y. Wang, K.C. Ho, S.L. Kuo, N.L. Wu, *J. Electrochem. Soc.* 153 (2006) A75.

285. Y. Zhang, Y. Gui, X. Wu, H. Feng, A. Zhang, L. Wang, T. Xia, *Intern. J. hydrogen energy* 3 4 (2 0 0 9) 2 4 6 7.

286. M. Wu, J. Gao, S. Zhang, A. Chen, *J. Porous Mater.* 13 (2006) 407.

287. D. Zhao, W. Zhou, H. Li, *Chem. Mater.* 19 (2007) 3882.

288. M.S. Wu, H.-H. Hsieh, *Electrochim. Acta* 53 (2008) 3427.

289. J. Li, E.-H. Liu, W. Li, X.-Y. Meng, S.-T. Tan, *J. Alloys Compds.* 478 (2009) 371.

290. J. Li, Q.M. Yang, I. Zhitomirsky, *J. Power Sources* 185 (2008) 1569.

291. Y. Zheng, M. Zhang, P. Gao, *Mat. Res. Bull.* 42 (2007) 1740.

292. Y. Cao, J. Cao, M. Zheng, J. Liu, G. Ji, *J. Sol. State Chem.* 180 (2007) 792.

293. J.Y. Lee, K. Liang, K.H. Ana, Y.H. Lee, *Synthetic Metals* 150 (2005) 153.

294. F. Miao, B. Tao, P. Ci, J. Shi, L. Wanga, P.K. Chu, *Mat. Res. Bull.* 44 (2009) 1920.

295. H. Li, Y. Li, R. Wang, R. Cao, *J. Alloys Compds* 481 (2009) 100.

296. J. Chen, K. Huang, S. Liu, X. Hu, *J. Power Sources* 186 (2009) 565.

297. J. Chen, K. Huang, S. Liu, *Electrochem. Commun.* 10 (2008) 1851.

298. N. L. Wu, S. Y. Wang, C. Y. Han, D. S. Wu, and L. R. Shiue, *J. Power Sources* 113 (2003) 173.

299. Y. Wang, W. Yang, C. Chen, D.G. Evans, *Journal Power Sources* 184 (2008) 682.

300. S.-L. Kuo, N.-L. Wu, *Electrochem. Solid-State Letters* 8 (2005) A495.

301. J. Chen, K. Huang, S. Liu, *Electrochim. Acta* 55 (2009) 1.

302. M. Mallouki, F. Tran-Van, C. Sarrazina, C. Chevrot, J.F. Fauvarque, *Electrochim. Acta* 54 (2009) 2992.

303. F. Tao, Y.-Q. Zhao, G.-Q. Zhang, H.-L. Li, *Electrochem. Commun.* 9 (2007) 1282.

304. Y. Yu, G. Ji, J. Cao, J. Liu, M. Zheng, *J. Alloys Compd.* 471 (2009) 268.

305. Z. Zheng, L. Huang, Y. Zhou, X. Hu, X. Ni, *Solid State Sciences* 11 (2009) 1439.

306. J. Wang, T. Golden, K. Varughese and I. El-Rayes, *Anal. Chem.* 61 (1989) 509.

307. Z. Chen, Y. Zhou, *Surface and Coating Technology* 201 (2006) 2419.

308. C.J. Brinker, G.W. Scherer, *Sol-Gel Science: The Physics and Chemistry of Sol-Gel Processing*. Academic Press (1990). ISBN 0121349705.

309. K.B. Blodgett, *J. Amer. Chem. Soc.* 56 (1934) 495.

310. http://en.wikipedia.org/wiki/Chemical_vapor_deposition (Accessed online, September 15, 2009).

311. T. Trindade, O. O˘ıBrien, N.L. Pickett, *Chem. Mater.* 13 (2001) 3843.

312. B. Oregan, M. Gratzel, *Nature* 353 (1991) 737.

313. A.P. Baioni Torre, M. Vidotti, P.A. Fiorito, E.A. Ponzio, S.I. C´ordoba de Torresi, *Langmuir* 27 (2007) 6796.

314. M. Haruta, N. Yamada, T. Kobayashi, S. Iijima, *J. Catal.* 115 (1989) 301.

315. J. Wang, M. Musameh, *Anal. Chem.* 75 (2003) 2075.

316. P.A. Fiorito, V.R. Goncales, E.A. Ponzio, S.I. C´ordoba de Torresi, *Chem. Commun.* (2005) 366.

317. V.M. Rotello. *Nanoparticles: Building Blocks for Nanotechnology*. 1st Ed. New York: Springer; 2003.

318. N.L. Rosi, C.A. Mirkin, *Chem. Rev.* 105 (2005) 1547.

319. Y. Ju-Nam, J.R. Lead, *Science of the Total Environment* 400 (2008) 396.

320. C.P. Poole, F.J. Owens, *Introduction to Nanotechnology*. Hoboken: Wiley-Interscience; 2003.

321. M.C. Daniel, D. Astruc, *Chem. Rev.* 104 (2004) 293.

322. V.S. Bagotsky, Fundamental of Electrochemistry, 2nd Edition, John Wiley & Sons, Inc., New Jersey, 2006.

323. P.J. Pearce, A.J. Bard, J. Electroanal. Chem. 114 (1980) 89.

324. R.H. Wopschall, I. Shain, Anal. Chem. 39 (1967) 1514

325. H.X. Ju, L. Donal, *J. Electroanal. Chem.* 484 (2000) 150.

326. C.A. Gervasi, P.E. Alvarez, M.V. Fiori Bimbi, M.E. Foilquer, *J. Electroanal. Chem.* 601 (2007) 194.

327. E. Le Bourhis, G. Patriarche, Micron 38 (2007) 377.

328. The Free Encyclopedia, http://en.wikipedia.org/wiki/Atomic_force_microscope (accessed online 24 August, 2009).

329. J.B. Hudson, *Surface Science: An Introduction*, John Wiley&Sons, New York, 1998.

330. X. Jiang, T. Wang, *Applied Surface Science* 252 (2006) 8029.

331. D. Briggs, M.P. Seah, *Practical Surface Analysis* by Auger and X-Ray Photoelectron Spectroscopy, Eds. New York: Wiley 1983.

332. *The Free Encyclopedia,* http://en.wikipedia.org/wiki/X-ray-diffraction (accessed online 24 August, 2009).

333. H.H. Willard, L.L. Merritt, J.A. Dean, F.A. Settle, Instrumental Methods of Analysis, 7th Edition, Belmont, Calif: Wadsworth, 1988.

334. *The Free Encyclopedia,* http://en.wikipedia.org/wiki/Ultraviolet-visible_spectroscopy (accessed online July, 2009).

335. K. Yamada, K. Yasuda, N. Fujiwara, Z. Siroma, H. Tanaka, Y. Miyazaki, T. Kobayashi, *Electrochem. Commun.* 5 (2003) 892.

336. R.A. Becker, L.R. Barrows, R.C. Shank, *Carcinogenesis* 2 (1981) 1181.

337. *Homeland Security Information Bulletin* US Department of Homeland Security: Washington DC May 2003.

338. G.G. Wildgoose, C.E. Banks, R.G. Compton, *Small* 2(2006) 182.

339. C.E. Banks, A. Crossley, C. Salter, S.J. Wilkins, R.G. Compton, *Angew Chem. Int. Ed.* 45: (2006) 2533.

340. J. Kruusma, N. Mould, K. Jurkschat, A. Crossley, C.E. Banks Electrochem. Commun. 9 (2007) 2330.

341. C.P. Jones, K. Jurkschat, A. Crossley, R.G. Compton, B.L. Riehl, C.E. Banks, *Langmuir* 23 (2007) 9501.

342. K. Jurkschat, X. Ji, A. Crossley, R.G. Compton, C.E. Banks, *Analyst* 132 (2007) 21.

343. Available at http://en.wikipedia.org/wiki/Chemica_warfare (Accessed online 15 April, 2009).

344. E. W. Hooijschuur, A. Hulst, A. de Long, L. de Reuver, S. van Krimpen, B. van Baar, E. Wils, C. Kientz, U.A. Brinkman, *Trends Anal. Chem. (TrAC)* 21 (2002) 116.

345. Y.Yang, *Acc. Chem. Res.* 32 (1999) 109.

346. C.L. Copper, G.E. Collins, *Electrophoresis*, 25 (2004) 897.

347. J. Wang, J. Zima, N.S. Lawrence, M.P. Chatrathi, *Anal. Chem.*, 76 (2004) 4721.

348. J. Pillay, K.I. Ozoemena, *Electrochem. Commun.*, 9 (2007) 1816.

349. C.A. Claudia, F. Bedioui, J.H. Zagal, *Electrochim. Acta* 47 (2002) 1489.

350. N.S. Bryan, *Free Radical Biol. Med.*, 41 (2006) 691.

351. E.T. Reichert, S.W. Mitchell, *Am. J. Med. Sci.* 159 (1980) 158.

352. C.J. Hunter, *Nat. Med.* 10 (2004) 1122.

353. A.V. Kozlov, *Shock* 15 (2001) 366.

354. N. Sparatu, T.N. Rao, D.A. Tryk, A. Fujishima, *J. Electrochem. Soc.* 148 (2001) E112.

355. H.J. Choi, G. Kwag, S. Kim, *J. Electroanal Chem.* 508 (2001) 105.

356. A.L. Leninger, D.L. Nelson, M.M. Cox, *Principles of Biochemistry*, 2nd ed., Worth Publishers, New York 1993, p. 689.

357. S.Y. Ha, S. Kim, *J. Electroanal. Chem.* 468 (1999) 131.

358. Z.H. Wen, T.F. Kang, *Talanta* 62 (2004) 351.

359. D. Giustarini, I. Dalle-Donne, R. Colombo, A. Milzani, R. Rossi, *Free Rad. Res.* 38 (2004) 1235.

360. W. Frenzel, J. Schulz-Brussel, B. Zinvirt, *Talanta* 64 (2004) 278.

361. S. Arias-Negrete, L.A. Jimenez-Romero, M.O. Soliis-Martiinez, J. Ramiirez-Emiliano, E.E. Avila, P. Cuella-Mata, *Anal. Biochem.* 328 (2004) 14.

362. A. Aydin, O. Ercan, S. Tascioglu, *Talanta* 66 (2005) 1181.

363. M.I.H. Helaleh, T. Korenaga, *J. Chromatogr. B* 744 (2000) 433.

364. X. Cai, Z. Zhao, *J. Electroanal. Chem.* 252 (1988) 361.

365. J.E. Newbry, M.P.L. de Haddad, *Analyst* 110 (1985) 81.

366. M. Trojanowicz, W. Matuszewski, B. Szostek, *Anal. Chim. Acta* 261 (1992) 391.

367. C.A. Caro, F. Bedioui, J.H. Zagal, *Electrochim. Acta* 47 (2002) 1489.

368. S.Q. Wang, Y.M. Yin, X.Q. Lin, *Electrochem. Commun.* 6 (2004) 259.

369. J.W. Mo, B. Ogorevc, *Anal. Chem.* 73 (2001)1196.

370. R.M. Wightman, L.J. May, A.C. Michael, *Anal. Chem.* 60 (1998) 769A.

371. R.C. Retna, T. Okajima, T. Ohsaka, *J. Electroanal. Chem.* 543 (2003) 127.

372. T. Selvaraju, R. Ramaraj, *J.Electroanal. Chem.* 585 (2005)290.

373. P. Zhang, F.H. Wu, G.C. Zhao, X.W. Wei, *Bioelectrochem.* 67 (2005) 109.

374. N.Q. Jia, Z.Y. Wang, G.F. Yang, H.B. Shen, L.Z. Zhu, *Electrochem. Commun.* 9 (2007)233.

375. Y.F. Zhao, Y.Q. Gao, D.P. Zhan, H. Liu, Q. Zhao, Y. Kou, Y.H. Shao, M.X. Li, Q.K. Zhuang, Z.W. Zhu, *Talanta* 66 (2005) 51.